

University of Windsor

## Scholarship at UWindor

---

Electronic Theses and Dissertations

Theses, Dissertations, and Major Papers

---

2011

### Water absorption of Wood Plastic Composite and Biopolymer reinforced with Switchgrass-fiber Biocomposite Materials

Ganesh Muralidhar Venukadasula  
*University of Windsor*

Follow this and additional works at: <https://scholar.uwindsor.ca/etd>

---

#### Recommended Citation

Venukadasula, Ganesh Muralidhar, "Water absorption of Wood Plastic Composite and Biopolymer reinforced with Switchgrass-fiber Biocomposite Materials" (2011). *Electronic Theses and Dissertations*. 8258.

<https://scholar.uwindsor.ca/etd/8258>

This online database contains the full-text of PhD dissertations and Masters' theses of University of Windsor students from 1954 forward. These documents are made available for personal study and research purposes only, in accordance with the Canadian Copyright Act and the Creative Commons license—CC BY-NC-ND (Attribution, Non-Commercial, No Derivative Works). Under this license, works must always be attributed to the copyright holder (original author), cannot be used for any commercial purposes, and may not be altered. Any other use would require the permission of the copyright holder. Students may inquire about withdrawing their dissertation and/or thesis from this database. For additional inquiries, please contact the repository administrator via email ([scholarship@uwindsor.ca](mailto:scholarship@uwindsor.ca)) or by telephone at 519-253-3000ext. 3208.

# **Water absorption of Wood Plastic Composite and Biopolymer reinforced with Switchgrass-fiber Biocomposite Materials**

by

Ganesh Muralidhar Venukadasula

A Thesis

Submitted to the Faculty of Graduate Studies  
through the Department of Chemistry and Biochemistry  
in Partial Fulfillment of the Requirements for  
the Degree of Master of Science at the  
University of Windsor

Windsor, Ontario, Canada

2011

© 2011 Ganesh M. Venukadasula



Library and Archives  
Canada

Published Heritage  
Branch

395 Wellington Street  
Ottawa ON K1A 0N4  
Canada

Bibliothèque et  
Archives Canada

Direction du  
Patrimoine de l'édition

395, rue Wellington  
Ottawa ON K1A 0N4  
Canada

*Your file Votre référence*  
ISBN: 978-0-494-81743-8  
*Our file Notre référence*  
ISBN: 978-0-494-81743-8

#### NOTICE:

The author has granted a non-exclusive license allowing Library and Archives Canada to reproduce, publish, archive, preserve, conserve, communicate to the public by telecommunication or on the Internet, loan, distribute and sell theses worldwide, for commercial or non-commercial purposes, in microform, paper, electronic and/or any other formats.

The author retains copyright ownership and moral rights in this thesis. Neither the thesis nor substantial extracts from it may be printed or otherwise reproduced without the author's permission.

#### AVIS:

L'auteur a accordé une licence non exclusive permettant à la Bibliothèque et Archives Canada de reproduire, publier, archiver, sauvegarder, conserver, transmettre au public par télécommunication ou par l'Internet, prêter, distribuer et vendre des thèses partout dans le monde, à des fins commerciales ou autres, sur support microforme, papier, électronique et/ou autres formats.

L'auteur conserve la propriété du droit d'auteur et des droits moraux qui protègent cette thèse. Ni la thèse ni des extraits substantiels de celle-ci ne doivent être imprimés ou autrement reproduits sans son autorisation.

---

In compliance with the Canadian Privacy Act some supporting forms may have been removed from this thesis.

While these forms may be included in the document page count, their removal does not represent any loss of content from the thesis.

Conformément à la loi canadienne sur la protection de la vie privée, quelques formulaires secondaires ont été enlevés de cette thèse.

Bien que ces formulaires aient inclus dans la pagination, il n'y aura aucun contenu manquant.

  
**Canada**

## **DECLARATION OF ORIGINALITY**

I hereby certify that I am the sole author of this thesis and that no part of this thesis has been published or submitted for publication.

I certify that, to the best of my knowledge, my thesis does not infringe upon anyone's copyright nor violate any proprietary rights and that any ideas, techniques, quotations, or any other material from the work of other people included in my thesis, published or otherwise, are fully acknowledged in accordance with the standard referencing practices. Furthermore, to the extent that I have included copyrighted material that surpasses the bounds of fair dealing within the meaning of the Canada Copyright Act, I certify that I have obtained a written permission from the copyright owner(s) to include such material(s) in my thesis and have included copies of such copyright clearances to my appendix.

I declare that this is a true copy of my thesis, including any final revisions, as approved by my thesis committee and the Graduate Studies office, and that this thesis has not been submitted for a higher degree to any other University or Institution.

## **ABSTRACT**

Biocomposites have become widely used materials these days. Due to their light weight and ability to be tailored for specific end uses they have gained a considerable ground in the high performance applications, such as aerospace and automobile industry. However, the use of polymers that can be recycled with carbon and other niche fibers renders the composite non-recyclable.

The objective of this present research work was to study the resistance of the Biocomposite and Wood Plastic Composite materials to water. A Biocomposite made up of biopolymer reinforced with switchgrass fibers and a WPC prepared from High density polyethylene reinforced with wood flour fillers were studied for the water absorption behaviour at three different temperatures were evaluated. In addition, density changes, dimensional stability and acoustic properties of the WPC and switchgrass/biopolymer composite were evaluated.

## **DEDICATION**

To

My mother Padmasri

## **ACKNOWLEDGEMENT**

I would like to express my sincere thanks to my research advisor Prof. Elena Maeva for her excellent support and guidance throughout my studies at the University of Windsor.

I would like to thank Dr. Ina Seviaryna for her valuable time. Her patience in explaining instruments and helpful suggestions were big contributions to my projects and thesis.

I would like to thank Dr. Fedar Severin for his instructions regarding the Ultrasonic Pulse-receiver instrument.

I would like to thank Sharon Lackie for help in teaching and attaining the images from the Scanning Electron Microscopy.

I would like to thank our collaborators Dr. Manjusri Misra and Dr. Saswatha Sahoo for their efforts in preparing the switchgrss/biopolymer composite materials, which were used in my research.

I would like to thank Joe Lichaa for his help.

I would like to thank all my friends Ranith, Satya, Jogi, Preetham, Vekat Subramanyam, Venkat Anathapalli, Sandeep Sing, Navneet, Devang, Mukesh, Siddu, Sumanth, Rinku, Abhineeth, Harsha, Subbu, Srinu, Sriram reddy, Gurram, Ranadheer, Raghavan, Akhil, Anil, Chandu, Srikanth, Vinay, Srikanth Reddy, Vamsi, Vinod, Akhilesh, Sai, Sunil, Ravikanth, Anjan, Omprakash, Teja, and Himadri for their support during my stay in Canada. I would like to thank my college friends Dali Naidu, Shekar Reddy and Sravan Kumar for their patience and support.

I would like to thank my cousin Mr. Vindo Gurijala and Rajitha akka, for their support and valuable suggestions regarding life and my career.

I would like to thank Rani and Venkat for their support when I really needed help.

I cannot forget my brother Phanindra Venukadasula for his support and help. Whatever I am today in regards to my career, was primarily his influence. When I left India, I was grown up and strong at heart; ready to take up any challenges that came my way. All this is due to my brother, Phani and his support and encouragement.

My greatest strength is my family. I can proudly say I am who I am because my mother, Padmasri and father Prabhakar. Mom, you have always supported me in no matter what I pursue and I am eternally grateful. I hope that I have made you proud and hope I can continue to build on the values you have taught me in life. I am grateful to my elder brother Venumadhav and Sharvani vadina, Chandrika vadina, for their support during my toughest phase in life. My lovely nephew Sathwik and niece Sumedha, your innocent questions and childish interest, are what allowed me to relax and laugh. I can't tell you how much this helped in stressful times.



## TABLE OF CONTENTS

DECLARATION OF ORIGINALITY .....	III
ABSTRACT .....	IV
DEDICATION .....	V
ACKNOWLEDGEMENT .....	VI
LIST OF TABLES .....	XII
LIST OF FIGURES .....	XIII
Introduction .....	1
1.1 Background .....	1
1.2 Problem statement/objectives .....	2
1.3. Thesis outline .....	3
Literature Review .....	4
2.1 Definition .....	4
2.2 Natural fibers as fillers .....	4
2.3 Different matrices .....	6
2.3.1 Thermoplastic matrices .....	6
2.3.2 Thermosetting matrices .....	6
2.3.3 Rubber matrices .....	6
2.3.4 Biodegradable matrices .....	7
2.4 Additives .....	7
2.4.1 Coupling agent (CA) .....	8
2.5 Biocomposites and their interactions with the environment .....	9
2.5.1 Emission of volatiles and low molecular weight compounds from biocomposites .....	10
2.5.2 Degradation of Biocomposites .....	11
2.5.2.1 Abiotic degradation by water absorption .....	11
2.5.2.2 Hydrothermal degradation .....	12
2.5.2.3 Thermo- and Photo-Oxidation .....	13
2.6 Water absorption .....	14

2.7 Chemical Effect on Biocomposites .....	18
2.7.1 Natural fibers .....	18
2.7.2 Mechanism of Chemical modifications.....	20
2.7.2.1 Alkali treatment .....	20
2.7.2.2 Acetylation .....	21
2.7.2.3 Silane Treatment.....	22
2.7.3 Chemical Modification Characterization of Natural fibers .....	24
2.7.3.1 Aspen Fiber composites.....	24
2.7.3.2 Bagasse fiber Composites.....	24
2.7.3.3 Coir fiber composites.....	25
2.7.3.4 Flax fiber composites.....	26
2.7.3.5 Ramie fiber composites .....	27
2.8 Fourier transform infrared spectroscopy .....	28
2.9 Mechanical Properties .....	29
2.9.1 Effect of Water Absorption on Mechanical Properties of Biocomposites.....	30
2.10 Thermal properties.....	31
3. Materials and Methods .....	34
3.1 Materials.....	34
3.2 Water absorption .....	34
3.3 Diffusion coefficient (D) .....	34
3.4 Density Determination.....	35
3.5 Thickness Swelling Determination.....	36
3.6 Dehydration .....	37
3.7 Scanning Acoustic Microscopy .....	37
3.8 Pulse-echo Technique.....	41
3.9 Scanning Electron Microscope:.....	42
3.10 STATISTICS .....	45
4. Results and Discussion .....	46

4.1 Water absorption .....	46
4.1.1. Wood Plastic Composite (WPC) .....	47
4.1.2. switchgrss/biopolymer composite .....	48
4.1.3. WPC vs. switchgrss/biopolymer composite Discussion.....	50
4.2 Diffusion Coefficient (D) .....	51
4.3 Density of WPC and switchgrss/biopolymer composite .....	55
4.4 Dimensional stability of WPC and switchgrss/biopolymer composite .....	56
4.5 Dehydration .....	58
4.6 Morphology .....	59
5. Acoustic measurements .....	67
5.1 Ultrasonic wave speed Measurements in WPC .....	68
5.1.1 Ultrasonic wave speed Measurements in WPC at 2.25MHz.....	68
5.1.2 Ultrasonic wave speed Measurements in WPC at 3.5MHz.....	69
5.1.3 Ultrasonic wave speed in WPC vs. Weight change% at 2.25MHz .....	70
5.1.4 Ultrasonic wave speed in WPC vs. Weight change% at 3.5MHz .....	71
5.2. Attenuation measurements in WPC.....	72
5.2.1 Attenuation Measurements in WPC at 2.25MHz .....	72
5.2.2 Attenuation Measurements in WPC at 3.5MHz .....	73
5.2.3 Attenuation in WPC vs. Weight change% at 2.25MHz.....	74
5.2.4 Attenuation in WPC vs. Weight change% at 3.5MHz.....	75
5.3 Ultrasonic wave speed Measurements in switchgrss/biopolymer composite.....	76
5.3.1 Ultrasonic wave speed measurements in switchgrss/biopolymer composite at 2.25MHz .....	76
5.3.2 Ultrasonic wave speed measurements in switchgrss/biopolymer composite at 3.5MHz .....	77
5.3.3 Ultrasonic wave speed measurements in switchgrss/biopolymer composite at 10MHz .....	78
5.3.4 Ultrasonic wave speed in switchgrss/biopolymer composite vs. Weight Change% at 2.25MHz .....	79
5.3.5 Ultrasonic wave speed in switchgrss/biopolymer composite vs. Weight Change% at 3.5MHz	80
5.3.6 Ultrasonic wave speed in switchgrss/biopolymer composite vs. Weight Change% at 10MHz	81
5.4 Attenuation measurements in switchgrss/biopolymer composite.....	82

5.4.1 Attenuation in switchgrss/biopolymer composite at 2.25MHz .....	82
5.4.2 Attenuation in switchgrss/biopolymer composite at 3.5MHz .....	83
5.4.3 Attenuation in switchgrss/biopolymer composite at 10MHz .....	84
5.4.4 Attenuation in switchgrss/biopolymer composite vs. Weight change% at 2.25MHz.....	85
5.4.5 Attenuation in switchgrss/biopolymer composite vs. Weight change% at 3.5MHz.....	86
5.4.6 Attenuation in switchgrss/biopolymer composite vs. Weight change% at 10MHz.....	87
5.5 Acoustic Images .....	88
5.6 Histograms.....	90
CONCLUSIONS .....	92
REFERENCES .....	94
<i>VITA AUCTORIS</i> .....	103

## **LIST OF TABLES**

Table 1: Natural and biodegradable matrices	7
Table 2: Water absorption values at equilibrium (wt. %) and time to reach equilibrium (hours)	50
Table 3: Diffusion Coefficient of WPC and switchgrass/biopolymer at different temperatures	54

## LIST OF FIGURES

	PAGE
Figure 2.1. Classification of Natural Fibers.	5
Figure 2.2. Mechanism of PP-MA reacting with Lignocellulosic hydroxyl group	9
Figure 2.3. The function of the compatibilizing agent in the Lignocellulosic filler-polyolefin composite system	15
Figure 2.4. Chemical structures of anti-hydrolysis agent and trimethylolpropane trifunctional monomer	16
Figure 2.5. Structure of Biofiber.	19
Figure 2.6. Lattice structure of Cellulose I and Cellulose II	21
Figure 2.7. Scheme for interaction of silanes with cellulosic fibers	23
Figure 2.8. Hypothetical reaction of silane with KFAB.	27
Figure 3.1. Schematic representation of (a) the principle of acoustic scanning (b) scanning acoustic microscope	38
Figure 3.2. Schematic representation of the acoustic image formation (a) B-scan	38
Figure 3.3. Schematic image of the acoustic lens	39
Figure 3.4. Schematic representation of the principle of pulse-echo method	42
Figure 3.5. Schematic representation of principle of BSE	44
Figure 3.6. Schematic representation of principle of SE	44
Figure 4.1. Water absorption of WPC at different temperatures	48
Figure 4.2. Water absorption of switchgrass/biopolymer composite at different temperatures	49
Figure 4.3. Initial part of the water absorption slopes for WPC at 20°C, 40°C & 70°C	52

Figure 4.4. Initial part of the water absorption slopes for switchgrass/biopolymer composite at 20°C, 40°C & 70°C	52
Figure 4.5. Diffusion Coefficient of WPC at three different temperatures	53
Figure 4.6. Diffusion Coefficient of switchgrass/biopolymer composite at three different temperatures	54
Figure 4.7. Change in density of WPC at three different temperatures	55
Figure 4.8. Change in density of switchgrass/biopolymer composite at three different temperatures	56
Figure 4.9. Thickness swelling of WPC at three different immersion temperatures	57
Figure 4.10. Thickness swelling of switchgrass/biopolymer composite at three different immersion temperature	58
Figure 4.11. Dehydration of WPC and switchgrass/biopolymer composite at room temperature	59
Figure 4.12. SEM micrographs of the fractured surface of WPC, (a) completely dry sample, (b) Drying after 20°C water immersion	61
Figure 4.12. SEM micrographs of the fractured surface of WPC, (c) Drying after 40°C water immersion, (d) Drying after 70°C water immersion	62
Figure 4.12. SEM micrographs of the fractured surface of WPC, (e) 20°C water immersion, (f) 40°C water immersion	63
Figure 4.13. SEM micrographs of the fractured surface of switchgrass/biopolymer composite (a) completely dry sample, (b) Drying after 20°C water immersion	64
Figure 4.13. SEM micrographs of the fractured surface of switchgrass/biopolymer composite (c) Drying after 40°C water immersion, (d) Drying after 70°C water immersion,	65
Figure 4.13. SEM micrographs of the fractured surface of switchgrass/biopolymer composite (e) 20°C water immersion, (f) 40°C water immersion	66
Figure 5.1. Ultrasonic wave speed of WPC for 2.25MHz at three different temperatures	68
Figure 5.2. Ultrasonic wave speed of WPC for 3.5MHz at three different temperatures	69
Figure 5.3. Ultrasonic wave speed of WPC vs. Weight% for 2.25MHz at three different temperatures	70

Figure 5.4. Ultrasonic wave speed of WPC vs. Weight% for 3.5MHz at three different temperatures	71
Figure 5.5. Attenuation of WPC for 2.25MHz at three different temperatures	72
Figure 5.6. Attenuation of WPC for 3.5MHz at three different temperatures	73
Figure 5.7. Attenuation of WPC vs. Weight% for 2.25MHz at three different temperatures	74
Figure 5.8. Attenuation of WPC vs. Weight% for 3.5MHz at three different temperatures	75
Figure 5.9. Sound speed of switchgrss/biopolymer composite for 2.25MHz at three different temperatures	76
Figure 5.10. Sound speed of switchgrss/biopolymer composite for 3.5MHz at three different temperatures	77
Figure 5.11. Sound speed of switchgrss/biopolymer composite for 10MHz at three different temperatures	78
Figure 5.12. Sound speed of switchgrss/biopolymer composite vs. Weight% for 2.25MHz at three different temperatures	79
Figure 5.13. Sound speed of switchgrss/biopolymer composite vs. Weight% for 3.5MHz at three different temperatures	80
Figure 5.14. Sound speed of switchgrss/biopolymer composite vs. Weight% for 10MHz at three different temperatures	81
Figure 5.15. Attenuation of switchgrss/biopolymer composite for 2.25MHz at three different temperatures	82
Figure 5.16. Attenuation of switchgrss/biopolymer composite for 3.5MHz at three different temperatures	83
Figure 5.17. Attenuation of switchgrss/biopolymer composite for 10MHz at three different temperatures	84
Figure 5.18. Attenuation of switchgrss/biopolymer composite vs. Weight% for 2.25MHz at three different temperatures	85
Figure 5.19. Attenuation of switchgrss/biopolymer composite vs. Weight% for 3.5MHz at three different temperatures	86
Figure 5.20. Attenuation of switchgrss/biopolymer composite vs. Weight% for 10MHz at three different temperatures	87



5.21. Acoustic images of the switchgrass/biopolymer composite samples exposed to water for different time intervals. a) 0hrs b) 24hrs c) 120hrs d) 360hrs 89

5.22 Histograms of the switchgrass/biopolymer composite samples exposed to water for different time intervals. A) 0hrs B) 24hrs C) 120hrs D) 360hrs 91

## LIST OF ABBREVIATIONS

AAPP	Acrylic acid grafted polypropylene
AA	Acrylic acid
BRAF	Bleached red algae fiber
BR	Butadiene rubber
BSE	Backscatter electrons
CR	Chloroprene rubber
CA	Coupling agent
CIDIC	Isocyanate derivative of cardanol
DMA	Dynamic mechanic analyzer
EPDM	Ethylene propylene diene rubber
EVA	Ethylene vinyl acetate
EVOH	Ethylene vinyl alcohol copolymer
EFB	Empty fruit bunch
FTIR	Fourier transform infrared spectroscopy
HDPE	High Density Polyethylene
HDT	Heat deflection temperatures
IFSS	Interfacial shear strength
IIR	Butyl rubber
KOH	Potassium hydroxide
KFAB	Permanganate acetone solution
KsFAB	Permanganate acetone solution and silane solution
KF-PP	Kenaf polypropylene
LiOH	Lithium hydroxide
MS	Mass Spectrometry

MRI	Magnetic resonance imaging
MA	Maleic anhydride
MAPP/PP-MA	Maleated polypropylene
MAPE/PE-MA	Maleated polyethylene
NP	Newsprint
NR	Natural rubber
NP-PP	Newsprint polypropylene
NBR	Nitrile rubber
NaOH	Sodium hydroxide
OPT	Oil palm trunk
PP	Polypropylene
PE	Polyethylene
PLA	Poly(Lactic Acid)
PLA-MA	Maleic anhydride-grafted poly(lactic acid)
PHA	Polyhydroxy Alkanoate
PP-RHF	Polypropylene Rice-husk flour
PBS	Polybutylene Succinate
PBS-MA	Maleic anhydride-grafted poly(butylene succinate)
PLLA	Poly(L-lactic Acid)
PHBV	Poly (3-hydroxybutyrate-co-3-hydroxyvalerate)
PS	Polystyrene
PC	Polycarbonate
PEEK	Polyether ether ketone
PCL	Poly(caprolacton)
RH	Relative humidity

RH-PP	Rice hull polypropylene
SBR	Styrene butadiene rubber
SEBS-MA	Maleic anhydride grafted poly(styrene-b-ethylene-co-butylene-b-styrene) triblock copolymer
SEM	Scanning electron microscopy
SE	Secondary electrons
SAM	Scanning acoustic microscopy
TDP	4,4'- thiodiphenol
TGA	Thermo gravimetric analysis
TMVS	Trimethoxyvinyl silane
UF	Urea formaldehyde
WPC	Wood plastic composite
WF-PP	Wood flour polypropylene
XPS	X-ray photoelectron spectroscopy

# **Chapter I**

## **Introduction**

### **1.1 Background**

Traditional composite materials are made up of aramid, glass or carbon fibers reinforced with phenolics, epoxy, polyurethanes or unsaturated polyester resins. Their removal, use and manufacturing was scrutinized from a legislative and an environmental perspective<sup>1</sup>. The traditional composites are made from two dissimilar materials. Recycling and waste disposal of these materials after their life span has become a problem because they are stable<sup>1</sup>. Landfills of traditional composites cannot be reused or recycled; hence environmentally compatible alternative materials such as biocomposites will need to be used.

Researchers have shown interest in biocomposites due to their low density, low cost and very good mechanical properties, as well as adequate supply of these natural fibers from renewable resources<sup>2</sup>. There are 3 different types of biocomposites: (1) Partially biodegradable, (2) Completely biodegradable, (3) Hybrid biodegradable. Biocomposites made up of natural fibers are biodegradable whereas traditional thermosets (unsaturated polyesters) and thermoplastics (like polyethylene and polypropylene) are non-biodegradable. These can be referred to as “partially biodegradable” biocomposite. In case the polymer matrix is biodegradable, a natural fiber-reinforced biopolymer composite is referred to as a “completely biodegradable” biocomposite. If two or more natural fibers are combined with a polymer matrix it is referred to as “Hybrid” biocomposite.

The preparation of natural fiber-reinforced composites attracted many scientists because these biocomposites are substitutes to the ever diminishing petroleum resources. Biocomposites’

main advantages are: environmentally friendly, fully sustainable and biodegradable. They can be easily disposed of at the end of life their span without harming the environment.

## **1.2 Problem statement/objectives**

There have been a lot of investigations in new composites development during the last decades. However, the biocomposites are not as widely accepted in industry as they deserve.

One of the limiting factors is low water resistance of the materials. Biocomposites may suffer from water attacks when exposed to service conditions.

It is important to understand the dynamics of water absorption by biocomposites. The work in this Thesis is planned to study water sorption of the natural fibre based composites. By characterizing changes in density, dimensional stability as well as acoustic properties of two types of biocomposites and to establish the correlation between acoustic and other parameters. This correlation could help in developing fast and nondestructive techniques for identification of water content in composites.

The objectives of this study are:

- To characterize water absorption by two types of biocomposites at various temperatures;
- To establish a correlation between acoustic parameters of composites and water absorbance;
- To visualize the changes in microstructure of composites during the water absorption process.

### **1.3. Thesis outline**

This thesis starts with a literature review on biocomposites (chapter II). The instruments, materials and methods used in this research are described in chapter III. In chapter IV the results and discussion are presented and focus on water absorption by WPC and switchgrass/biopolymer composite at different temperature and diffusion coefficient values. Chapter V discusses acoustic measurements (velocity, attenuation), acoustic images and Histograms of the samples. Chapter VI presents the conclusions and recommendations of this work.

## Chapter II

### Literature Review

#### 2.1 Definition

Biocomposites are composite materials made from bio/natural fiber and a biodegradable polymer (Polylactic Acid (PLA), Polyhydroxy Alkonates (PHA)) or petroleum derived nonbiodegradable polymers (Polypropylene (PP), Polyethylene (PE)). Biocomposites derived from bio/crop-derived plastic (**bioplastic/biopolymer**) and plant-derived fiber (**bio/natural fiber**) are found to be more eco-friendly and such composites are called green composites.

Using excess petroleum products has become a big problem (i.e. diminishing petroleum resources and entrapment of plastics in the environment and food chain). Excessive use of plastics results in increased pollution and emissions during degradation which is affecting the water we drink, the air we breathe and the food we eat. It is threatening our very ability to survive. The effort to develop biodegradable plastics was initiated because of the limited supply of petroleum-based resources. Bioplastics are based on renewable agricultural products and plants but can compete with petroleum-derived products which currently dominate the market. 100% biobased material production is not presently an economical solution for replacement of petroleum based products. Combining petroleum and biobased resources would be a more viable solution to develop a cost-effective product that can have broad applications. Synthetic polymers or biopolymers reinforced with bio or natural fibers are a viable alternative to glass fiber composites.

#### 2.2 Natural fibers as fillers

Generally natural fibers can be classified based on their origin. Natural fibers can be extracted from animals, plants or minerals. Plant fibers are the most popular choice in material



science because of their physical properties, sustainability and recyclability. Based on the part of the plant they originate from, plant fibers are further categorized. Figure<sup>3</sup> 2.1 provides classification of natural fibers.

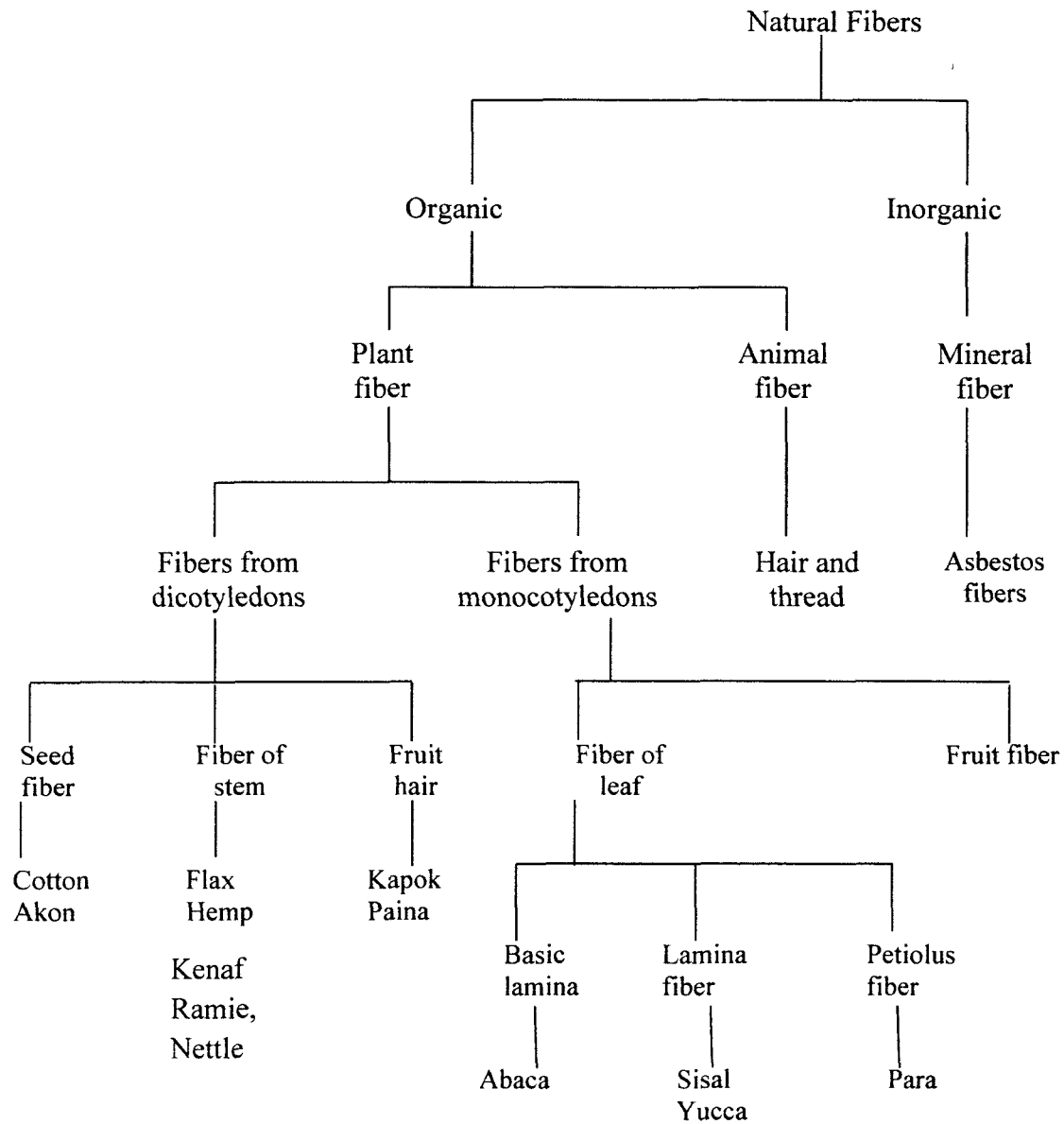


Figure 2.1. Classification of Natural Fibers.<sup>3</sup>

## **2.3 Different matrices**

### **2.3.1 Thermoplastic matrices**

Thermoplastic polymers soften or melt upon heating. These polymers consist of branched or linear chain molecules having strong intramolecular bonds but weak intermolecular bonds. Solidification and melting of these polymers are reversible and they can be reshaped by applying pressure and heat. The structure of these polymers is either amorphous or semicrystalline. The following are examples of thermoplastics: Polystyrene (PS), polyethylene (PE), polycarbonate (PC), nylons, polyamide-imide, polyacetals, polysulphone polyphenylene sulphide, polyether-ether ketone (PEEK) and polyether imide.

### **2.3.2 Thermosetting matrices**

A thermosetting plastic has a network or crosslinked structures, and consists of covalent bonds between all molecules. Upon heating, thermosetting plastics decompose. They cannot be reshaped once they have been solidified by crosslinking. Epoxides, polyesters and phenol formaldehydes are a few common examples of thermosetting polymers.

### **2.3.3 Rubber matrices**

Styrene butadiene rubber (SBR), natural rubber (NR), butadiene rubber (BR), butyl rubber (IIR), nitrile rubber (NBR), ethylene propylene diene rubber (EPDM), chloroprene rubber (CR), silicon rubber and polyurethane rubbers are used for the preparation of composites. Natural rubber is most widely used as a rubber matrix.

### 2.3.4 Biodegradable matrices

Researchers are developing a new class of biodegradable green composites by combining bio/natural fibers with biodegradable matrices. The main advantages of green composites are that they are eco-friendly, sustainable and fully degradable. They can easily be disposed of at the end of their life without harming the environment. A number of biodegradable and natural matrices, which can be used in the preparation of green composites, are listed in the table 1.

Table 1 Natural and biodegradable matrices<sup>4</sup>

Natural	Synthetic
Polysaccharides	Poly(amides)
Starch	Poly(anhydrides)
Cellulose	Poly(amide-enamines)
Chitin	Poly(vinyl alcohol)
Proteins	Poly(vinyl acetate)
Collagen/gelatin	Polyesters
Casein, albumin, fibrogen, silks	Poly(glycolic acid)
Polyhydroxyalkanoates	Poly(lactic acid)
Lignin	Poly(caprolactone)
Lipids	Poly(orthoesters)
Shellac	Poly(ethylene oxides)
Natural rubber	Poly(phosphazines)

### 2.4 Additives

Various additives are used in biocomposites to improve the preparation during their life time or to achieve specific needs during the manufacturing process. Commonly used additives

are antioxidants, coupling agents, pigments, stabilizers, biocides or lubricants. Biocides in biocomposites and bioplastics may be more significant compared to the other composite materials because of their ability to suppress the growth of microorganisms (fungi, bacteria) which are responsible for biological degradation of the materials.

#### **2.4.1 Coupling agent (CA)**

A coupling agent (CA) is a chemical substance, added to a biocomposite material to improve the fiber matrix interface. Interfacial adhesion between natural fibers and the polymer matrix determines the biocomposite's final properties, hence it is very important to use a CA. Maier et al<sup>5</sup> reported that CAs are bifunctional molecules. One end of the CA reacts with organic, nonpolar substrates while the other end reacts with polar, inorganic materials. Commonly used coupling agents are titanate, silane and maleic anhydride grafted to the polymers like polyethylene grafted maleic anhydride (PE-MA); and polypropylene grafted maleic anhydride (PP-MA). As well, aluminates and zirconate are used in polymer industries. PE-MA and PP-MA coupling agents are used with thermoplastics. These coupling agents are characterized by the percentage of the maleic anhydride grafted to the polymer and their molecular weight. Natural fibers based on cellulose are hydrophilic in nature, and hence show inherent incompatibilities with a hydrophobic polymer (polyolefins) matrix. This leads to poor interfacial adhesion between cellulose-based fibers and a polypropylene or ethylene matrix. Maleic anhydride grafted polyolefin is one of the most efficient CA used for composites composed of polyolefin matrixes and cellulose-based materials (fillers or fibers). The composite materials prepared by the melting mixing technique with MA-PP as a coupling agent showed drastically improved mechanical properties improved drastically. The strong interfacial adhesion was caused by esterification between hydroxyl groups of cellulose and anhydride groups (Figure 2.2) of MA-PP<sup>6</sup>.

Pathapulakkal et al<sup>7</sup> used CAs such as ethylene-(acrylic ester)-glycidylmethacrylate and ethylene-(acrylic ester)- maleic anhydride with high density polyethylene (HDPE) which gave significant strength and rigidity to the composite materials.

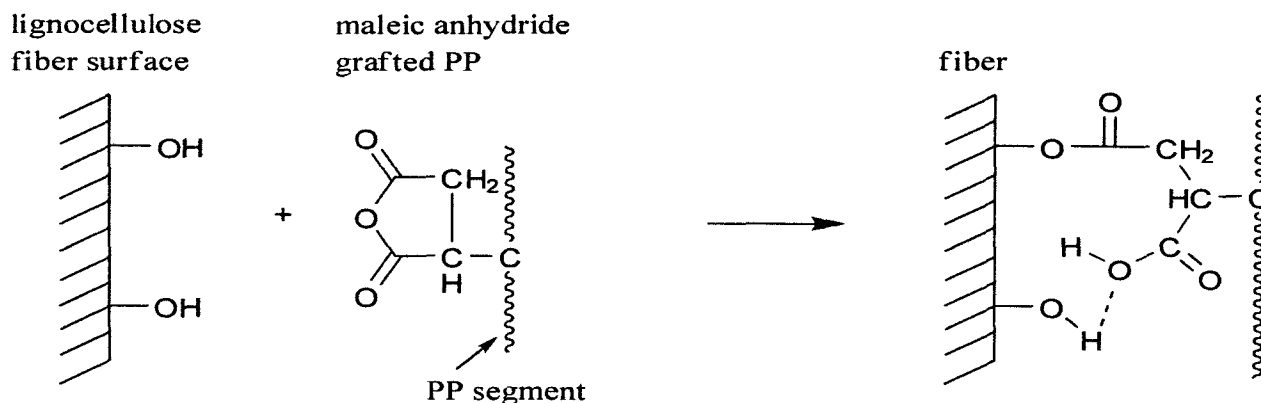


Figure 2.2. Mechanism of PP-MA reacting with Lignocellulosic hydroxyl group.<sup>8</sup>

## 2.5 Biocomposites and their interactions with the environment

Every manufacturer has to make sure when they are preparing biocomposites that they pose no danger to the environment or to human health throughout their service life. Regarding the design of biocomposites the following important issues need to be discussed: (i) the possible emission of odours, (ii) the release of nanosized fillers and low molecular weight compounds, (iii) high moisture absorption, and (iv) chemical modifications.

### **2.5.1 Emission of volatiles and low molecular weight compounds from biocomposites**

Generally reinforced biocomposites possess limited thermal stability during thermo-mechanical processing at the required temperatures, which may contribute to the formation of low molecular weight compounds as a result of the degradation of either the lignocellulosic fibers or the polymeric matrix used as reinforcement. This causes the release of unwanted odours during service life and processing, which limits the applicability of biocomposites in automotive components and indoor construction applications. Extrusion (including foaming, reactive extrusion, film and sheet forming), injection moulding and compression moulding are the most common procedures for the thermo-mechanical processing of biocomposites<sup>9</sup>. The pyrolysis of (bio)polymers and natural fibers as well as thermal degradation have been widely reported in the literature, mostly from the perspective of biomass pyrolysis and residue incineration<sup>10,11</sup>.

Thermogravimetric analysis (TGA) is a common technique used for the investigation of decomposition kinetics and to assess the thermal stability of the (bio)polymeric matrix, natural fibers and their composites. Mass spectrometry (MS) or TGA combined with FTIR provides the information about volatiles released during the process. Thermal stability of biocomposites is enhanced by the presence of natural fibers, due to the strong interactions between the components; hence degradation of the products is prevented<sup>12,13</sup>. The reverse phenomena is observed in other cases, where any constituent of the biocomposite which is thermally susceptible may promote earlier degradation of the overall material<sup>12,13,14</sup>. To decrease the formation of degradation products that could be released as odorous and volatile compounds during the service life of the products, contributing to poor indoor air quality, it is very important to assess the thermal stability of biocomposites

## **2.5.2 Degradation of Biocomposites**

Studies of the degradation process must be performed to assure that materials are structurally stable during their use as well as to confirm that they are biodegradable and bioassimilable without ecotoxicological properties when being disposed of. The degradation process in polymer can be classified as (i) chemical degradation (caused by chemical agents such as water (hydrolysis), oxygen (oxidation), bases or acids), (ii) mechanical degradation (by external stress), (iii) degradation by radiation (including electromagnetic and UV light exposure), (iv) thermal degradation (by temperature), or (v) biological degradation (by biological entities). Degradation studies of composite materials must be carried out in controlled environmental chambers, where the external factors can be adjusted and recorded while observing the degradation process and their effects.

### **2.5.2.1 Abiotic degradation by water absorption**

A biocomposite material's performance is reduced by water absorption and hydrothermal degradation due to the hydrophilic nature of the polymeric matrix (bio)polymer and/or the natural reinforcement. In the preparation of biocomposite materials it is important to analyse the moisture absorption phenomenon, its degradative effects, and the ways to reduce them during service life. Composites prepared from a material which was exposed to high humidity were found to suffer more damage to the interfacial strength of the final composite than those experiencing post-fabrication water exposure<sup>15</sup>. Moisture absorption depends on the hygroscopic constituents present in the biocomposite material. There are three different mechanisms through which water penetrates the composite material: (1) water molecules diffuse inside the microgaps between the polymer chains; (2) due to incomplete wettability and impregnation, capillary transport of water molecules into the gaps and flaws at the interface between polymer and fibers;

and (3) during the compounding process micro cracks are formed in matrix, and water molecules transported in to these microcracks<sup>16</sup>. There are several factors affecting the moisture absorption in biocomposite materials: fiber loading (increase in fiber content shows a rise in water absorption), the chemical nature of lignocellulosic fibers (lignin is hydrophobic and hence permits lower water absorption), fiber geometry and compatibilization between fiber and matrix (improved adhesion between fiber and matrix results in smaller and fewer microgaps where water uptake may occur)<sup>17,18</sup>. In biocomposites with a hydrophobic polymer matrix reinforced with lignocellulosic fibers, increased water absorption is expected. However, in biocomposites with a hydrophobic biopolymer as a matrix and natural fibers showed greater water resistance, due to fiber-matrix interactions that are absent in the former matrix. This was observed in starch-based composites reinforced with sisal fillers<sup>19,20</sup>.

### **2.5.2.2 Hydrothermal degradation**

Moisture absorption and its resulting hydrothermal degradation irreversibly affects the morphology and properties of lignocellulosic fibers and the polymer matrix, and severely damages the matrix-fiber interface. This leads to poor stress transfer from matrix to reinforcement<sup>21</sup>. For hydrothermal degradation, the proposed mechanism begins with water absorption by the hydrophilic constituents of the composite (matrix and/or fibers). The presence of moisture causes swelling of the reinforcement. As a result of this, stress may develop at the interface and around the swollen fibers causing matrix micro-cracks to develop. Chain reorientation and shrinkage effects also occur in the matrix structure. Moisture absorption and its resulting effects contribute to the loss of compatibility between matrix and fiber. Hydrogen bonds between the hydrophilic constituents of the biocomposite fibers and water molecules are formed, resulting in weakening and debonding of the interface adhesion<sup>18,22</sup>. Natural fiber



degradation occurs by hydrolytic mechanisms due to hydrothermal ageing. The main damage induced by water absorption is weakening of the fiber/matrix interface<sup>23</sup>.

### **2.5.2.3 Thermo- and Photo-Oxidation**

The effect of thermo- and photo-oxidation on the properties of biocomposite materials are not widely studied compared with other traditional degradative processes. This may be due to the fact that other degradative mechanisms damage the biocomposites in a more selective manner than long term oxidative exposure in a dry environment. Thomas et al.<sup>24</sup> studied prolonged exposure to elevated temperature (100°C) resulting in decrease in fiber strength. This is due to the decomposition of volatile extractables present on the surface of the fiber. Even though cellulose constituents are stable up to 160°C, thermo-oxidative reactions might occur during prolonged exposure, which leads to fiber degradation. Voids then develop in the interface and result in loss of interfacial adhesion between fiber matrix. Chemical modifications of the fiber or incorporation of bonding agents is used to increase the compatibility between fiber and matrix. This retains the mechanical properties during thermo-oxidation<sup>25</sup>. Synthetic thermoplastic reinforced with natural fibers may offer a protective effect against photo-oxidation and similarly for thermo-oxidation. Ultraviolet radiation stimulates photo-oxidation in materials and is responsible for chain breaking in the thermoplastic matrix and the surface cracks which appear in the composites<sup>26, 27</sup>. The generation of such defects and cracks can be minimized by increasing fiber load<sup>26</sup> and by increasing adhesion between the matrix and fiber<sup>28</sup> (either by the addition of compatibilizers or by fiber treatment).

## 2.6 Water absorption

The hydrophilic nature of the natural fibers plays a vital role in the ageing of biocomposites by immersion in water or in a wet atmosphere. Moisture absorption has become a big hurdle in the development of the use of the natural fibers in composite materials due to degradation and decrease in the properties of composites in wet conditions. Biocomposites used for outdoor applications need to be investigated for mechanical properties in a moist environment.

H.S. Yang et al.<sup>29</sup> proved that the PP-RHF 30wt.%-MAPP 3 wt.% biocomposite exhibited significantly less thickness swelling than the other PP-RHF bio-composites, because the MAPP chemically bonded with the –OH groups in the lignocellulosic filler and this limits the water absorption ( shown in Figure 2.3)<sup>29</sup>

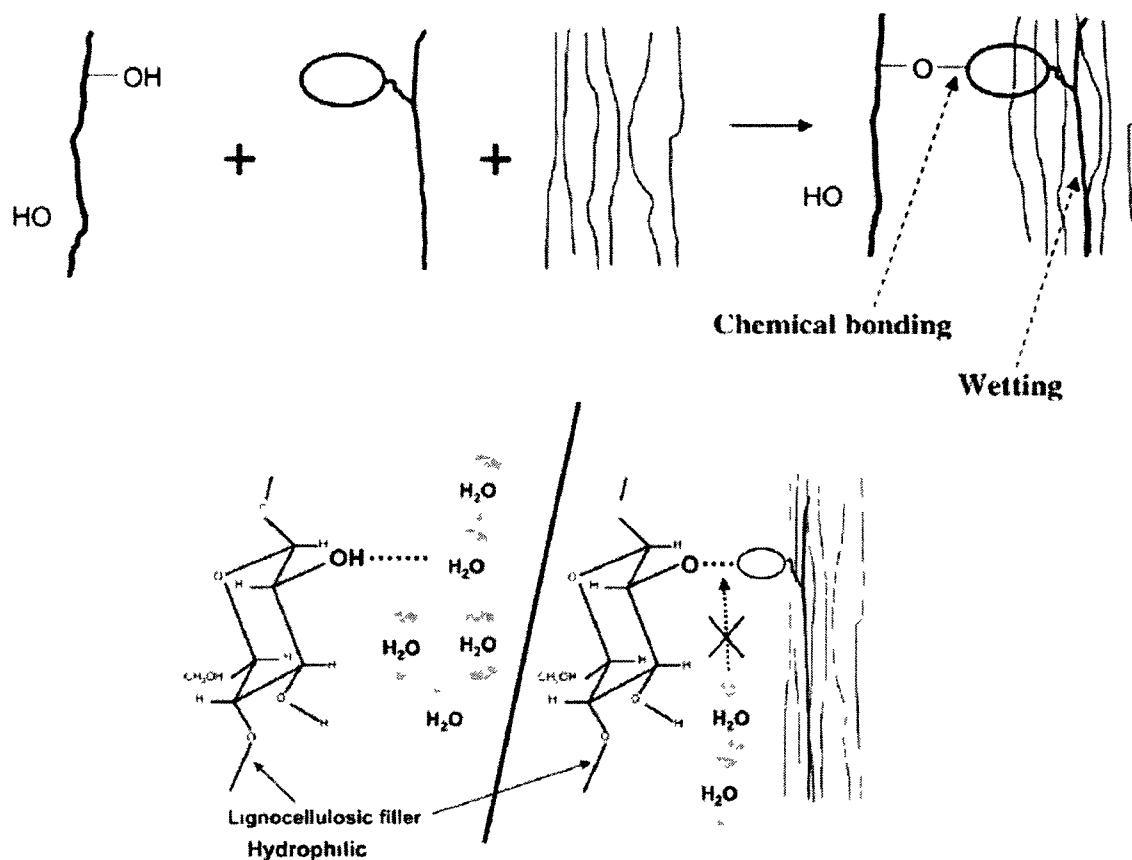
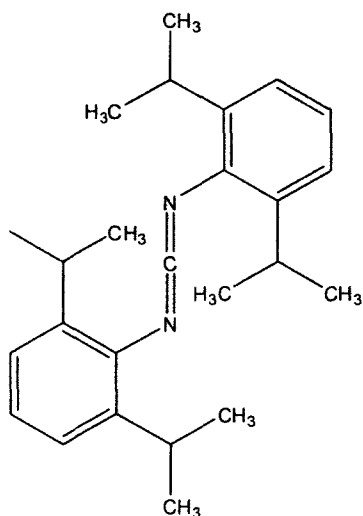
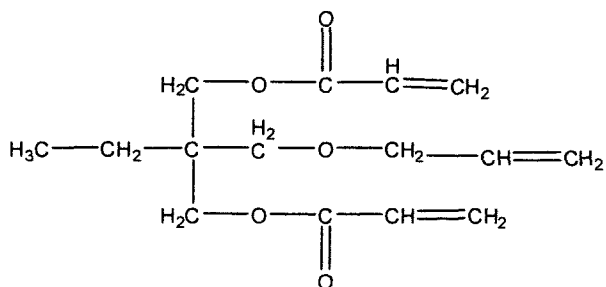


Figure 2.3. The function of the compatibilizing agent in a lignocellulosic filler-polyolefin composite system<sup>29</sup>.

The experiments carried out by Yang et al.<sup>29</sup> showed that biocomposite samples containing MAPP and MAPE showed lower thickness swelling and water absorption, that the thickness swelling and water absorption of the composites are directly proportional to the filler loadings and that the compatibilizing agents have a positive effect on the thickness swelling and water absorption. The strong interfacial bonding between the filler and matrix polymer caused by the compatibilizing agents limits the thickness swelling and water absorption of the composites.



Bis-(2,6-diisopropylphenyl) Carbodiimide



trimethylolpropane triacrylate

Figure 2.4. Chemical structures of anti-hydrolysis agent and trimethylolpropane trifunctional monomer.<sup>31</sup>

J.S.Kim et al.<sup>30</sup> used an anti-hydrolysis agent and a trifunctional monomer (Figure 2.4) to conduct a thermal analysis of degradation and hydrolysis of biocomposites and biodegradable polymers such as Polybutylene Succinate (PBS) at 50°C and 90% relative humidity (RH). They proved that addition of trimethylolpropane triacrylate and an anti-hydrolysis agent is an effective method of reducing the degradation and hydrolysis of biocomposites and biodegradable polymers under high humidity conditions.

Tajvidi et al.<sup>31</sup> prepared composites of polypropylene by using kenaf fibers, newsprint fibers, wood flour and rice hulls (25 and 50% by weight content) including 1 and 2% compatibilizers. Long-term water absorption tests were performed on these samples at room temperature for 5 weeks. From their experimental results they found that, RH/PP (rice hull / polypropylene), WF/PP (wood flour / polypropylene) exhibits minimum water absorption compared to KF/PP (kenaf / polypropylene) and NP/PP (Newsprint) composites. The composites

with higher fiber content resulted in higher water absorption, this is because of “the hydrophilic lignocellulosic fraction in a composite increases by increasing fiber content”. At longer immersion times the effect of fiber content on water absorption is more pronounced. The water diffusion coefficient of these composites found to be 3 times higher than that of pure polypropylene.

Rouison et al<sup>32</sup> conducted water absorption tests on hemp fiber/unsaturated polyester composites by exposing them to air with a relative humidity of 94% or by immersing them in water. The moisture absorption process follows a diffusion mechanism, confirmed/proved by using images obtained with a magnetic resonance imaging (MRI) system. Here the longitudinal direction diffusion method is more important than transverse direction. The longitudinal diffusion coefficient was found to be  $3 \times 10^{-11} \text{ m}^2/\text{s}$ . As the fiber content increases, the diffusion coefficient of the water in the samples increases and water absorption also increases. They conclude: the best way to lower “the rate of water absorption was to keep the fibers properly sealed within the matrix”.

Karlsson et al<sup>18</sup> have taken fibers from pine or eucalyptus wood and also one-year crops such as sisal, coir, etc. to be used in polypropylene composites preparation. Water absorption tests were studied by immersion of these composites in water at three different temperatures 70°C, 50°C and 25°C. The process of water absorption of natural fiber/PP composites was found to follow the kinetics and mechanisms described by Fick’s theory. Mechanical properties of these composites were found to be decreased by water absorption. Water-saturated composites present poor mechanical properties such as stress at maximum load and Young’s modulus values are low. Use of 3 wt% of ethylene vinyl acetate copolymer (EVA) in a PP composition shows improved resistance to water absorption. EVA is a copolymer of ethylene, which helps in

adhesion to PP matrix, the acetate groups in EVA bond to hydroxyl groups on fibers and by this, compatibility between fibers and matrix is improved.

## **2.7 Chemical Effect on Biocomposites**

### **2.7.1 Natural fibers**

Natural fibers are hydrophilic in nature. These fibers are obtained from lignocellulose and contain polar hydroxyl groups. These fibers are incompatible with hydrophobic polymers, such as polyolefins (PP, PE). There are several limitations for natural fibers as reinforcements with polymer matrix, such as (1) poor interfacial adhesion between the nonpolar hydrophobic polymer matrix and polar hydrophilic fiber, (2) orientation of the fibers (during the composite preparation fibers orient along the flow direction of the matrix, and hence vary in mechanical properties in different directions), and (3) Fiber dispersion (poor dispersion of fibers results in a loose bundle, which will show less reinforcing potential than a single fiber). In order to develop strength in a composite material, there should be a strong interface between the fiber and matrix. When a load is applied externally on the surface of the matrix, this load will be transferred to the fibers on the surface and continue from fiber to fiber through the matrix. If the fiber-matrix interface is poor then the load distribution is not effectively achieved, and thus the composite material demonstrates poor mechanical properties. However, a strong interface between fiber and matrix can assure that the composite is able to bear the load and, even if several fibers are broken, the load applied on the interface of a composite can be transferred to the intact portions of unbroken, as well as broken fibers. For any composite material a poor interface is always a drawback, e.g. when the composite is subjected thermal stress, premature failure can occur at a weak interface because of differential thermal expansion of the fibers and matrix. Hence, adhesion between

matrix and fibers is an important factor in determining the response of the interface and its integrity under stress.

A lignin and hemicellulose matrix helps hold hollow cellulose fibrils together, hence natural fibers can be considered as composites.<sup>33</sup> Figure 2.5 shows that the fiber cell wall is not a homogenous membrane<sup>34</sup>. Each fiber consists of primary and secondary walls. The primary wall is thin and it is the first layer formed during cell growth. The fiber's secondary wall made up of three layers. The mechanical properties of the fibers can be determined by the thick middle layer of secondary wall. The middle layer of the secondary wall consists of a series of cellular microfibrils (helical in nature). These cellular microfibrils are formed from long chain cellulose molecules. Each microfibril has a diameter in the range of 10-30nm and they are made up of 30-100 cellulose molecules and give mechanical strength to the fibers. The amorphous matrix phase in a cell wall consists of lignin, hemicellulose and in some cases (pectin).

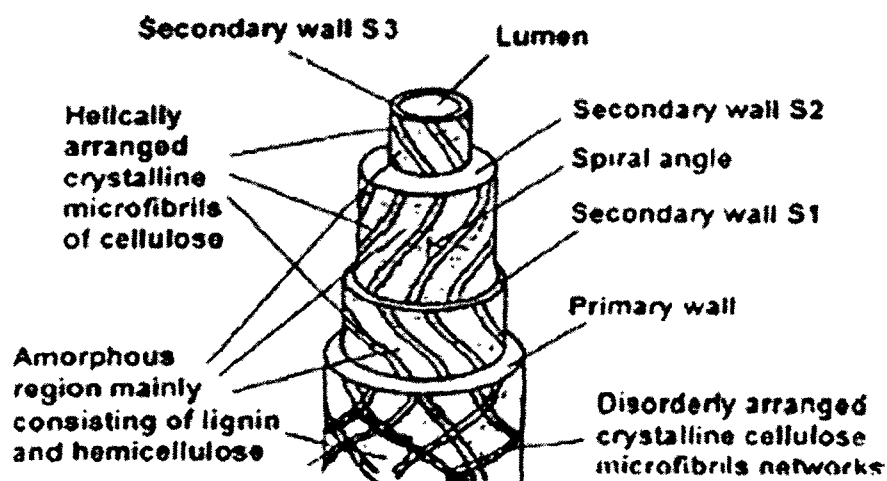


Figure 2.5. Structure of Biofiber.<sup>35</sup>

The cellulose molecules are hydrogen bonded with hemicellulose. This acts as cement matrix between the cellulose microfibrils and forms the hemicellulose-cellulose network. Lignin is

hydrophobic in nature, its network acts as a coupling agent causing the cellulose/hemicellulose composite stiffness to increase.

## **2.7.2 Mechanism of Chemical modifications**

Surface modification of composite materials includes: (1) physical treatment (such as extraction of solvent), (2) physical-chemical treatment (such as the use of plasma and corona discharges<sup>36</sup>, (3) and chemical modifications (direct condensation of the cellulose surface with coupling agents or by its grafting by ionic or free-radical polymerization).

A few common chemical treatments adopted for natural fibers explained below.

### **2.7.2.1 Alkali treatment**

There is an increase in the amount of amorphous cellulose at the expense of crystalline cellulose in alkali treatment. Removal of hydrogen bonds in the network structure is the important modification in alkali treatment.

Alkali treatment reaction:



Cellulose fibers undergo a swelling reaction as a result of alkali treatment. The natural crystalline structure of the cellulose relaxes during this time. Figure 2.6 shows alkali-cellulose and cellulose-II forms. KOH, LiOH and NaOH are different types of alkali chemical used for alkali treatment. Na<sup>+</sup> are able to widen the smallest pores in between the lattice planes and enter into them. Therefore when treated with NaOH a higher amount of swelling was observed. This leads to the formation of a lattice (Na-Cellulose-I) with relatively large distances between the cellulose molecules and water molecules. There is an increase in the dimension of the molecules



in this structure due to -OH groups of the cellulose being converted to -ONa groups. The linked Na-ions were removed by rinsing with water which converted the cellulose to cellulose-II (is a new crystalline structure). Thermodynamically cellulose II is more stable than cellulose I. From cellulose I to cellulose II a complete lattice transformation can occur using NaOH. Figure 2.6 shows that other alkalis produced only partial lattice transformation. The alkali solutions also influence the noncellulosic components such as hemicellulose, lignin and pectin<sup>37</sup>.

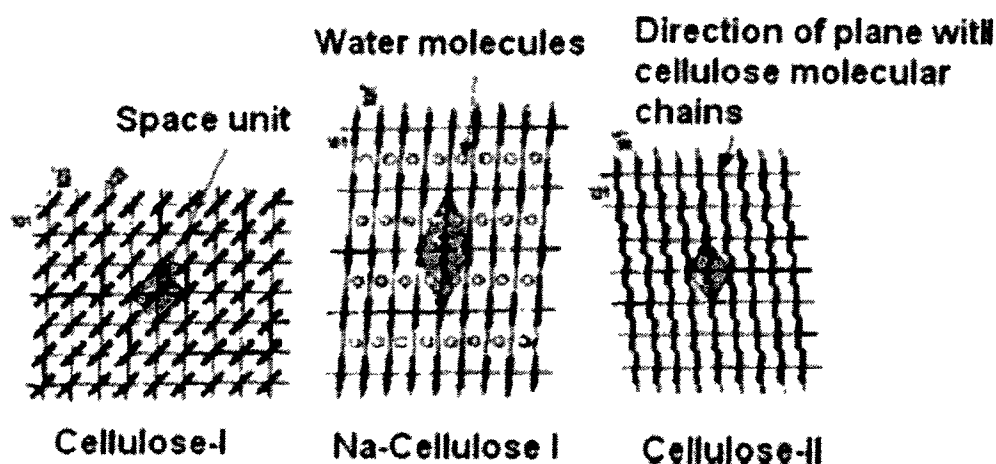
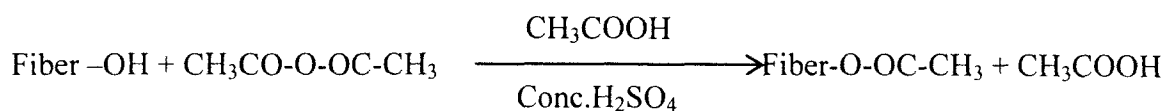


Figure 2.6. Lattice structure of Cellulose I and Cellulose II.<sup>37</sup>

### 2.7.2.2 Acetylation

One of the important methods used to modify the surface of natural fibers is acetylation. The main principle of the method is that acetyl groups ( $\text{CH}_3\text{CO}$ ) reacts with the hydroxyl groups (OH) of the fibers and make the fiber surface more hydrophobic. The hydroxyl groups of natural fibers in the crystalline regions are closely packed with strong interchain bonding and are inaccessible for chemical reagents. The following reaction represents the acetylation of the -OH group in cellulose.



Acetylation proved to be beneficial in reducing water absorption of fibers. The acetylated jute fibers and pine fibers have shown reduction in moisture absorption by 50% and 65%, respectively<sup>38</sup>. The interface between flax fiber and PP composites was found to be increased by Acetylation<sup>39</sup>

### **2.7.2.3 Silane Treatment**

With silane chemicals, different groups attached to one end of the silicon react with the hydrophilic fiber and the other end reacts with matrix silicone. This acts as a bridge between them. There are a number of factors depends on uptake of silane such as temperature, pH, hydrolysis time and organofunctionality of silane. Silanols reacts with hydroxyl groups of the fibers and form poly-siloxane structures<sup>40</sup>. Figure 2.7 shows the chemical reaction of silane treatment.

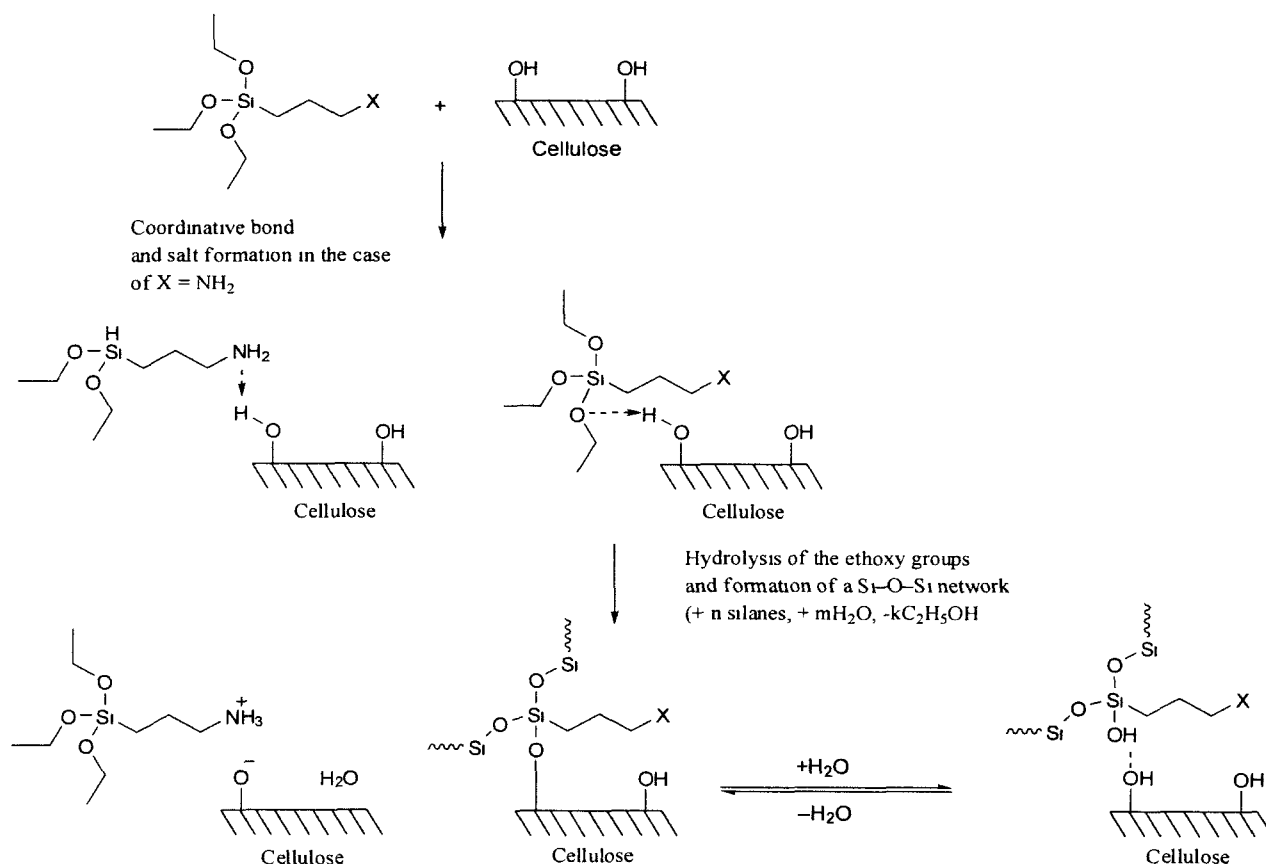


Figure 2.7. Scheme of interaction of silanes with cellulosic fibers.<sup>41</sup>

Amino silane molecules react with the hydroxyl groups of cellulose through the Bronsted basic amino groups. Herrera-Franco et al.<sup>42,43,44</sup> investigated the properties of henequen fiber-reinforced polymer composites by using different silane coupling agents. These authors proved that the reaction between silanes and cellulose takes place only at temperatures above  $70^\circ\text{C}$  by using FTIR and XPS spectroscopy.

### **2.7.3 Chemical Modification Characterization of Natural fibers**

Chemical modifications of natural fibers are amenable due to the presence of –OH groups. These –OH groups within the cellulose molecule may form hydrogen bonds. New moieties can be introduced by activating these groups that form an effective interlocking system. Chemical modifications of fibers can improve surface characteristics such as adhesion, wetting, surface tension and porosity. Some of the work on fiber modifications are cited below.

#### **2.7.3.1 Aspen Fiber composites**

Xue et al.<sup>45</sup> studied the effect of maleic anhydride-grafted polypropylene (MAPP) as a coupling agent on the mechanical properties of aspen fiber/PP composites. Adhesion between the matrix and fibers improved with the coupling agent, further more tensile properties of these composites increased. By using a compatibilizer, the flexural and tensile strength increase by 15% and 40%, respectively. Colom et al.<sup>46</sup> investigated the interfacial characteristics of aspen-HDPE composites by using different chemical modification methods. The addition of two coupling agents such as  $\gamma$ -methacryloxypropyl trimethoxy silane (Silane A-174) and maleated polyethylene (epolene C-18) improved interaction between aspen fibers and HDPE. The authors proved that silane A-174 was a better compatibilizer than epolene. This indicates that when these composites are modified with epolene coupling agent, adhesion occurs due to multiple mechanisms of interdiffusion and adsorption, while the silane-treated composites showed a chemical mechanism of adhesion with the formation of hydrogen bridges and also covalent bonds. This increases the adhesion between the matrix and fiber.

#### **2.7.3.2 Bagasse fiber Composites**

Zheng et al.<sup>47</sup> investigated the effect of benzoic acid chemical modifications on bagasse fibers in polyvinyl chloride composites. The tensile strength increased by 35% in modified

composites, which indicates better reinforcement. The tensile strength was found to be 38 MPa for untreated fibers containing composites, whereas for modified fibers containing composites, it was found to be 52 MPa. Cao et al.<sup>48</sup> investigated the effect of alkali treatment on the mechanical properties of bagasse fiber-reinforced polyester composites. 1, 3 and 5% concentrations of NaOH were used for chemical modification. Composites made from 1% NaOH-treated bagasse fibers were found to have superior properties. Due to the chemical modifications, these composites showed 14% improvement in flexural strength, 13% in tensile strength and 30% in impact resistance.

### **2.7.3.3 Coir fiber composites**

Brahamakumar et al.<sup>49</sup> investigated the influence of the natural waxy surface layer of coir fiber-reinforced PE composites. To determine the effect of the waxy layer on interfacial bonding between the fiber and matrix, surface-modified coconut fibers were obtained by grafting an isocyanate derivative of cardanol (CIDIC). Coconut fibers with wax-free surface were also used. The coconut fiber's natural waxy surface layer provides a strong interfacial bonding between the fiber and polymer matrix. Removal of the natural waxy layer of the coir fiber resulted in a poor interfacial bonding and decreased the composite modulus and tensile strength by 60% and 40% respectively. Due to the polymeric nature of the wax layer, there was a large difference in matrix/fiber bonding as compared to that of a grafted layer of a C15 long alkyl chain molecule onto the wax-free fiber.

Nam et al.<sup>50</sup> developed poly(butylene succinate) (PBS) biodegradable composites reinforced with coir fibers. The authors investigated the effect of alkali treatment on the mechanical properties and surface morphology of coir fibers, as well as the mechanical properties and interfacial shear strength (IFSS) of coir fiber/PBS composites. The coir fibers

treated with 5% NaOH solution for 72 hrs at room temperature showed a IFSS increase of 55.6%. Alkali-treated coir fibers increased the wettability and the interfacial bonding strength of the fibers with PBS resin which lead to an improvement in the mechanical properties of the composites. Increasing fiber content up to 25% increases the mechanical strength and modulus of the composites. Increases above 25% fiber content in composites showed decrease in modulus and tensile strength.

#### **2.7.3.4 Flax fiber composites**

Weyenberg et al.<sup>37</sup> studied the effect of alkali treatment on flax fibers. The authors mainly concentrated on optimizing parameters such as concentration of NaOH and time, in order to develop a continuous process for the fabrication and the treatment of unidirectional flax fiber-epoxy composites. The transverse strength of the composites increased by 30% when the material was treated with 4% NaOH solution for 45s.

Elsabbagh et al.<sup>51</sup> investigated the effect of NaOH solution on the properties of flax fibers and the matrix. Trimethoxyvinyl silane (TMVS) and acrylic acid (AA) were used to treat a selected groups of fibers. The PP matrix is functionalized with liquid TMVS, AA and maleic anhydride (MA). As a result, the coupling agents of TMVS, AAPP and MAPP are formed. The stiffness of modified AAPP matrix increased fourfold compared to that of untreated flax/PP composites. Lower water absorption values and improved mechanical properties were observed for a MAPP-modified matrix. NaOH-TMVS/TMVS-MAPP and NaOH/MAPP show 300% and 285% increase in stiffness at 40 %wt, respectively. Modification by MAPP is considered superior in impact resistance and water absorption. A significant difference between matrix treatments on the tensile strength is difficult to detect. Considering the surface modification of the fiber, TMVS was well known for strength and stiffness, while NaOH washing was enough

considering water absorption and impact. NaOH-TMVS/AAPP and NaOH-TMVS/MAPP systems proved their applicability as compared to the classical NaOH/MAPP system.

### 2.7.3.5 Ramie fiber composites

Chem et al.<sup>52</sup> showed the effect of surface treatment of biocomposites based on Poly(L-Lactic Acid) (PLLA) and ramie fiber. Ramie fiber absorbs less water compared to jute, kenaf, sisal, hence it was a preferable reinforcing material. Dynamic mechanical analyzer (DMA) results showed an increase in storage modulus of treated PLLA (Figure 2.8) Ramie fiber treated with permanganate acetone solution (KFAB) and ramie fiber treated with permanganate acetone solution and silane solution (KsFAB)) compared to untreated PLLA. After UV irradiation, a hydrothermal aging test on treated PLLA (KFAB and KsFAB) showed at good mechanical properties were not maintained. The reason for this is that the high water absorption of KFAB and KsFAB can accelerate the water permeation rate in PLLA biocomposites. This plays a key role in the decline of interfacial adhesion strength of KsFAB/PLLA.

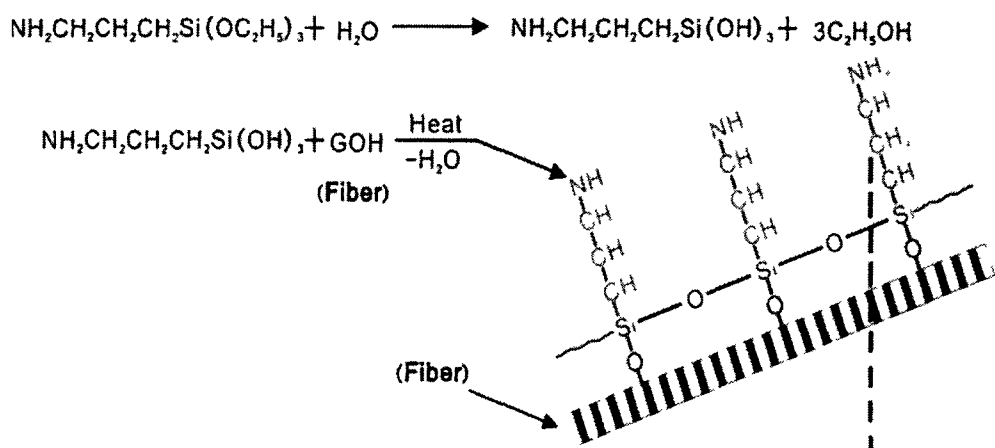


Figure 2.8. Hypothetical reaction of Silane with KFAB.<sup>52</sup>

## 2.8 Fourier transform infrared spectroscopy

The Fourier transform infrared spectroscopy (FTIR) technique is used to characterize the surface of a fiber. From this, interfacial adhesion information can be obtained<sup>53</sup>. George et al.<sup>54</sup> used an IR (infrared) technique to characterize the interface and modified fiber surface of the pineapple leaf fiber PE (poly ethylene) composites. Colom et al.<sup>46</sup> conducted different chemical modifications on aspen fibers to study the interfacial characteristics of aspen fiber reinforced with HDPE composites. With the addition of two coupling agents,  $\gamma$ -methacryloxy-propyl trimethoxy silane (silane A-174) and maleated PE (epolene C-18) to the above composites, the interaction between aspen fibers and HDPE was found to be improved. The lowest absorbance value corresponds to the composites modified with maleated polypropylene (PPMA) and the highest value to that of untreated composites. FTIR was used to examine the interface of wood fibers reinforced with PP composites by Hristov and vasileva<sup>55</sup>. The authors modified polypropylene matrix with poly (butadiene styrene) rubber and PPMA. From the FTIR spectra of the treated composites they confirmed that the coupling agent was attached to the wood fibers either by hydrogen or ester bonds.

Mwaikambo and Ansell<sup>56</sup> studied chemical modifications of different fibers using different microscopic and spectroscopic methods. One of the techniques was FTIR: this was used to analyse sisal, jute, kapok and hemp fibers after treatment with NaOH. Kapok fiber was found to be the most reactive among the fibers, followed by jute, sisal and hemp. Adhesion between fiber and resin was improved by alkalisation, thereby increasing the thermal and mechanical stability of the composites. Wong et al.<sup>57</sup> studied the influence of 4,4' -thiodiphenol (TDP) on the interfacial properties of flax fiber reinforced with poly(3-hydroxybutyrate). The added TDP



forms hydrogen bonds with various functional groups. Hydrogen bonding in the composite, as revealed by FTIR, brought beneficial changes in the mechanical properties of the composite.

Kim et al.<sup>58</sup> analysed chemically treated natural wood fiber (lignocel C120) by FTIR spectroscopy. This gave clear evidence of crystalline structure transformation in observing a wave number shift from Cell-I to Cell –II. Using NaOH treatment and attachment of benzoyl or silane coupling agents, they confirmed the transformation of crystalline cellulose structure in wood fiber with FTIR spectra.

The FTIR technique advantage is less experimental complexity, further more interpretation of the spectrum is simplified. FTIR is more precise than the infrared technique. The disadvantages of the FTIR technique are lower sensitivity than infrared and need to use compact samples.

## **2.9 Mechanical Properties**

Bledzki et al.<sup>59</sup> studied the effect of reinforcing poly(3-hydroxy butyrate-co-3-hydroxy valerate) (PHBV) and Polylactic acid biopolymers on the mechanical properties. PLA and PHBV both are reinforced with jute, abaca and man-made cellulose fibers. The results of these biopolymer composites were compared with the polypropylene(PP) composites which have the same reinforcing fibers. The biopolymer composites showed an increase in strength (>50%), stiffness and notch impact strength (>250%) compared to common natural fiber reinforced polypropylene. Due to the advantageous geometry and good mechanical performance, man-made cellulose proved to be a favorable reinforcing fiber. Sawpan et al.<sup>60</sup> studied mechanical properties of PLA composites reinforced with chemically treated aligned long fiber and random short hemp fiber were investigated over 0-40 wt% range of fiber content. Short hemp fiber

reinforced PLA composites showed an increase in impact strength, Young's modulus and tensile strength with increased in fiber content (10-30%)

### **2.9.1 Effect of Water Absorption on Mechanical Properties of Biocomposites**

Tajvidi et al.<sup>61</sup> studied the mechanical properties and water absorption behavior of polypropylene composites containing three different types of natural fillers such as wood flour, waste paper fibers and purified  $\alpha$ -cellulose. The samples were prepared with fiber contents 15, 25 and 35% by weight and 2% maleic anhydride polypropylene (MAPP) is added to these samples as a compatibilizer agent. Water absorption by cellulose fibers/PP composites is found to be lower than the paper fibers and wood flour composites. The reason for lower water absorption is the better interaction of fibers with the polymer matrix which leads to better coverage of the fibers by the polymer. This result disagrees with the literature.<sup>62</sup> Composites with 15% filler of any type show sharp reduction in the values of elongation at break and there is no significant change in the values between 25 and 35% filler contents. Tensile strength for 15% fiber content of any type decreased slightly but generally increased by addition of more fibers. As the fiber content increased in the composites, the modulus of elasticity also increased. There is no significant difference in the values of modulus at 35% fiber content of any type. Energy at the proportional limit is reduced as the fiber content increased in the samples.

Bledzki et al.<sup>63</sup> studied the potential of grain by-products such as rye husk or wheat husk as reinforcement for composite materials and as an alternative to softwood fibers. Rye husk and wheat husk are thermally stable as low as 210°C and 235°C, respectively. Wheat husk and rye husk contains 45% and 43% proportions structural polymers (cellulose and starch), respectively, whereas softwood contains 42%. Wheat husk and rye husk were found to have a carbon-rich surface compared to softwood fibers. More surface silicon was found in wheat husk than

softwood fiber. A 15% better charpy impact strength was shown by wheat husk composites than softwood composites. 110% better elongation was shown by rye husk at break as compared to soft wood composites.

## 2.10 Thermal properties

When a composite is manufactured, the behavior of the natural fiber as well as the physical properties of the natural fiber contained in a composite can be affected by temperature. The main obstacle in the preparation of biocomposites is the low thermal stability of natural fibers. To avoid the degradation of natural fibers, the temperature for processing was kept below the natural fibers' degradation temperature. The degradation of natural fibers leads to poor mechanical integrity and brittleness of the thermoplastic composites. Ng<sup>64</sup> reported that natural fiber degradation is undesirable and the results include decrease in mechanical strength, rise in brittleness and the biocomposites darken.

Thermogravimetric analysis (TGA) is the most commonly used technique to investigate the thermal stability of natural fibers. In this method, a specimen is heated up in a helium or nitrogen environment and is thermally oxidized or decomposed. The degree of decomposition can be calculated from the sample weight loss compared to the reference, corresponding to the temperature. Lee et al.<sup>65</sup> used red algae (*Gelidium Elegance*) fibers as a reinforcing material in poly(butylene succinate) to fabricate biocomposites and also studied the effect of reinforcement content on the thermal properties in terms of thermal expansion and thermal stability. Fibers from red algae were generated effectively by extracting and bleaching processes. The bleached red algae fiber (BRAf) showed thermal and crystalline properties similar to crystalline cellulose.

Higher thermal stability, with the maximum thermal decomposition temperature 356.6°C, was shown by bleached red fiber compared to that of crystalline cellulose.

Kim et al.<sup>66</sup> studied the interfacial adhesion mechanical and thermal properties of biocomposites treated with CAs. The dynamic storage modulus ( $E'$ ), values of maleic anhydride-grafted poly(lactic acid) (PLA-MA) and maleic anhydride-grafted poly(butylene succinate) (PBS-MA) treated biocomposites slightly increased as well as the  $T_g$  (glass transition temperature) values of PLA-MA and PBS-MA treated biocomposites as compared to untreated composites. The heat deflection temperatures (HDT) of PLA-MA- and PBS-MA-treated biocomposites were found to be greater than the maleic anhydride-grafted polypropylene (MAPP) and untreated maleic anhydride-grafted poly(styrene-*b*-ethylene-co-butylene-*b*-styrene) triblock copolymer (SEBS-MA) treated biocomposites. The use of MA-grafted polymer matrix as a CA in biocomposites improves the mechanical and thermal properties as well as increases the interfacial adhesion of fiber/matrix.

Rosa et al.<sup>67</sup> studied the thermal and mechanical properties of starch/EVOH/coir biocomposites. Coir fibers are treated by three different methods: alkali treatment (mercerization), washing with water, and bleaching. These chemically modified fibers are incorporated into starch/ethylene vinyl alcohol copolymer (EVOH) blends. Washing, mercerization and bleaching treatments removed impurities on the surface of the fibers, produced modifications on the fiber surface and improved thermal stability of both fiber-reinforced biocomposites and fibers. Treated fibers showed moisture release at higher temperatures because of the improved wetting of the finely separated coir fibers by polymer matrix.

Bhat et al.<sup>68</sup> studied mechanical, physical and thermal properties of hybrid biocomposites prepared from oil palm trunk (OPT) and oil palm empty fruit bunch (EFB). 450 and 250 g/m<sup>2</sup> of urea formaldehyde (UF) were used as gluing agent in the preparation of the above hybrid composite. The hybrid biocomposites with a glue spread level of 450 g/m<sup>2</sup>, showed better thermal stability than plywood with a glue spread level of 250 g/m<sup>2</sup>. Moriana et al.<sup>69</sup> studied the improved thermal stability of starch-based thermoplastic biocomposites (Mater-Bi KE 03B1) by the addition of three different natural fibers, hemp, kenaf and cotton and the compatibilization between matrix and natural fibers through morphological and viscoelastic properties. Pure Mater-Bi KE natural fibers act as thermal stabilizer, by increasing the activation energy and the thermal stability associated to the thermal decomposition process. Kenaf and hemp fibers showed better interfacial adhesion with pure Mater-Bi KE, due to the compatibilizer effect of partly lignin and hemicellulose with both the synthetic polyester and thermoplastic starch contained in the polymeric matrix. Therefore, kenaf and hemp fibers act as better thermal stabilizers than cotton fibers for pure Mater-Bi KE. Cotton fibers provided the lowest decrease in the thermal expansion coefficient associated with the glass transition and the highest increase in the modulus.

## Chapter III

### 3. Materials and Methods

#### 3.1 Materials

WPC is a commercial composite that consist of HDPE and wood flour. Biocompsite material provided by University of Guelph is a true Biocompsite consisting of biopolymer and 30% switchgrass fibers. The composition of switchgrass is 37% cellulose, 29% hemicellulose, 19% lignin.

#### 3.2 Water absorption

WPC and switchgrss/biopolymer composite were used to observe the water absorption at different temperatures (20°C, 30°C and 70°C). Samples were dried prior to the test in a desiccator for 24hr. These samples were first weighed ( $W_0$ ), then immersed in distilled water at different temperature in water bath. At certain time intervals these samples were removed from the water and dried with filter paper to remove the water on surface of composites and weighed ( $W_t$ ). The amount of water absorbed by the composite and WPC was calculated by the weight difference between the samples immersed in water to the dry samples. The total water absorption was calculated by using following equation.

$$WA (\%) = \frac{W_t - W_0}{W_0} \times 100\% \quad (1)$$

#### 3.3 Diffusion coefficient (D)

Diffusion coefficient ( $D$ ) was calculated using the following equation from the initial slope of the plot of  $M_t/M_m$  against  $\sqrt{t}$  (time).<sup>18,32</sup>

$$\frac{M_t}{M_m} = \frac{4}{h} \times \left( \frac{D}{\pi} \right)^{0.5} t^{0.5} \quad (2)$$

where

$M_t$  = moisture content at time,

$M_m$  = moisture content at equilibrium,

$h$  = thickness of the sample,

$t$  = soaking time.

The  $M_m$  values were taken from the water absorption vs. time graphs for certain material and temperature.  $M_m$  (maximum water absorption) was calculated as the average value from a series of measurements that showed no additional moisture absorption. The importance of measuring the diffusion coefficient is that it gives a measure of the rate of water absorption

### 3.4 Density Determination

A Sartorius analytical tool was used to determine the density of WPC and switchgrass/biopolymer composite samples. The Archimedeian principle was applied to determine the density of these composite materials. Density ( $\rho$ ) was calculated using the following equation.

$$\rho = \frac{W(a) \cdot \rho(fl)}{W(a) - W(fl)} \quad (3)$$

where

$W(a)$  = weight of the solid in air,

$W(fl)$  = weight of the solid in liquid,

$\rho$  (fl) = density of the liquid,

$\rho$  = specific gravity of the liquid.

In this method the mass of the sample measured in air and then immersed in distilled water. When a sample is immersed in water, water is subjected to the force of buoyancy. The value of this force is equal to the weight of the water displaced by the volume of the sample. When a composite material is submerged in water air bubbles may appear on the surface of the specimen. These air bubbles acts as a part of the sample and displaces additional water. This will increases the volume of the material. All air bubbles should be removed thoroughly from the surface of the sample for proper measurement. If not, there will be an error in measured mass of the sample and the calculated density.

### 3.5 Thickness Swelling Determination

Dimensional stability was determined by measuring the thickness of the samples as a function of their exposure to water. The samples were soaked in water at different temperatures until they reach equilibrium. The thickness swelling of the WPC and switchgrass/biopolymer composite material was calculated using the following equation.

$$G\% = \left( \frac{h_2}{h_1} \right) \times 100 \quad (4)$$

where

G% = thickness swelling of the sample,

$h_2$  (mm) = thickness swelling of the sample at time,



$h_1$  (mm) = thickness of the dry sample.

### **3.6 Dehydration**

WPC and switchgrass/biopolymer composite material were stored in distilled water at room temperature for 360hrs (reaches equilibrium) and then dehydrated for 1152hrs (room temperature). Weight of these samples periodically measured. The moisture content in WPC and switchgrass/biopolymer composite materials at specified time intervals were plotted versus dehydration time to observe the trend of moisture removal. Equation no. 1 was used to calculate moisture content in the samples.

### **3.7 Scanning Acoustic Microscopy**

Scanning acoustic microscopy (SAM) is helpful in material characterization. The ultrasonic testing method is based on transmission of high-frequency elastic sound waves through the sample. There are several configurations of the acoustic microscope based on shape of the ultrasonic signal and the type and relative position of the transducers. Ultrasonic testing primarily consists of two methods: (1) the pulse-echo method, (2) the through-transmission method. In the pulse-echo test method, a transducer emits a pulse of ultrasonic signal and detects the echo reflections. This method is especially useful for imaging the internal structure of a material. The transducers used in this method stimulate the “spike” of a high-voltage pulse for a period of 5-20ns and produce one or two periods of the acoustic wave. The ultrasonic sound waves penetrate through the coupling liquid into the material and reflect back from the voids and boundaries. The reflected sound wave is received by the transducer which converts it into an electrical signal with the voltage corresponding to the amplitude. After amplification, the

acoustic signal received by the transducer is digitized and stored in the computer memory for further analysis (Figure 3.1).

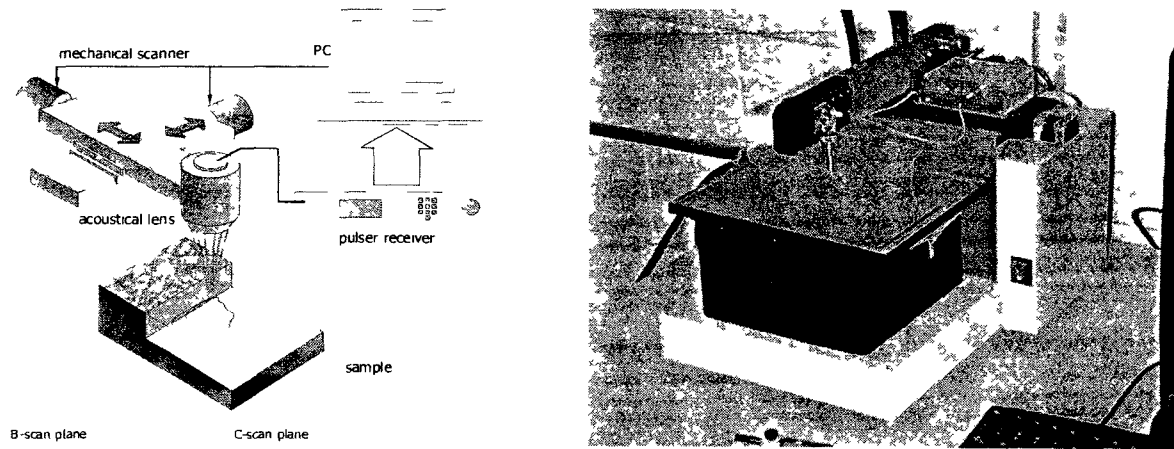


Figure 3.1. Schematic representation of (a) the principle of acoustic scanning (b) scanning acoustic microscope

Acoustic B-scan (Figure 3.2) is a 2-dimensional image, which is obtained by assembling several oscillograms. These oscillograms are collected in equidistant positions of the transducer along a straight line. Both the position of transducer (along one axis) and the time delay from the initial pulse (second direction) are related to each pixel position. Amplitude of the received signal is proportional to the brightness of the pixel. B-scans represent a vertical cross section of the sample, which can be obtained when transducer moves in one-dimension.

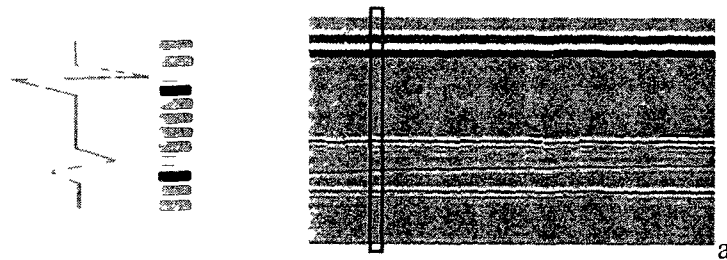


Figure 3.2. Schematic representation of the acoustic image formation (a) B-scan

B-scans are specifically useful to evaluate the depth-dependent material structure. Acoustic data from the sample volume can be collected when the transducer moves in two-dimensions parallel to the sample surface. A set of B-scans combined into three-dimensional cube of data is formed by multiple lines of mechanical raster scanning. C-scans (horizontal-cross section) represent the distribution of reflective properties of the materials at given depth. As a two-dimensional function of the transducer position, the C-scan is formed by the plotting of signal maximum inside the user-defined time window.

A focused transducer (acoustic lens) is the main part of acoustic microscope. Figure 3.3 shows an acoustic lens consisting of a buffer cylinder. The buffer cylinder is made from fused quartz with an attached piezoelement. The buffer has a spherical concave surface on the outer side. Which provides focusing of the acoustic beam. Plane acoustic waves generated by the transducer travel through the buffer and refract towards the focus when they cross the spherical surface.

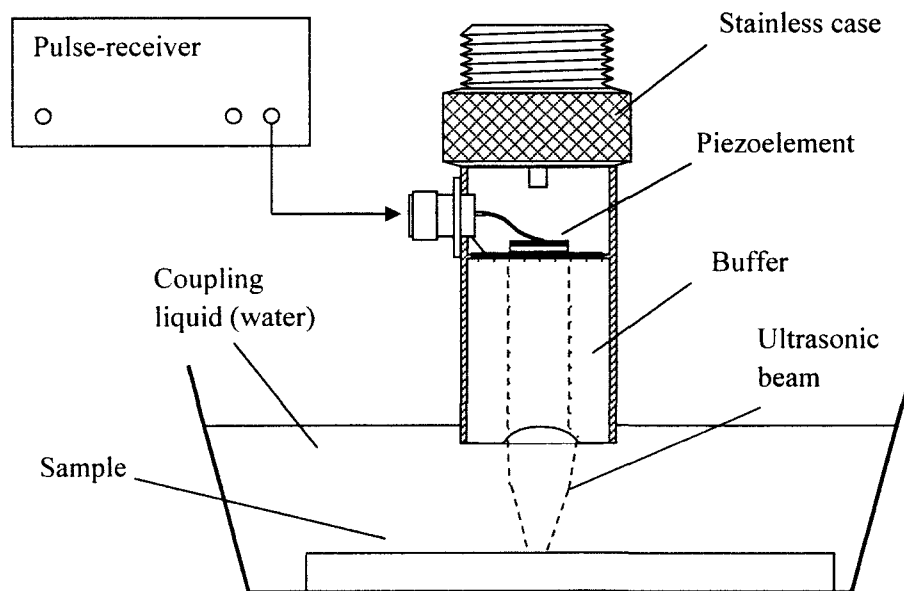


Figure 3.3. Schematic image of the acoustic lens.

The acoustic lens and the surface of the sample are coupled through an immersion medium. High impedance mismatch between the material and air can be reduced by using a coupling material. There are few cases where the use of immersion medium (couplant) can damage the sample (e.g. textiles, fiber webs or water sensitive samples). In scanning acoustic microscopy resolution depends on both the acoustic hardware and the material properties. The resolution of the ultrasonic microscopy method is capable of distinguishing two close reflectors on the C-scan (lateral resolution) and on the A-scan (axial resolution). These two values are proportional to the central frequency of the wave for the short pulse signal.

The Rayleigh criteria states that “the images of two points may be considered resolved if the principle diffraction maximum of one falls exactly on the first diffraction minimum of the other”. According to the above statement and Kino notes<sup>70</sup>, by using a focal spot size and Airy radius lateral resolution can be determined.

$$r_{Airy} = \frac{0.51\lambda}{\sin \theta} = \frac{0.51c}{f} \frac{F}{N.A} \quad (5)$$

The ideal numerical aperture has never been realized in practice. For focused acoustic waves, SAM uses a frequency range of 3MHz-2GHz, in this spatial resolution is limited to a few microns. By increasing the frequency an increase in acoustic image resolution cannot always be achieved, because the square of this frequency is proportional to the attenuation of the ultrasonic wave. Thus, when a sufficiently high frequency wave is used as a probe, it may not be possible to obtain information from the interior part of the sample as the wave may not penetrate far enough inside the specimen. Using attenuation in the coupling fluid the highest frequency level  $f$  is determined.

$$f \leq \sqrt{\frac{\alpha_{acc}}{2\alpha_0 q}} \quad (6)$$

where

$\alpha_{acc}$  = acceptable attenuation in the coupling media,

$\alpha_0$  = specific attenuation in liquid per Hz of acoustic frequency,

$q$  = focal length (proportional to velocity).

The resolution coefficient  $R_c$  is equal to

$$R_c = \sqrt{(C_0 \alpha_0)} \quad (7)$$

The smaller  $R_c$ , the better resolution can be achieved at shorter wavelength.

### 3.8 Pulse-echo Technique

From the transducer (Figure 3.4) a pulse is sent into the material. This pulse is reflected by the front and back surfaces of the specimen. The transducer receives the returned pulse at reduced amplitude. A recording oscilloscope is used to monitor the waveforms. From the amplitude and timing of the reflected waves, the attenuation (equation 9) and sound speed (equation 8) of the material can be determined.

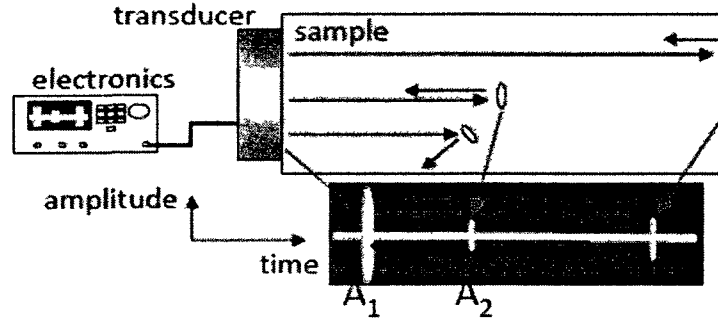


Figure 3.4. Schematic representation of the principle of pulse-echo method.

$$C = \frac{2h}{\Delta t} \quad (8)$$

where

h = thickness of the sample,

Δt = Time of flight.

$$\alpha = \frac{1}{2h} \ln \left( \frac{A_1}{A_2} \right) \quad (9)$$

where

h = thickness of the sample,

A<sub>1</sub> and A<sub>2</sub> = Amplitude of the signal,

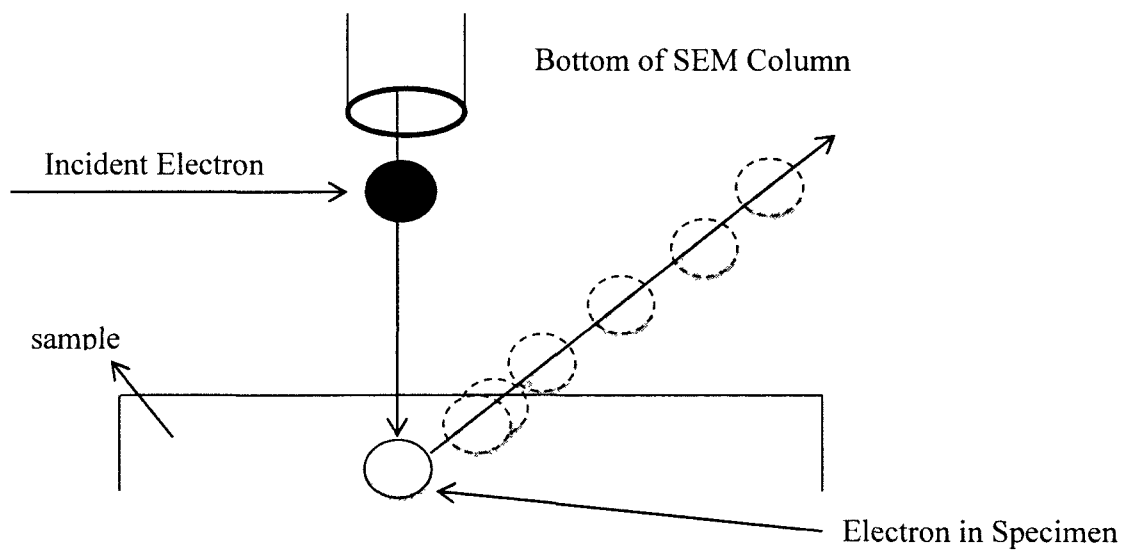
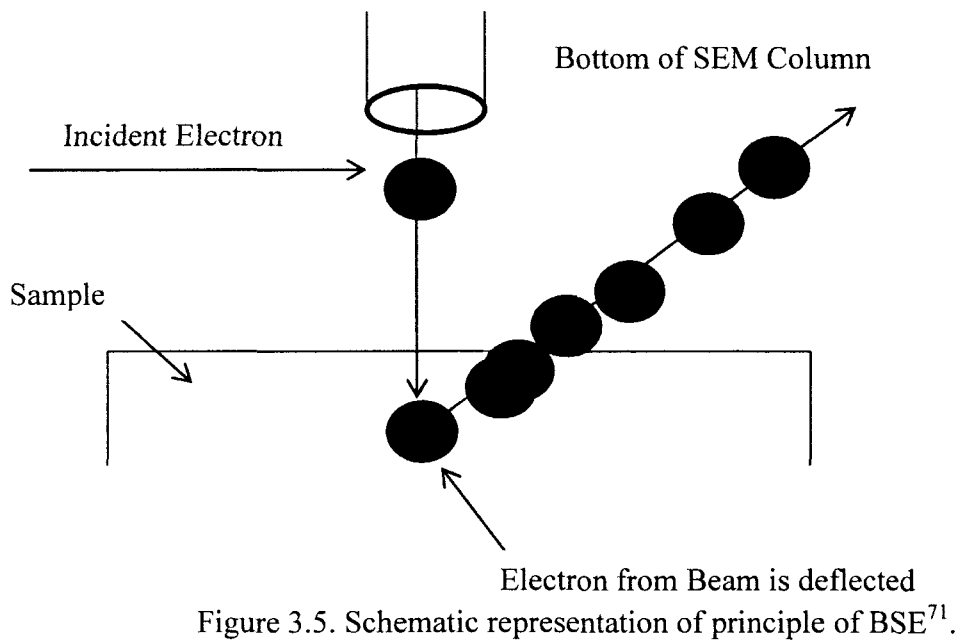
A = Attenuation.

### 3.9 Scanning Electron Microscope:

Scanning electron microscopy (SEM) experiments were performed in order to study the effect of water on the WPC and switchgrass/biopolymer composite structures. Fractured specimens were imaged in an FEI Quanta 200 FEG Environmental SEM. FEG means Field emission gun (it is one type of filament). This is an Environmental (TM) SEM, which means it can operate under High vacuum, Low vacuum and Environmental mode. The samples were

imaged under low vacuum (70pa) and at a pressure of 15kV (this is the operating pressure of the sample chamber). A scanning electron microscope (SEM) uses a beam of electrons to investigate the morphological characteristics of the material. The Large Field Secondary Electron Detector and a solid-state backscatter detector were used to detect the electrons. An SEM uses electrons from a heated tungsten wire filament accelerated down the column through a voltage potential. The electron beam penetrates into the sample in 3-dimensions. There are some important interactions that occur such as secondary electrons (SE), Backscatter Electrons (BSE). Secondary electrons (Figure 3.5) are lower in energy (<50 eV) and originate from the atoms in the sample itself. These SE originated from the top 100 Angstroms of the sample surface. Backscatter Electrons (Figure 3.6) are high energy electrons. These electrons leave from approximately a 3<sup>rd</sup> of the total penetration volume of the beam. BSE production is dependent on a material's atomic number. Therefore backscatter images reveal composition information. BSEs are higher in energy compared to than SEs. Since these electrons scattered back from the sample they are called Backscatter Electrons.

The SEM working principle under a low vacuum condition is: when the primary beam interacts with the gas molecules in the sample chamber some portion of gas molecules get ionized. Due to ionization, the molecules split into an environmental secondary electron and a positively charged ion. The positive ions will recombine with the electrons initially charging the specimen to form gas molecules again. Gas has only one function under low vacuum conditions: charge neutralization.





### **3.10 STATISTICS**

The water absorption experiments and acoustic data mentioned in the chapters IV and V at 20°C performed three times. At 40°C the experiment performed two times and at 70°C the experiment performed two times. The percentage was calculated by the average value of the last two points and the values of the initial point.

## CHAPTER –IV

### 4. Results and Discussion

#### 4.1 Water absorption

Moisture absorption is one of the main parameters to assess the quality of the biocomposite materials. Water absorption is considered a disadvantage due to its migration into the material, this can lead to disturbance of the matrix-fiber interface<sup>72</sup>. Natural fibers can also absorb moisture which initiates cracks or disturbances in the fiber-matrix interface interactions<sup>75</sup>. Water absorption affects the stability and reduces the overall strength of biocomposites<sup>72</sup>

There are three major mechanisms considered for moisture absorption into biocomposite materials. They are: (1) water molecules diffuse inside the microgaps between the polymer chains; (2) due to incomplete wettability and impregnation, capillary transport of water molecules into the gaps and flaws at the interface between polymer and fibers; (3) during the compounding process micro-cracks are formed in the matrix, water molecules are transported into these micro-cracks.<sup>76,77,78</sup>

One of the greatest problems in environmental durability of biofiber reinforced composites is their exposure to water in liquid or vapour form<sup>79, 80,81</sup>. High sensitivity of natural composites to water is due to the hydrophilic nature of natural fibers. Biofibers are rich in polar hydroxyl groups, which make them hydrophilic and sensitive to water exposure. There are several factors affecting the water absorption in biocomposite materials (1) loading of fibers (increase in % of fiber content shows increase in moisture absorption)<sup>31, 29,18</sup>, (2) chemical nature of lingocellulosic fibers (lignin is hydrophobic in nature, hence lower values of water

absorption)<sup>73</sup>, (3) fiber geometry, (4) matrix-fiber interface (improved adhesion between matrix and fibers would result in fewer and smaller microgaps where the water absorption occurs)<sup>17, 18</sup>. Exposure to the above conditions causes changes in mechanical properties and loss in composite strength<sup>18</sup>.

To study the water absorption of switchgrass/biopolymer composites, various approaches are used: total immersion in water at room or elevated temperatures, exposure to high humidity conditions at elevated temperatures, cyclic exposure to elevated temperatures, humidity and drying<sup>74</sup>. The first approach was used in this study as showing the most considerable effect on the composite properties.

WPC and switchgrass/biopolymer composite were used to evaluate water absorption. A WPC material is a commercial product which is designed to be used outdoors and we expect it to show good water resistance. The switchgrass/biopolymer composite is designed at the University of Guelph and is intended to use in car interior.

#### **4.1.1. Wood Plastic Composite (WPC)**

Figure 4.1 shows the weight change (in %) for WPC during its exposure to water at various temperatures. During water exposure, the weight of the composite sample increases due to water penetration in the material. Water absorbance increases as the temperature rises. For WPC at 20°C the maximum water absorbance (wt. %) is 8.37%, at 40°C it is 10.16% and at 70°C it is 10.6%. Water absorption in WPC reached its saturation level (where there is no further water absorption observed) at 312hrs at 20°C, at 216hrs for 40°C and at 72hrs for 70°C. This indicates that as the temperature increases the rate of water absorption increases as well, resulting in reduced time to saturation level.

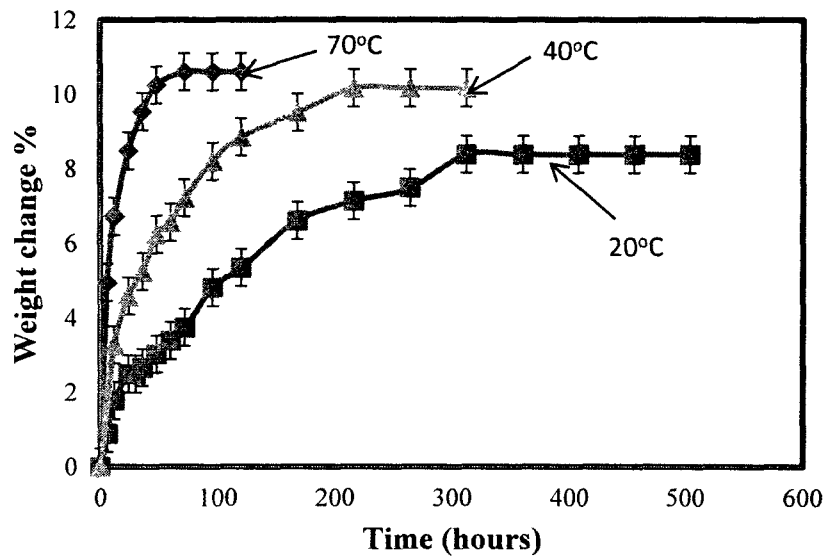


Figure 4.1. Water absorption of WPC at different temperatures.

Water absorption in sythetic polymers such as polypropylene and polyethylene is low due to their hydrophobic nature.<sup>29,31,61,82</sup> The slight water absorption in synthetic polymers is because of microgaps, which are formed during the composite preparation. Thus water absorption is mostly due to fibers.

#### 4.1.2. switchgrss/biopolymer composite

Figure 4.2 shows the values of the water absorption of switchgrss/biopolymer composite. The amount of water absorbed by the composite varies depending upon the water temperature. The switchgrss/biopolymer composite material shows the following maximum values of the weight increase:- 3.86% at 20°C, 3.91% at 40 °C and 6.63% at 70 °C. The switchgrss/biopolymer composite at 20°C reached the saturation level at 360hrs, for 40 °C the switchgrss/biopolymer composite reached the saturation level at 96hrs and for 70 °C it reaches saturation at 72hrs. This indicates that as the temperature of water increased, the rate of water absorption also increases.

The biopolymers such as poly(caprolacton) (PCL), poly(butylene succinate) (PBS), poly(lactic acid) (PLA) and poly(hydroxyalkanoates) (PHA) are widely used as matrices in biocomposites<sup>73</sup>. Poly(lactic acid) (PLA) is a biodegradable polymer with excellent thermal and mechanical properties. PLA contains aliphatic polyester groups, which are hydrophilic in nature. PLA can easily undergo hydrolysis when exposed to moisture. The products formed by hydrolysis are non-toxic to human beings<sup>88</sup>. Starch-filled PLA composites show an increase in water absorption compared to pure PLA<sup>83</sup>. Wang et al.<sup>84</sup> prepared PLA-starch blended with methylenediphenyl diisocyanate composites. They have demonstrated correlation of the increased water absorption with higher biodegradability for both composite and PLA polymer<sup>84,87</sup>.

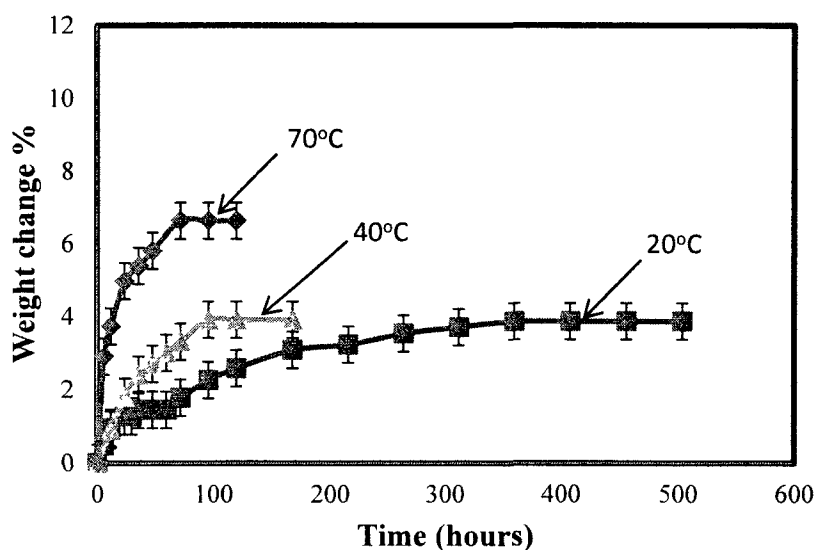


Figure 4.2. Water absorption of switchgrass/biopolymer composite at different temperatures.

### 4.1.3. WPC vs. switchgrass/biopolymer composite Discussion

Table 2 shows values of saturation levels in water absorption, when the process reaches the equilibrium and times to reach the equilibrium for both materials at various temperatures. The data are obtained from the Figures 4.1 and 4.2. Water absorption in WPC is higher compared to that of switchgrass/biopolymer composite for same time period immersed in water at different temperatures. The difference is greater for lower temperatures (more than twice) and decreases at 70°C (1.6 time). Time to reach equilibrium is almost the same for both composites at 20°C, 70°C

Table2: Water absorption values at equilibrium (wt. %) and time to reach equilibrium (hours)

Temperature, °C	Water absorption% at equilibrium		Time to reach an equilibrium (hours)	
	WPC	switchgrass/biopolymer composite	WPC	switchgrass/biopolymer composite
20°C	8.37	3.86	312	360
40°C	10.16	3.91	216	96
70°C	10.6	6.63	72	72

Thus, in spite of better water resistance of synthetic polymer matrix in WPC, the composite shows greater susceptibility to water. This may be explained by increased surface of fiber-matrix interface or wood flour used in WPC contains high percentage of cellulose, which shows high water absorption due to their inherent hydroxyl groups. These hydroxyl groups of cellulose form hydrogen bonds with water molecules.

## 4.2 Diffusion Coefficient (D)

The ability of the water molecules to penetrate inside switchgrass/biopolymer composite material can be described by the diffusion coefficient. Diffusion coefficient ( $D$ ) was calculated using the following equation from the initial slope of the plot of  $M_t/M_m$  against  $\sqrt{t}$  (time)<sup>16,85</sup>:-

$$\frac{M_t}{M_m} = \frac{4}{h} \times \left( \frac{D}{\pi} \right)^{0.5} t^{0.5} \quad (2)$$

where

$M_t$  = moisture content at time,

$M_m$  = moisture content at equilibrium,

$h$  = thickness of the sample,

$t$  = soaking time.

Diffusion coefficient gives a measure of the rate of water absorption. The diffusion coefficient value allow us quantitatively describe the water absorption process

Data from the Table 2 were used for calculations. Figures 4.3 and 4.4 show the  $M_t/M_m$  values versus the square root of time (in seconds) for both materials at all measured temperatures. From these graphs, the slopes of the approximately linear portion of the curves were obtained. Diffusion coefficients were calculated from these slope values. For diffusion coefficient calculation, the sum of all three mechanisms assumed to take place simultaneously.

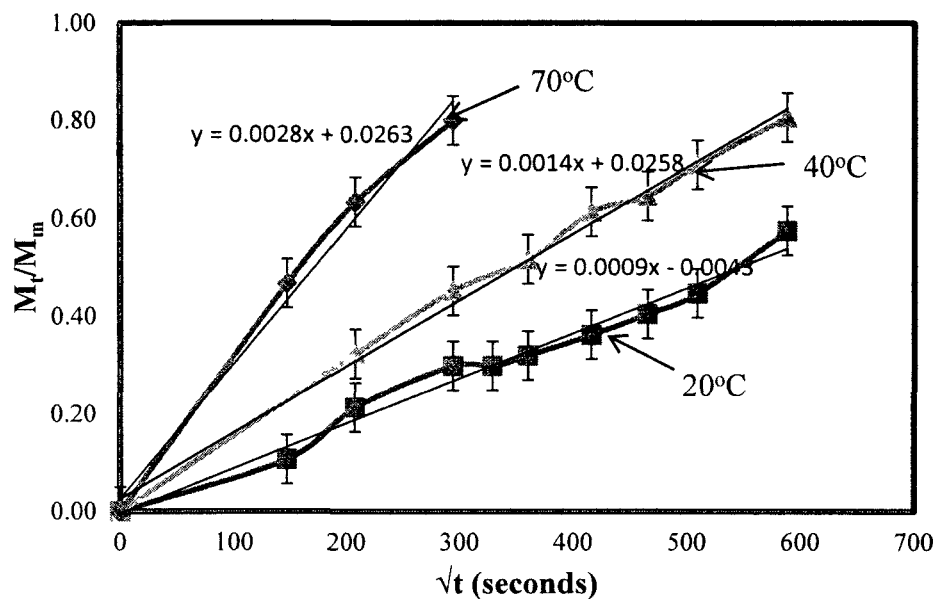


Figure 4.3. Initial part of the water absorption slopes for WPC at 20°C, 40°C & 70°C.

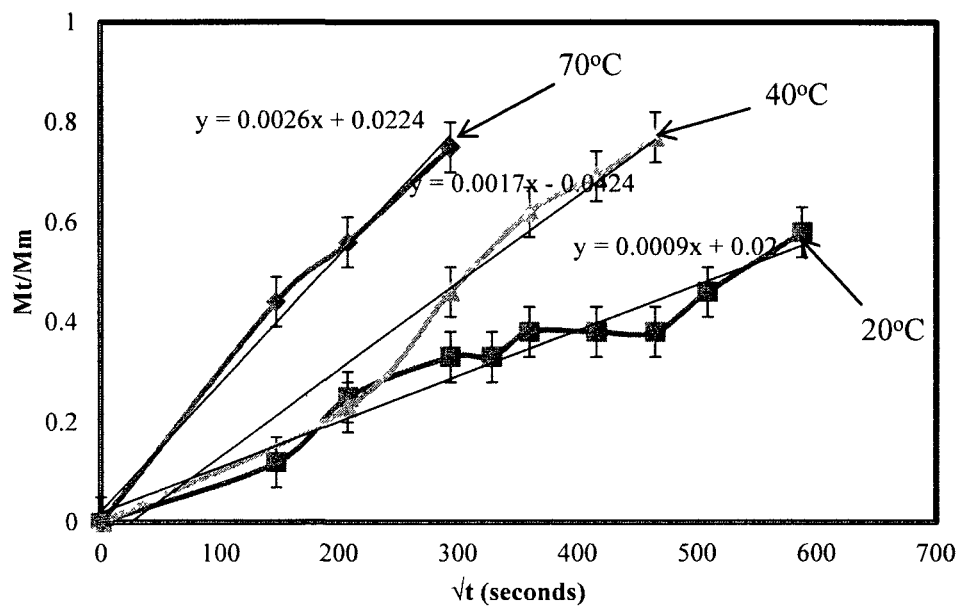


Figure 4.4. Initial part of the water absorption slopes for switchgrass/biopolymer composite at 20°C, 40°C & 70°C.



Figure 4.5 and 4.6 shows the mean of the diffusion coefficient results for each temperature. The calculated diffusion coefficient values are also listed in Table 3. From the Figures 4.5 and 4.6, it can be concluded that increase in immersion temperature increases the diffusion coefficient values for both WPC and switchgrass/biopolymer composite.

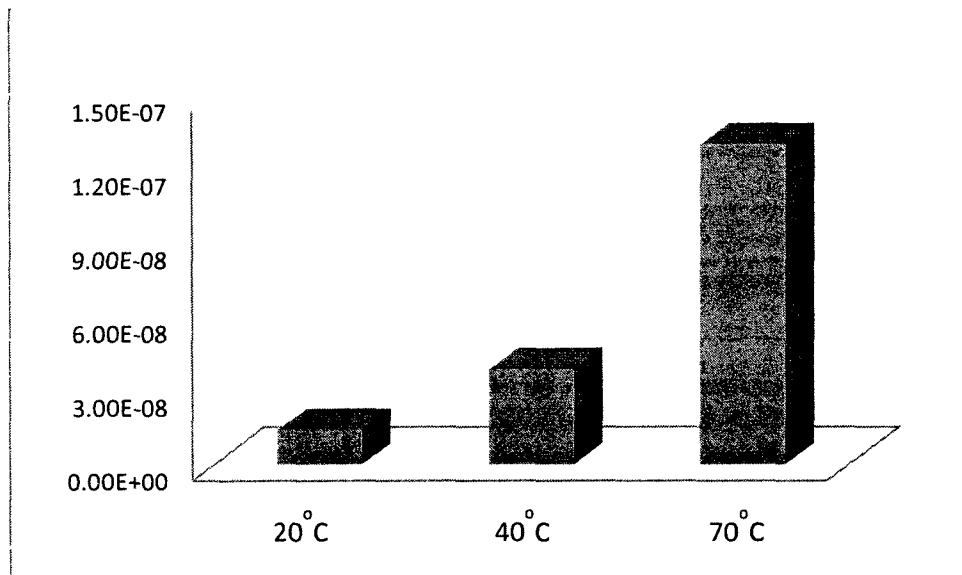


Figure 4.5. Diffusion Coefficient of WPC at three different temperatures.

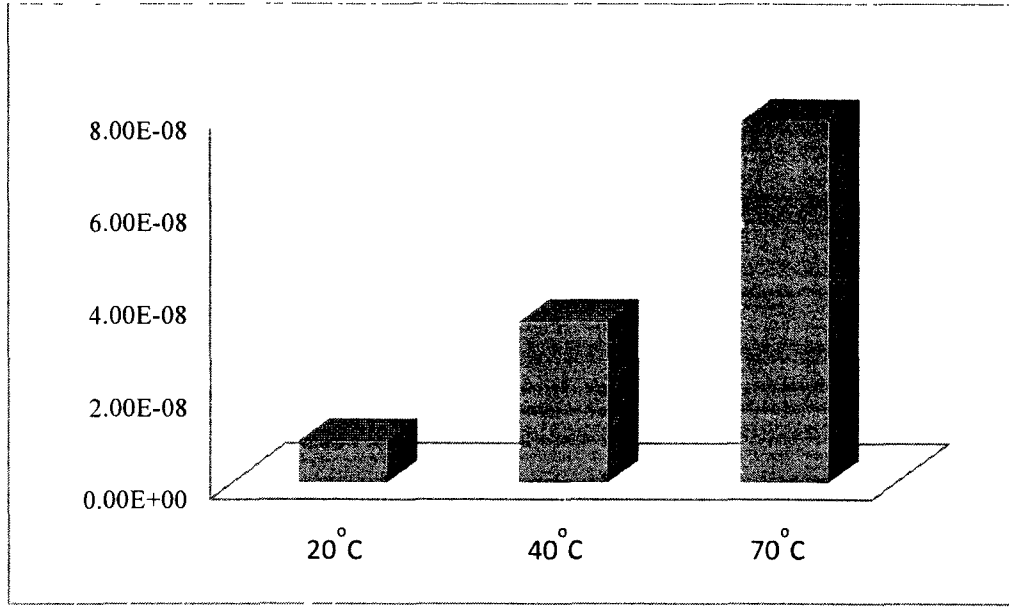


Figure 4.6. Diffusion Coefficient of switchgrss/biopolymer composite at three different temperatures.

Table 3: Diffusion Coefficient of WPC and switchgrss/biopolymer composite at different temperatures

Material	Diffusion Coefficient cm <sup>2</sup> /s		
	20°C	40°C	70°C
WPC	1.40x10 <sup>-8</sup>	3.86x10 <sup>-8</sup>	1.30x10 <sup>-7</sup>
Switchgrss/biopolymer composite	9.06x10 <sup>-9</sup>	3.49x10 <sup>-8</sup>	7.83x10 <sup>-8</sup>

According to the above results, the values of diffusion coefficient for natural fiber reinforced composites fall in the order of  $10^{-7}$  to  $10^{-9}$  cm<sup>2</sup>/s, these values are in agreement with the range of values reported for other natural fiber reinforced composites: short hemp-glass fiber hybrid polypropylene composite<sup>82</sup>, unsaturated polyester-woodflour composites<sup>86</sup>, polypropylene with natural cellulosic fibers from wood and sisal, coir, luffa composites<sup>18</sup>, hemp fiber-

unsaturated polyester composites<sup>32</sup>. The diffusion coefficient for switchgrass/biopolymer composite is two-fold lower than WPC at 20°C and 70°C. Lower diffusion coefficient values for switchgrass/biopolymer composites indicates that, it showed better water resistant even at higher temperatures compared to WPC. For 40°C the diffusion coefficient values are almost same for both materials, reason could be no. of microcracks are more in switchgrass/biopolymer composite material.

### 4.3 Density of WPC and switchgrass/biopolymer composite

Moisture content in composite material depends on density of that particular composite material. The lower the density, the higher the moisture absorbance in composite material.<sup>74</sup>

Figure 4.7 shows the density pattern of WPC at different temperatures. At 20°C the decrease in density for WPC is very low (0.14%). At 40°C the decrease in density for WPC was 0.2% and at 70°C the decrease in density for WPC was 1.2%.

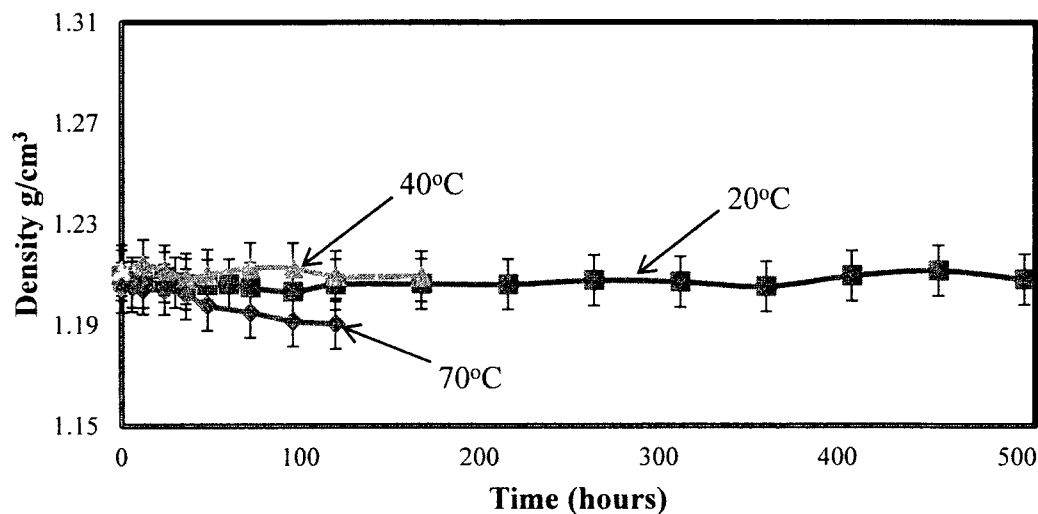


Figure 4.7. Change in density of WPC at three different temperatures.

Figure 4.8 shows the decrease in density of the switchgrass/biopolymer composite during water exposure at different temperatures. At 20°C and 40°C the decrease in density for switchgrass/biopolymer composite was 0.5% and 0.6% respectively. At 70°C the density reduces by 1.5%. As the temperature increases density decreases in both WPC and switchgrass/biopolymer composite materials. The decrease percentage for 70°C is almost same in both materials.

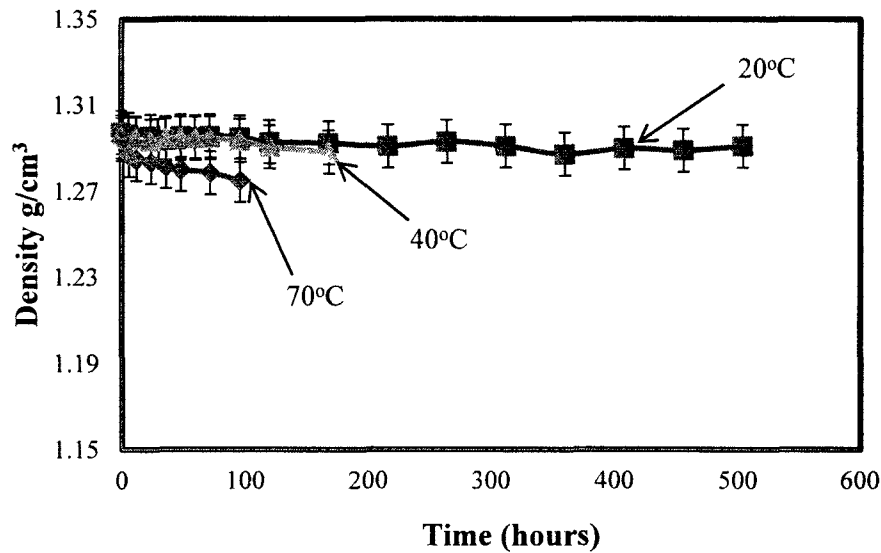


Figure 4.8. Change in density of switchgrass/biopolymer composite at three different temperatures.

#### 4.4 Dimensional stability of WPC and switchgrass/biopolymer composite

To test thickness swelling, samples were soaked in water at different temperatures until they reach equilibrium. The thickness swelling of the WPC and switchgrass/biopolymer composite material were calculated using the following equation.

$$G \% = \left( \frac{h_2}{h_1} \right) \times 100 \quad (4)$$

where

$G\%$  = thickness swelling of the sample,

$h_2$  (mm) = thickness swelling of the sample at time,

$h_1$  (mm) = thickness of the dry sample.

Thickness swelling of the composite material depends on both the matrix and the fibers used in it. Figure 4.9 and 4.10 show  $G\%$  (thickness swelling of samples) values versus time (in hours) for both WPC and switchgrass/biopolymer composite material at different temperatures. For WPC at 20°C the increase in thickness is 6.14%, at 40°C it is 8.16% and at 70°C the thickness swelling is 10%. The increased thickness swelling for switchgrass/biopolymer composite at 20°C is 3.38%, at 40°C it is 3.68% and at 70°C it is 5.88%.

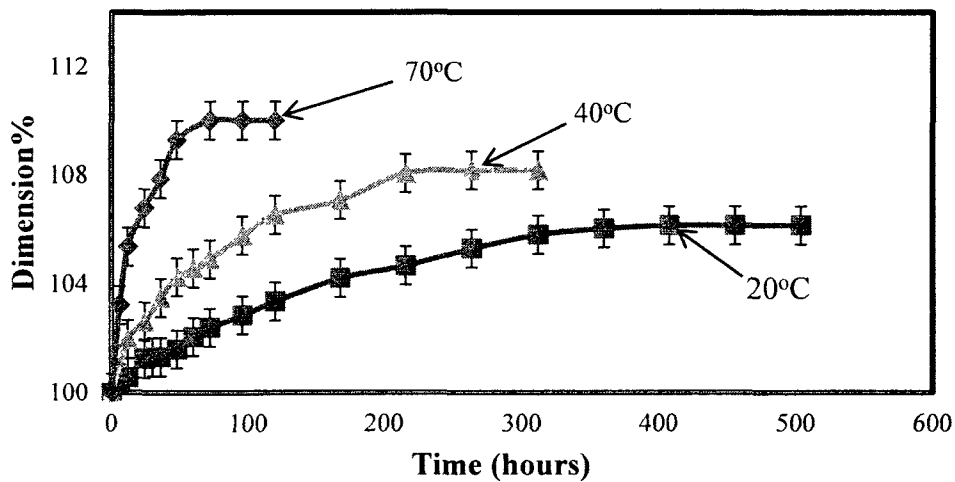


Figure 4.9. Thickness swelling of WPC at three different immersion temperatures.

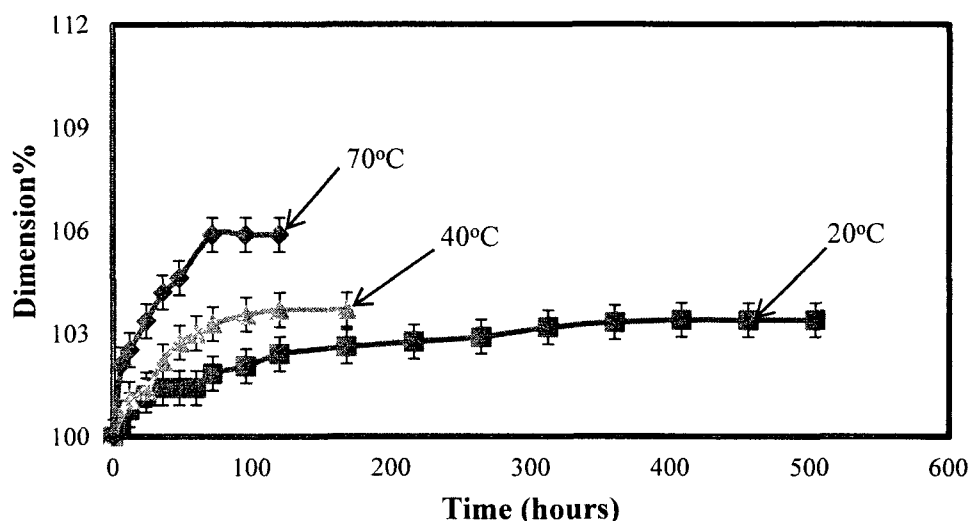


Figure 4.10. Thickness swelling of switchgrass/biopolymer composite at three different immersion temperatures.

This clearly indicates the thickness swelling of the WPC and switchgrass/biopolymer composite increases with an increase in the period of water exposure as well as rise in temperature. The thickness change for WPC was 1.81, 2.21 times more than switchgrass/biopolymer composite at 20°C and 40°C respectively. At 70°C WPC thickness swelling is 1.7 times higher than switchgrass/biopolymer composite. From the above results it can be concluded that WPC shows poor dimensional stability compared to that of switchgrass/biopolymer composite material.

## 4.5 Dehydration

A dehydration experiment was carried out in order to explain whether these composite materials will follow reversible process after removal of water. Graph 4.11 shows the progress

of dehydration process for WPC and switchgrass/biopolymer composite samples. The changes in moisture content of the material were plotted versus dehydration time.

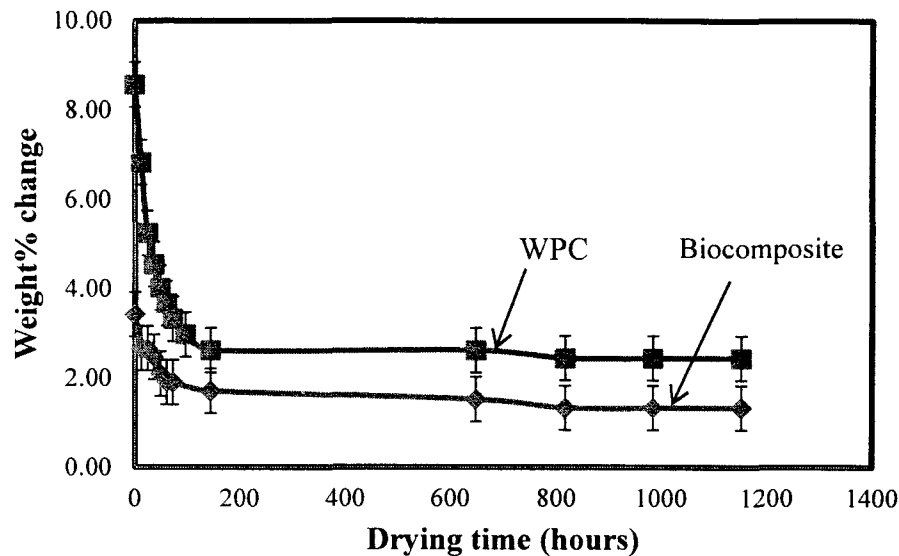


Figure 4.11. Dehydration of WPC and switchgrass/biopolymer composite at room temperature.

The dehydrated switchgrass/biopolymer composite and WPC material show the following moisture content values 38.8% and 28.6% respectively. There is no complete weight recovery observed in these samples even after exposing 1152hrs at room temperature. WPC shows high water absorption as well as high dehydration switchgrass/biopolymer composite exhibits lower water absorption and also lower dehydration. There was no discoloration of either material observed during the dehydration process.

## 4.6 Morphology

Morphology (fracture surface analysis) of the WPC and switchgrass/biopolymer composite materials was studied by scanning electron microscopy (SEM) analysis. Figure 4.12 (a)-(f) and Figure 4.13 (a)-(f) presents SEM micrographs of WPC and switchgrass/biopolymer

composite samples before and after water absorption, respectively, under similar conditions. SEM micrographs of WPC show high percentage of wood flour filler in the material. Due to high percentage presence of fillers the water absorption is high in the WPC samples. Because of higher amount of water absorption SEM images show poor interfacial bonding at many places and the number of fiber pullouts was also more. All samples of WPC (Figure 4.12a-f) micrographs at three different temperatures showed poor interfacial bonding between polymer matrix and fibers (as implied by circles and arrows). Whereas in Figures 4.13a-f (except 'd') of switchgrass/biopolymer composite material, it can be observed that there is a good adhesion between the switch grass fibers and the biopolymer matrix seen on the fracture surfaces (as indicated by arrows). These micrographs have shown a minimum number of fiber pullouts indicating their good interfacial interaction. Water absorption by switchgrass/biopolymer composite material at 20°C and 40°C is much less due to strong interfacial bonding between the fiber and matrix. A chemical linkage between hydroxyl groups of natural fibers with biopolymer is the main reason for better interfacial adhesion. Whereas for switchgrass/biopolymer composite material at 70°C, the micrograph Figure 4.13d show poor interfacial bonding between polymer matrix and fiber (because it has shown high amount of water absorption which leads to the poor interfacial bonding). SEM micrograph Figure 4.13a shows damaged fiber this was due to, when sample was fractured because of strong interfacial bonding fiber get damaged. As the water absorption increases instead of fiber damage, as fiber pullouts can be observed.





Figure 4 12 SEM micrographs of the fractured surface of WPC, (a) completely dry sample, (b) Drying after 20°C water immersion,

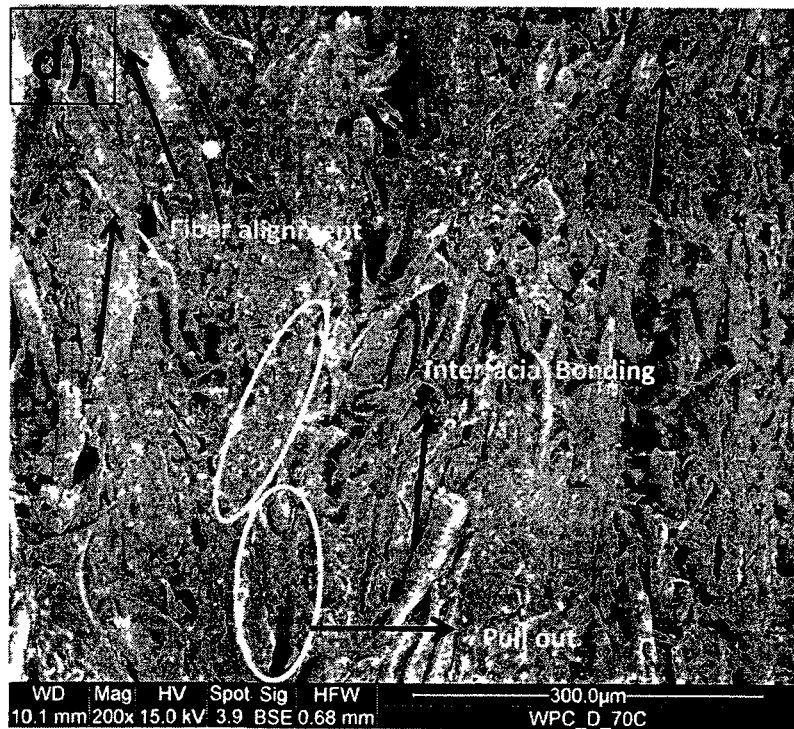
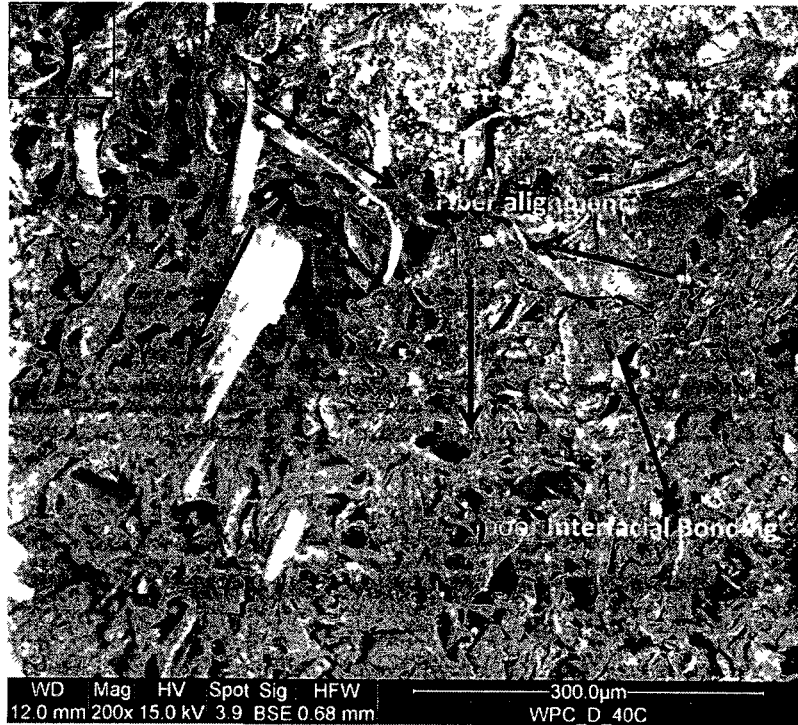


Figure 4.12. SEM micrographs of the fractured surface of WPC, (c) Drying after 40°C water immersion, (d) Drying after 70°C water immersion,

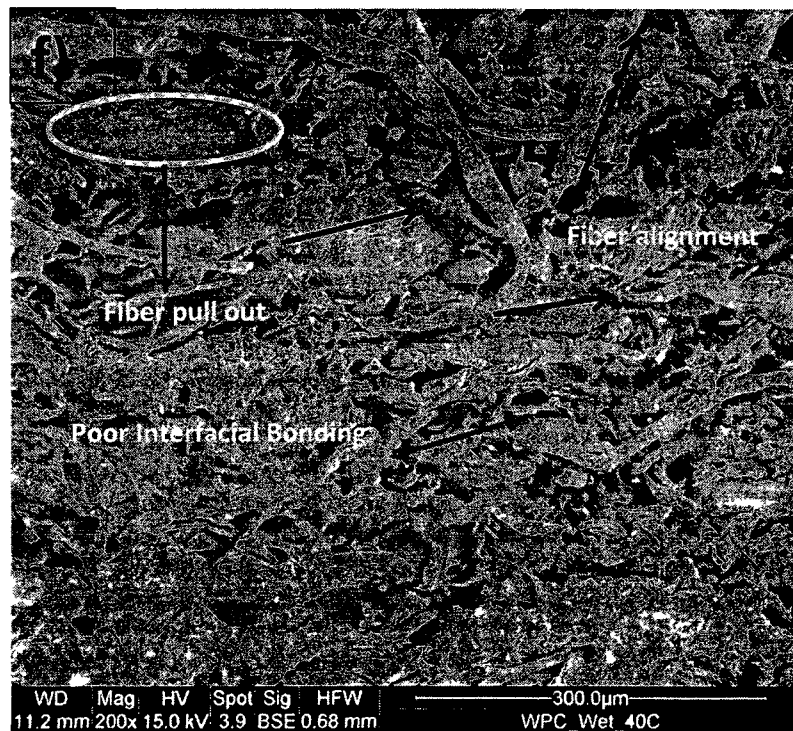
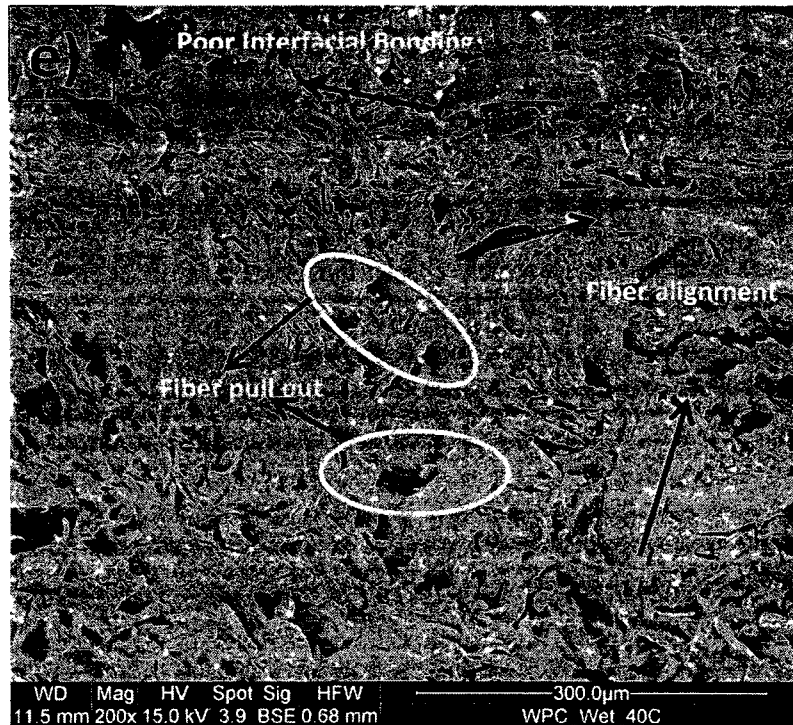


Figure 4.12. SEM micrographs of the fractured surface of WPC, (e) 20°C water immersion, (f) 40°C water immersion.

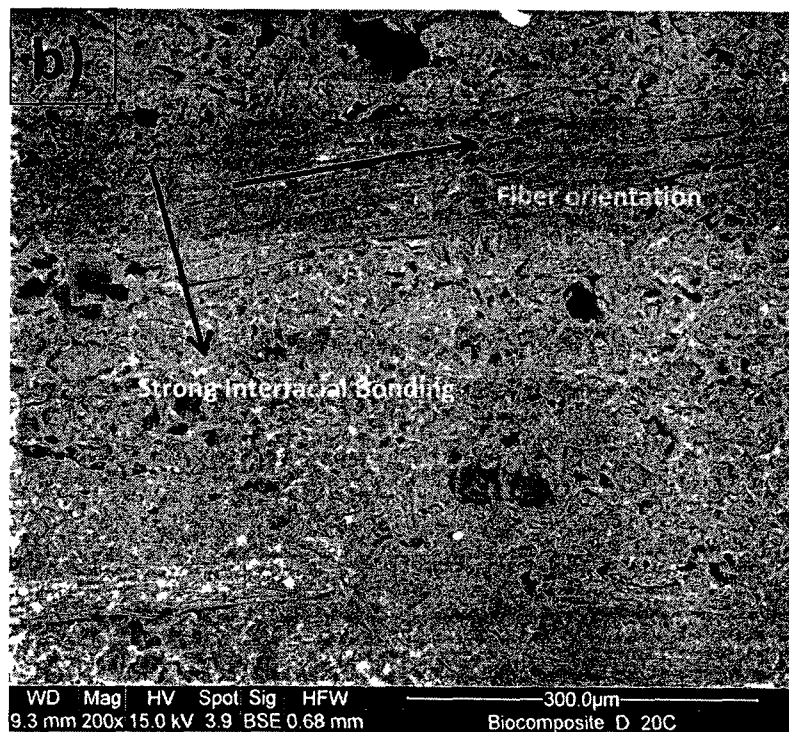


Figure 4.13. SEM micrographs of the fractured surface of switchgrass/biopolymer composite (a) completely dry sample, (b) Drying after 20°C water immersion,

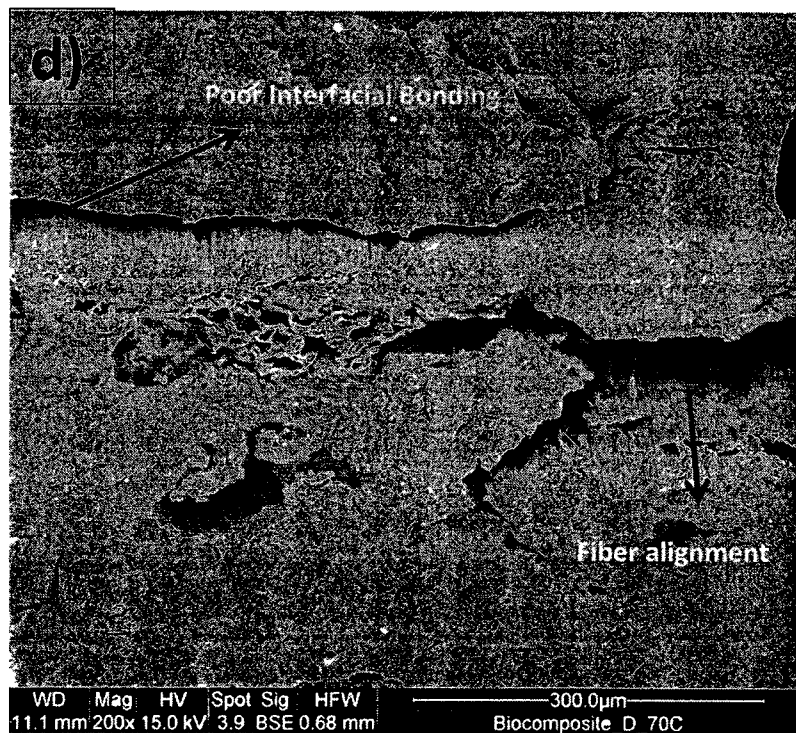
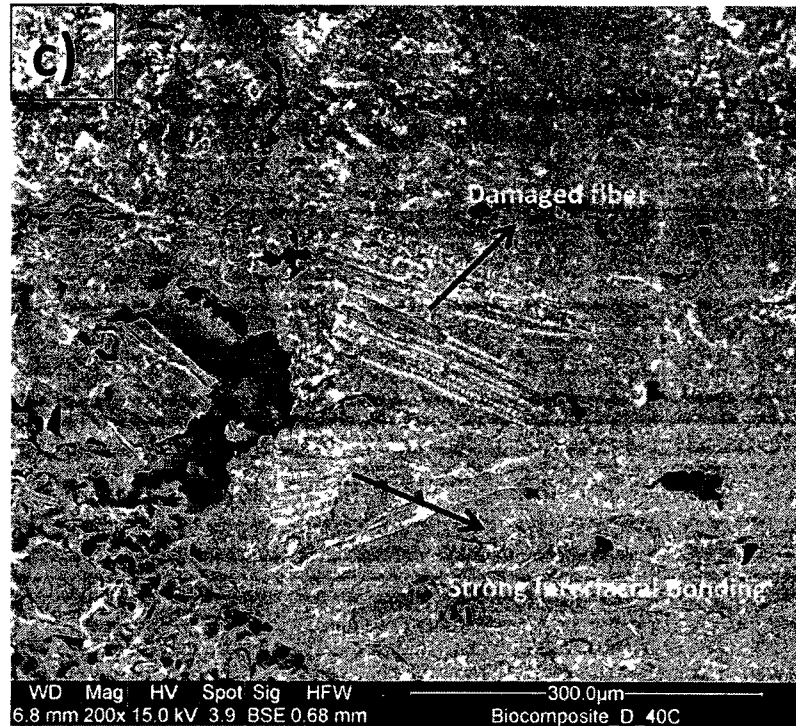


Figure 4.13 SEM micrographs of the fractured surface of switchgrass/biopolymer composite, (c) Drying after 40°C water immersion, (d) Drying after 70°C water immersion,



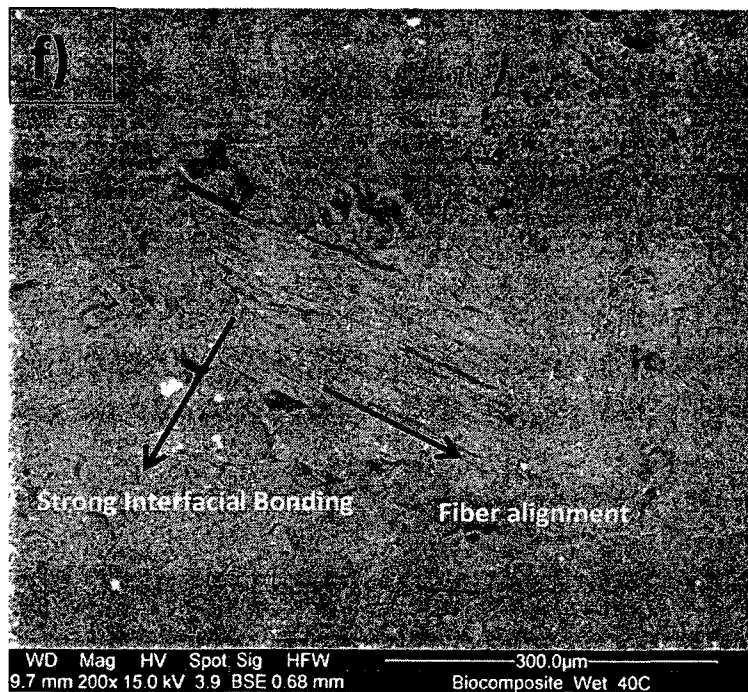
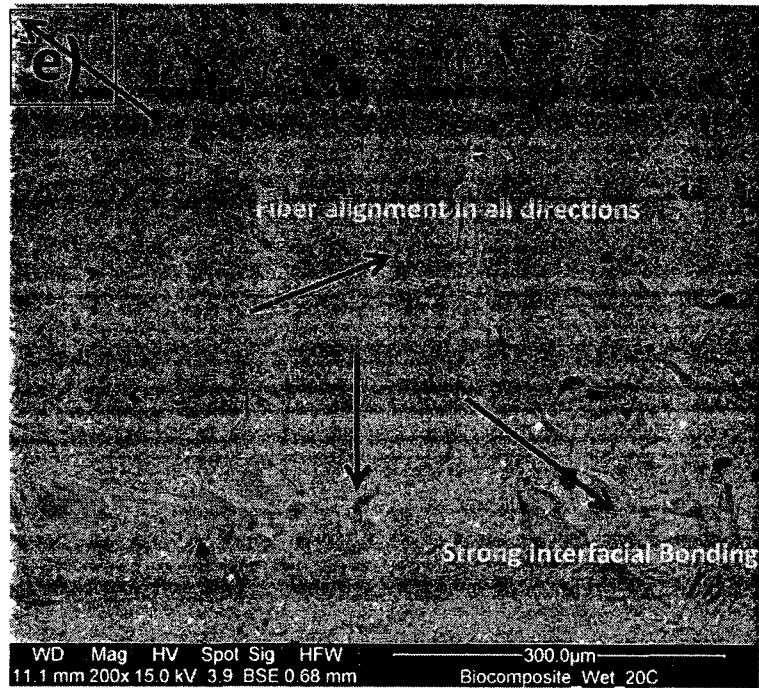


Figure 4.13. SEM micrographs of the fractured surface of switchgrass/biopolymer composite (e) 20°C water immersion, (f) 40°C water immersion.

## **Chapter V**

### **5. Acoustic measurements**

The ultrasonic non-destructive method is the most widely studied among all non-destructive techniques. This method helps determine sound speed, damping, attenuation characteristics and elastic constants, presence of flaws, fatigue behaviour and other defects in wood-based materials.<sup>89-92</sup>

In the ultrasonic investigation method, energy is coupled directly to the sample; in that a pulse propagates through a thin layer of coupling medium (glycerine water base gel is used to wet the composite surface) from the transducer into the composite sample. WPC and switchgrass/biopolymer composite samples with different moisture content were taken for acoustic measurements. High precision measurement methods are required as these samples absorb a low amount of water. The acoustic data was collected using 2.25MHz, 3.5MHz and 10MHz transducers.

## 5.1 Ultrasonic wave speed Measurements in WPC

### 5.1.1 Ultrasonic wave speed Measurements in WPC at 2.25MHz

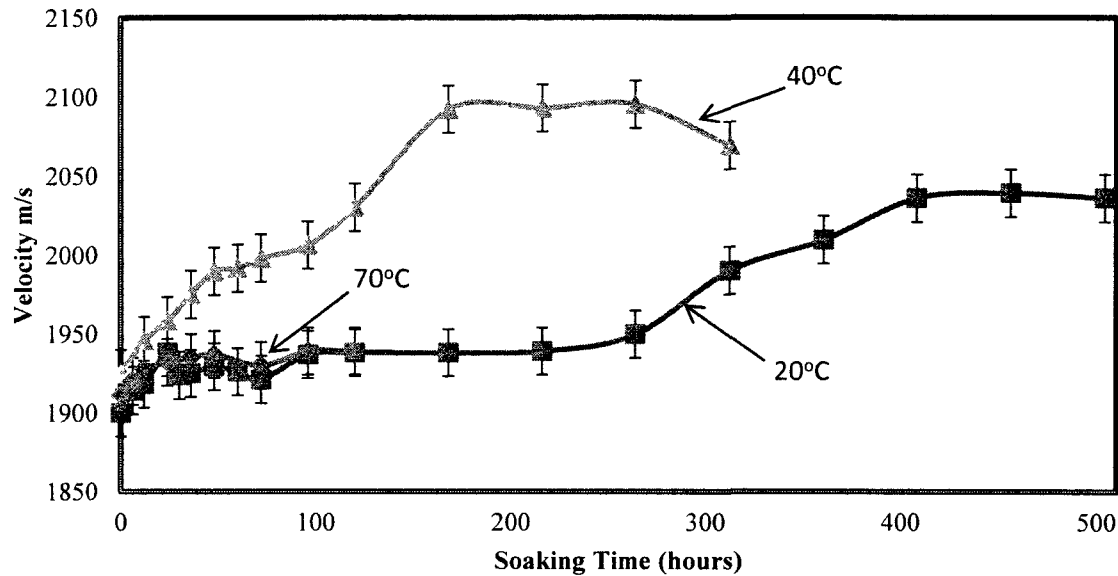


Figure 5.1. Ultrasonic wave speed of WPC for 2.25MHz at three different temperatures.

Figure 5.1 shows the velocity (ultrasonic wave speed) vs. soaking time of the WPC for 2.25MHz frequency to observe the sound speed change at different times as well as at various temperatures. As the soaking time increased, the ultrasonic wave speed of the WPC was also increased. For 20°C the increase in ultrasonic wave speed was 7%, at 40°C it was 7.5% and at 70°C it was 1.5%.



### 5.1.2 Ultrasonic wave speed Measurements in WPC at 3.5MHz

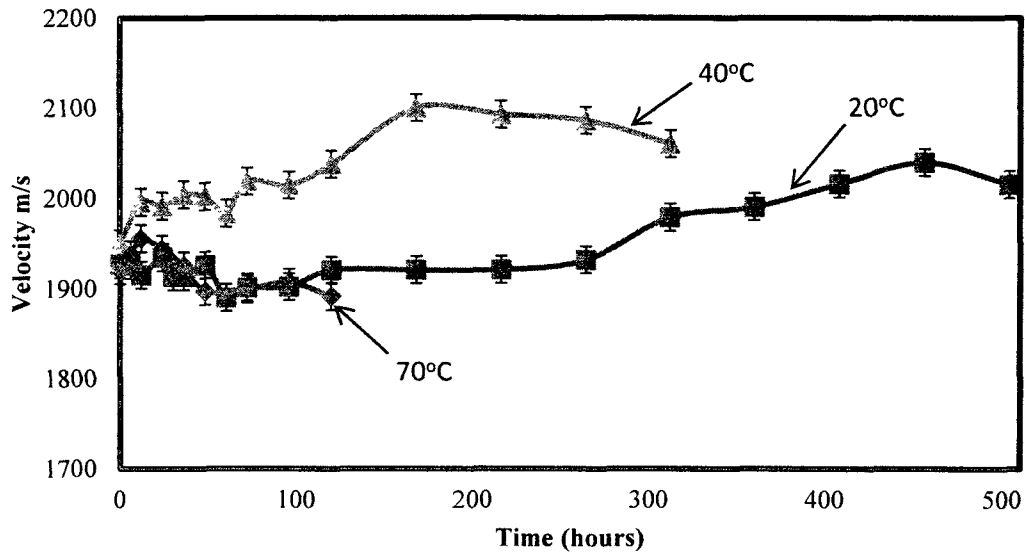


Figure 5.2. Ultrasonic wave speed of WPC for 3.5MHz at three different temperatures.

Figure 5.2 shows ultrasonic wave speed of WPC at 3.5MHz for each temperature. The increase in ultrasonic wave speed for WPC at 20°C was 5%, 6% was 40°C and 1.5% decrease in ultrasonic wave speed at 70°C. As the frequency increased from 2.25MHz to 3.5MHz, there was an increase in ultrasonic wave speed percentage for both 20°C and 40°C temperatures.

### 5.1.3 Ultrasonic wave speed in WPC vs. Weight change% at 2.25MHz

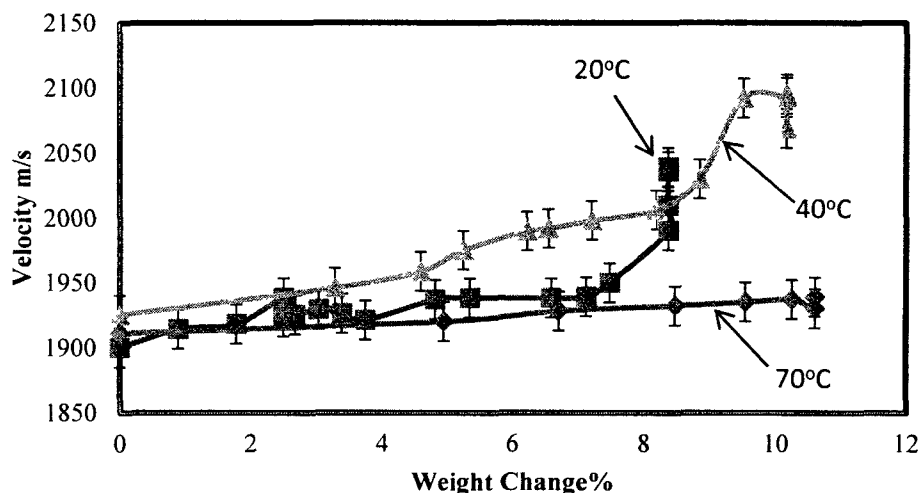


Figure 5.3. Ultrasonic wave speed of WPC vs. Weight% for 2.25MHz at three different temperatures.

Figure 5.3 presents the ultrasonic wave speed in WPC versus moisture content measured at 2.25MHz for three different temperatures. As the moisture content increased the ultrasonic wave speed in WPC also increased at all three temperatures. There was a slight increase in ultrasonic wave speed of WPC even after reaching the saturation level. This may be due to material properties which continue to change. At 20°C the increase in ultrasonic wave speed was found to be 7% for an increase in weight by 8.37% compared to initial material. For 40°C the increase in ultrasonic wave speed was 7.5% with an increase in mass by 10.16% compared to starting sample. For 70°C ultrasonic wave speed was increased by 1.5% with an increase in weight by 10.6% compared to dry sample.

#### 5.1.4 Ultrasonic wave speed in WPC vs. Weight change% at 3.5MHz

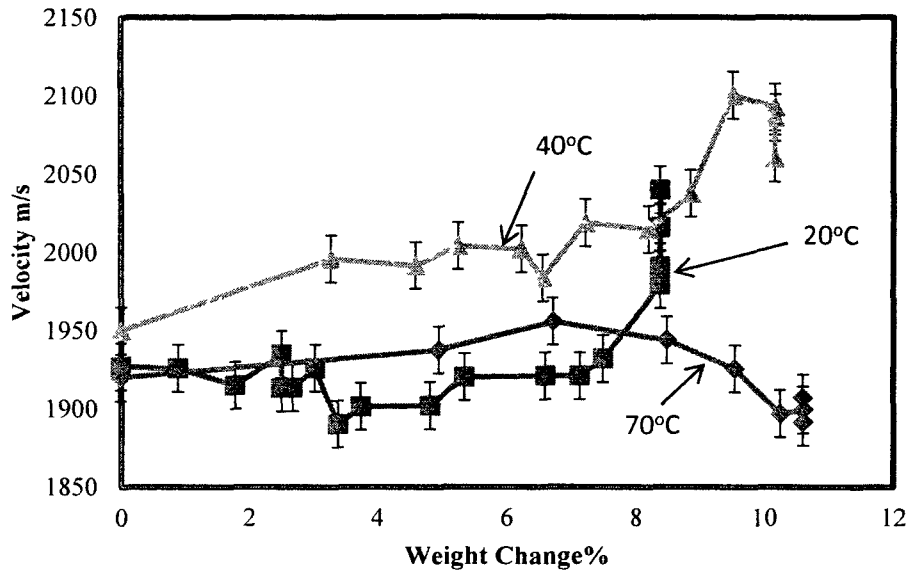


Figure 5.4. Ultrasonic wave speed of WPC vs. Weight% for 3.5MHz at three different temperatures.

Figure 5.4 presents the ultrasonic wave speed in WPC versus moisture content in the material measured at 3.5MHz for each temperature. There was an increase in ultrasonic wave speed by 5% in the final material and an increase in mass by 8.37% for dry samples at 20°C. For 40°C it was 6% increase in ultrasonic wave speed and an increase in mass by 10.16% for starting sample. At 70°C it was 1.5% decrease in ultrasonic wave speed and an increase in mass by 10.6% compared to dry material.

Polymer in WPC becoming much thicker as water is absorbed by filler swells the composite material; hence the velocity for the ultrasonic sound wave increases.

## 5.2. Attenuation measurements in WPC

### 5.2.1 Attenuation Measurements in WPC at 2.25MHz

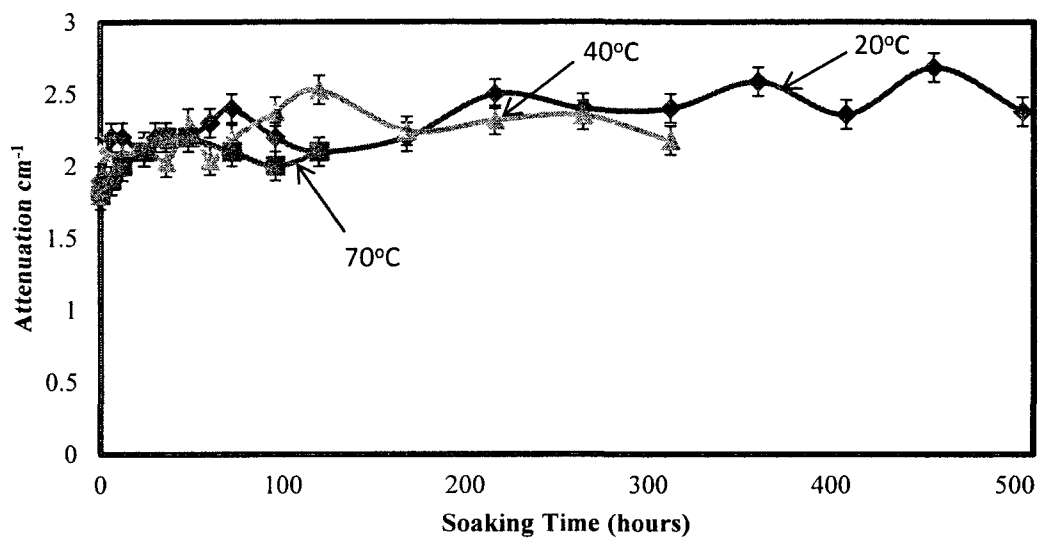


Figure 5.5. Attenuation of WPC for 2.25MHz at three different temperatures.

Figure 5.5 shows the attenuation values for WPC materials at 2.25MHz frequency. The attenuation values for WPC increase at different temperatures. Increase in attenuation percentage value at 20°C was 24%, at 40°C 5% and 70°C it was 16%.

### 5.2.2 Attenuation Measurements in WPC at 3.5MHz

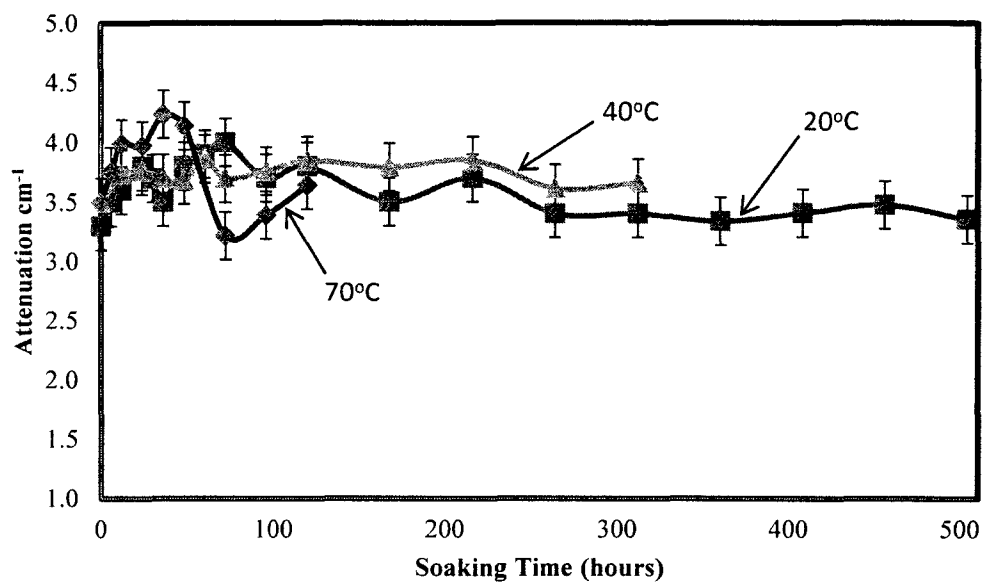


Figure 5.6. Attenuation of WPC for 3.5MHz at three different temperatures.

Figure 5.6 shows the increase in attenuation of the WPC sample for 3.5MHz frequency at various temperatures. At 20°C and 40°C the increase in attenuation was 3% and 6% respectively. As the temperature increased from 20°C to 40°C the attenuation percentage values also increased for 3.5MHz frequency. At 70°C it was 3% increase in attenuation.

### 5.2.3 Attenuation in WPC vs. Weight change% at 2.25MHz

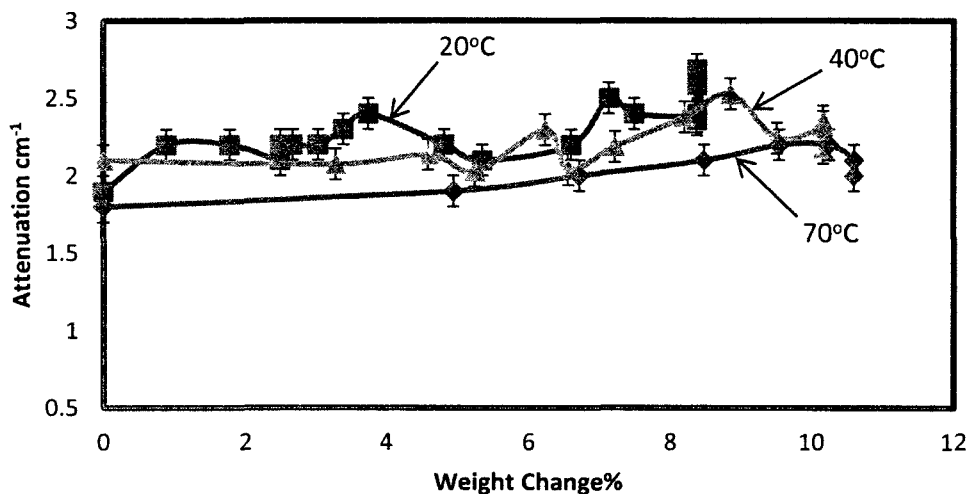


Figure 5.7. Attenuation of WPC vs. Weight% for 2.25MHz at three different temperatures.

Figure 5.7 presents the attenuation measured at 2.25MHz for WPC at various temperatures. The attenuation increased for WPC at different temperatures. Increase in attenuation value was 24% at 20°C with an increase in mass of 8.37% compared to dry sample. At 40°C attenuation was 5% higher in samples having an increase of 10.16% in mass than in the starting material. At 70°C, 16% higher attenuation was found in samples having a weight increase of 10.6% than the initial material

### 5.2.4 Attenuation in WPC vs. Weight change% at 3.5MHz

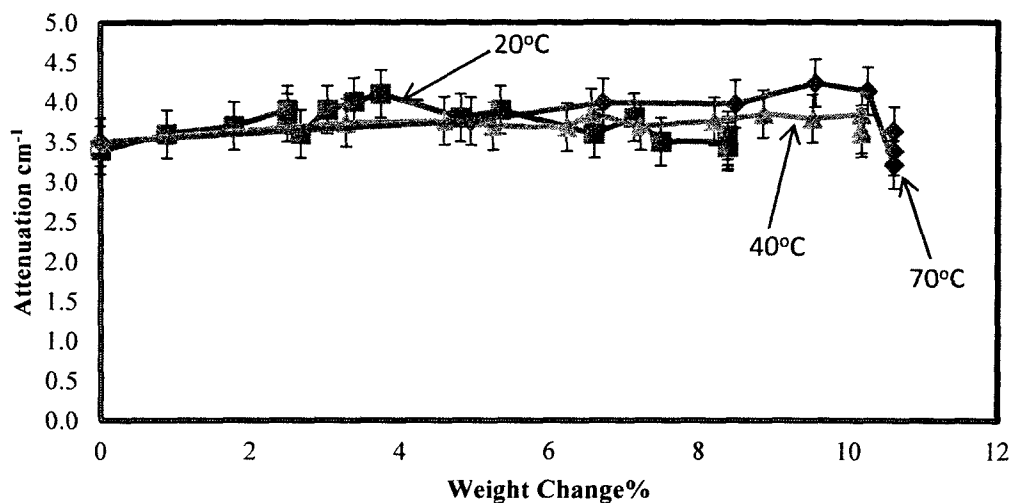


Figure 5.8. Attenuation of WPC vs. Weight% for 3.5MHz at three different temperatures.

Figure 5.8 presents the attenuation in WPC versus moisture content measured at 3.5MHz for three different temperatures. The attenuation increased by 3% at 20°C with an increase in weight of 8.37% compared to dry sample. For 40°C increase in attenuation is found to be 6% with an increase in weight of 10.16% compared to dry sample. At 70°C the increase in attenuation was 3% with an increase in mass of 10.6% compared to that of starting material.

## 5.3 Ultrasonic wave speed Measurements in switchgrss/biopolymer composite

### 5.3.1 Ultrasonic wave speed measurements in switchgrss/biopolymer composite at 2.25MHz

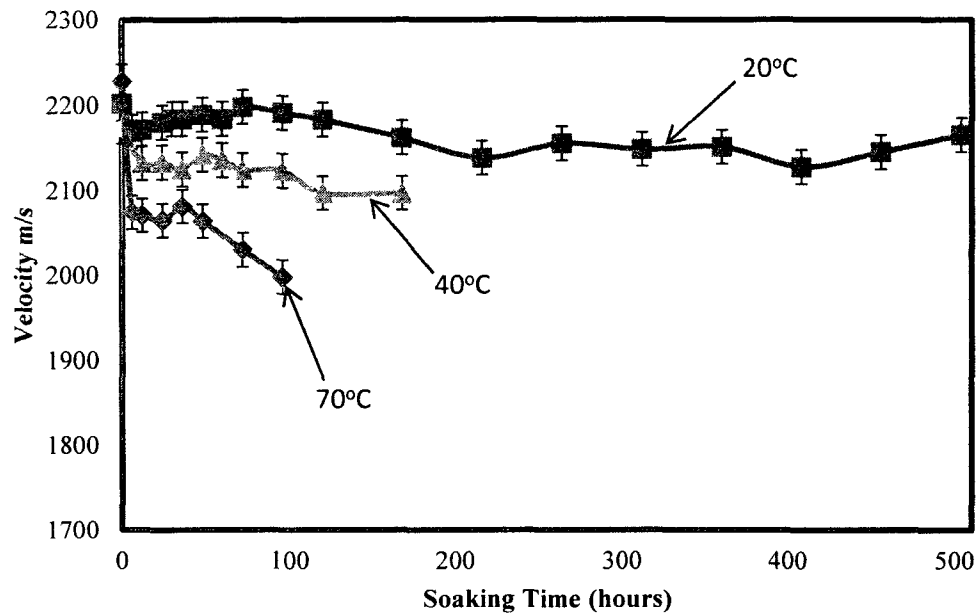


Figure 5.9. Sound speed of switchgrss/biopolymer composite for 2.25MHz at three different temperatures.

Figure 5.9 shows the values for the ultrasonic wave speed (2.25MHz) of the switchgrss/biopolymer composite at different temperatures. There was a decrease in ultrasonic wave speed values of the switchgrss/biopolymer composite material at three different temperatures. The decrease in ultrasonic wave speed was 2% at 20°C, 3.5% at 40°C and 10% at 70°C. This indicated that as temperature of water increased the ultrasonic wave speed decreased. There is a decrease in ultrasonic wave speed as water content increases in the switchgrss/biopolymer composite material. This was not observed in WPC material. The decrease in ultrasonic wave speed measured at 2.25MHz for switchgrss/biopolymer composite



sample at 40°C was 2 times lower and at 70°C it was 6 times lower compared to ultrasonic wave speed decrease at 20°C.

### 5.3.2 Ultrasonic wave speed measurements in switchgrass/biopolymer composite at 3.5MHz

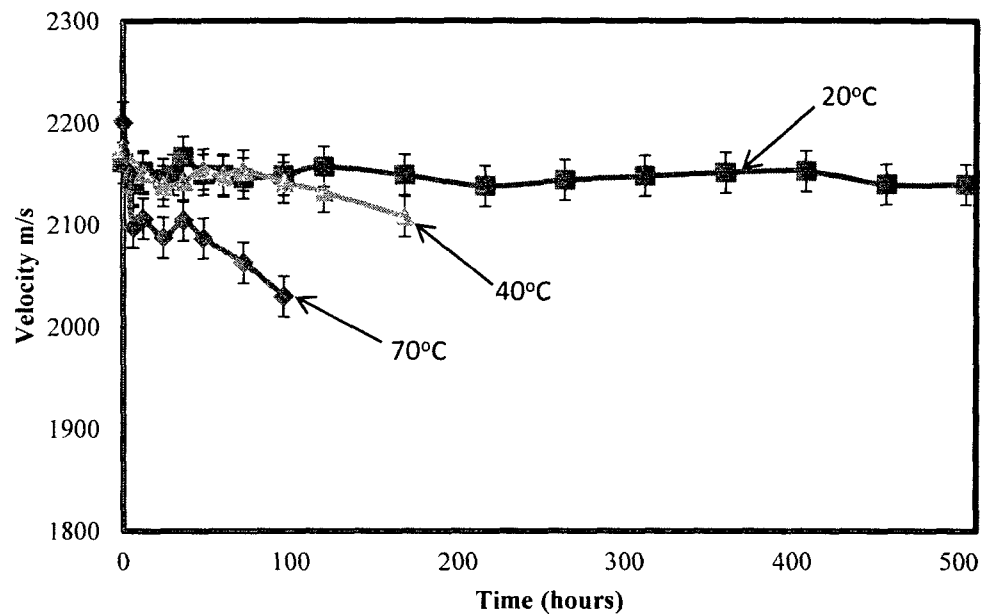


Figure 5.10. Sound speed of switchgrass/biopolymer composite for 3.5MHz at three different temperatures.

Figure 5.10 shows change in ultrasonic wave speed pattern at 3.5MHz in switchgrass/biopolymer composite material at different temperatures. At 20°C the decrease in ultrasonic wave speed for switchgrass/biopolymer composite was 1%, at 40°C it was 3 % and at 70°C it was 8%. As the temperature increased ultrasonic wave speed percentage also increased for switchgrass/biopolymer composite at 3.5MHz frequency. The decrease in ultrasonic wave speed at 40°C was 3 times lower and at 70°C it was 7 times lower than the decrease in ultrasonic wave speed at 20°C.

### 5.3.3 Ultrasonic wave speed measurements in switchgrass/biopolymer composite at 10MHz

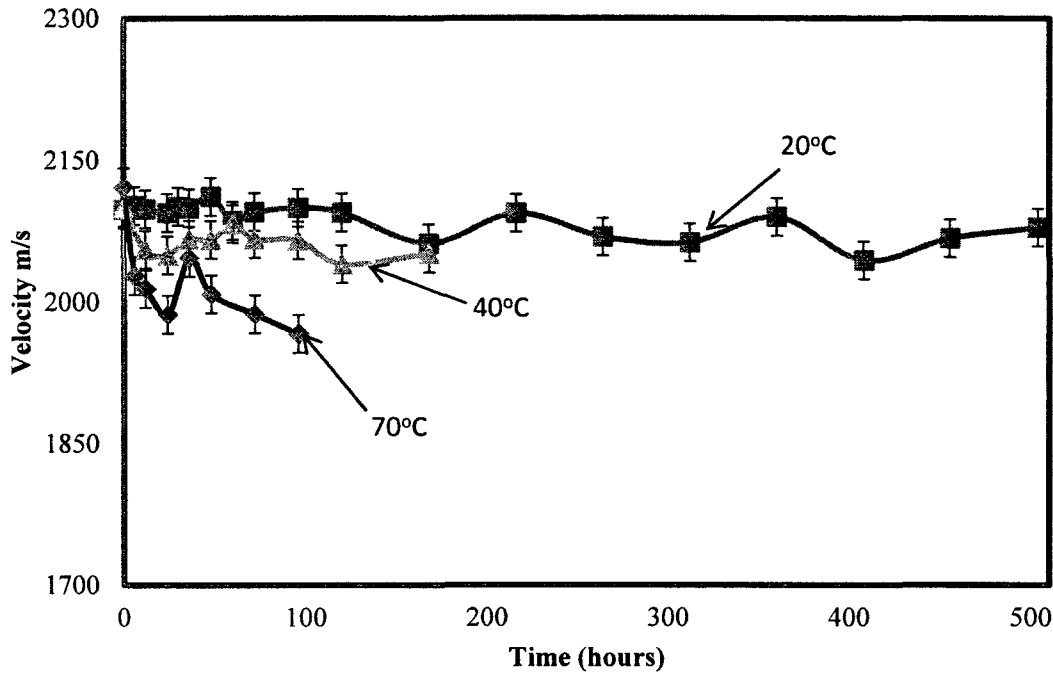


Figure 5.11. Sound speed of switchgrass/biopolymer composite for 10MHz at three different temperatures.

Figure 5.11 shows ultrasonic wave speed values of switchgrass/biopolymer composite versus the soaking time (in hours) for various temperatures at 10MHz frequency. From this Figure at 20°C the decrease in ultrasonic wave speed was 1%, at 40°C it was 2% and at 70°C it was 7%. As the temperature increased the sound speed percentage values was also increased for switchgrass/biopolymer composite material. For WPC material 10MHz data was not collected as WPC material is not sensitive at higher frequencies. The decrease in ultrasonic wave speed at 10MHz frequency for switchgrass/biopolymer composite at 40°C and 70°C was two, seven times lower than the decrease in ultrasonic wave speed at 20°C respectively.

### 5.3.4 Ultrasonic wave speed in switchgrass/biopolymer composite vs. Weight Change% at 2.25MHz

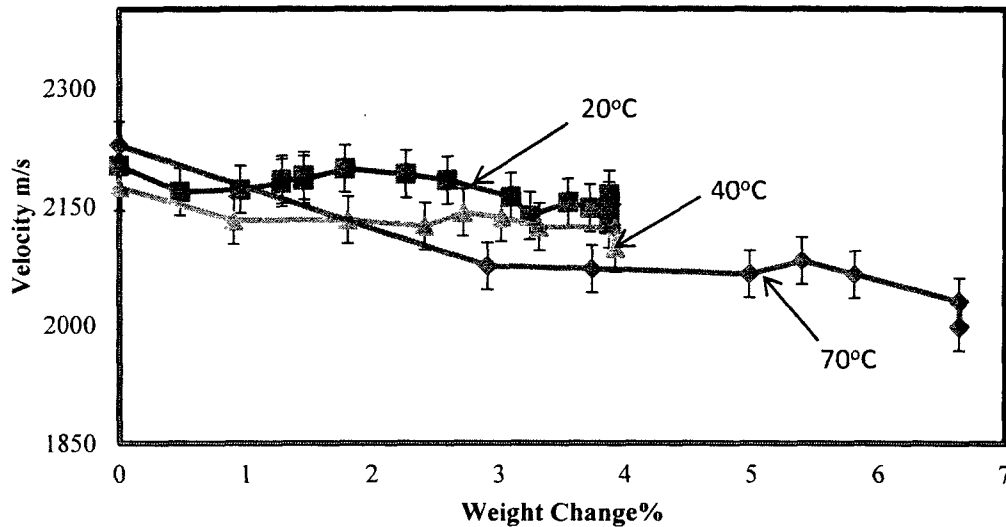


Figure 5.12. Sound speed of switchgrass/biopolymer composite vs. Weight% for 2.25MHz at three different temperatures.

Figure 5.12 shows the ultrasonic wave speed in switchgrass/biopolymer composite versus weight change at 2.25MHz for various temperatures. The ultrasonic wave speed was found to be 2% lower in samples having an increase in 3.86% in mass than in the dry switchgrass/biopolymer composite at 20°C temperature. For 40°C it was 3.5% lower in ultrasonic wave speed and had an increase of 3.91% in weight than in the dry material. For 70°C it was 10% decrease in ultrasonic wave speed for increase in 6.63% in weight than the starting material.

### 5.3.5 Ultrasonic wave speed in switchgrass/biopolymer composite vs. Weight Change% at 3.5MHz

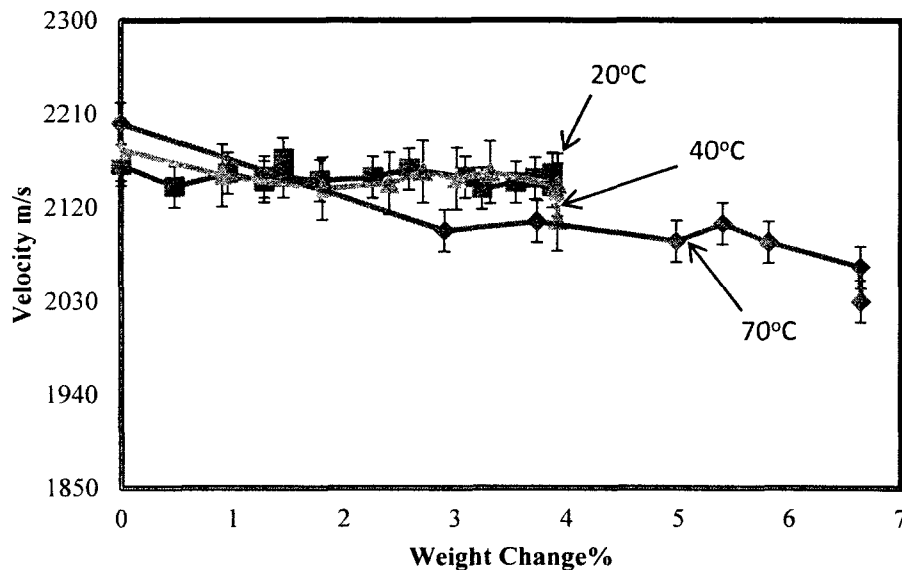


Figure 5.13. Sound speed of switchgrass/biopolymer composite vs. Weight% for 3.5MHz at three different temperatures.

Figure 5.13 shows ultrasonic wave speed in switchgrass/biopolymer composite versus weight change in the sample measured at 3.5MHz for three different temperatures. ultrasonic wave speed decreased by 1% at 20°C with an increase in mass by 3.86% in comparison with dry sample. At 40°C decrease in ultrasonic wave speed was 3% with an increase in weight by 3.91% compared to starting material. At 70°C ultrasonic wave speed decreased by 8% and an increase in mass 6.63% compared with dry material.

### 5.3.6 Ultrasonic wave speed in switchgrss/biopolymer composite vs. Weight Change% at 10MHz

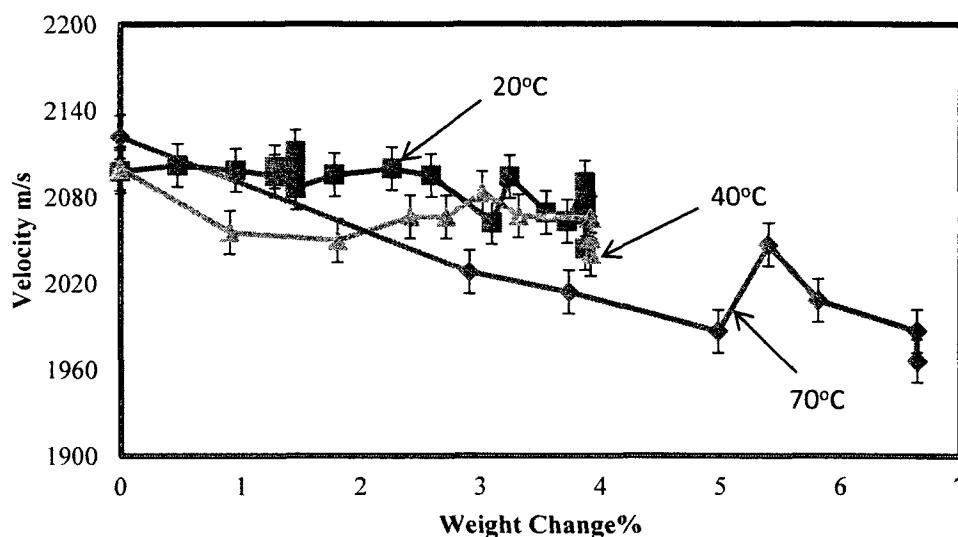


Figure 5.14. Sound speed of switchgrss/biopolymer composite vs. Weight% for 10MHz at three different temperatures.

Figure 5.14 presents the ultrasonic wave speed in switchgrss/biopolymer composite versus moisture content in the material measured at 10MHz for each temperature. At 20°C the decrease in ultrasonic wave speed was 1% with an increase in weight of 3.86% in comparison with starting material. For 40°C there was 2% decrease in ultrasonic wave speed with an increase in mass of 3.91% compared to initial sample. At 70°C there was a 7% decrease in sound speed with an increase in mass of 6.63% compared to dry sample.

Ultrasonic wave speed change observed in the switchgrss/biopolymer composite sample is related to water absorption. A decrease in ultrasonic wave speed was observed in switchgrss/biopolymer composite samples at high temperature. At high temperature (70°C) water absorption percentage increased. This is due to water molecules' penetrating quickly into the microcracks of the polymer matrix. The water absorption percentage at 40°C was slightly higher

than water absorption at 20°C. This is due to water molecules diffusing inside the microgaps between the polymer chains. At this temperature polymer molecules can move and because of this water molecules can enter and come outside the material. Water absorption of switchgrss/biopolymer composite samples at 20°C is because of capillary transport of water molecules into the gaps and flaws at the interface between polymer and fibers.

For switchgrss/biopolymer composites the fiber length is long, hence there were variations in ultrasonic wave speed. This could contribute to less sensitivity of the acoustics.

## 5.4 Attenuation measurements in switchgrss/biopolymer composite

### 5.4.1 Attenuation in switchgrss/biopolymer composite at 2.25MHz

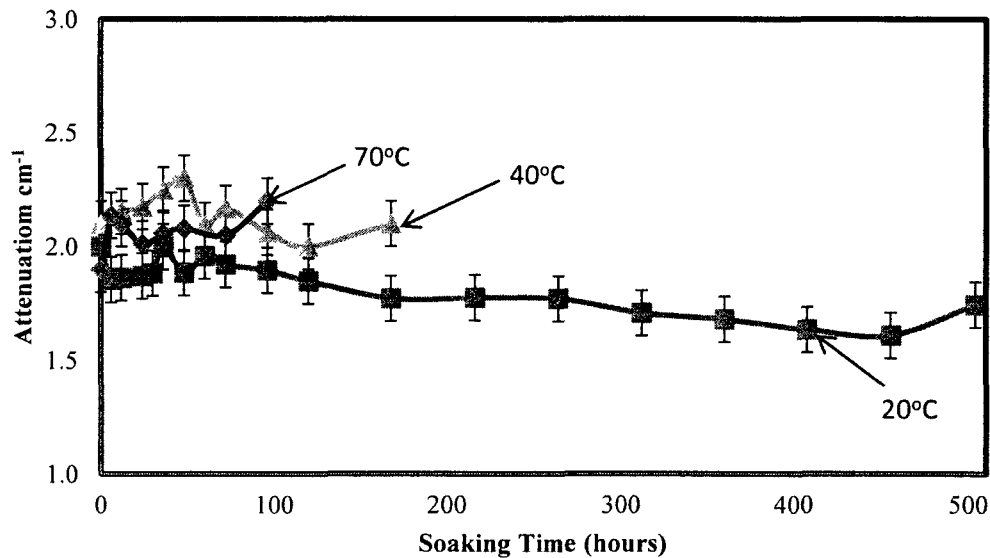


Figure 5.15. Attenuation of switchgrss/biopolymer composite for 2.25MHz at three different temperatures.

Figure 5.15 shows the attenuation values for switchgrss/biopolymer composite material at 2.25MHz frequency. For the switchgrss/biopolymer composite sample, attenuation values did not follow any pattern. At 20°C the decrease in attenuation percentage value was 15%, for 40°C

the 2.25MHz frequency was not sensitive (there was no overall change in attenuation values). At 70°C the increase in attenuation value was 16%.

#### 5.4.2 Attenuation in switchgrss/biopolymer composite at 3.5MHz

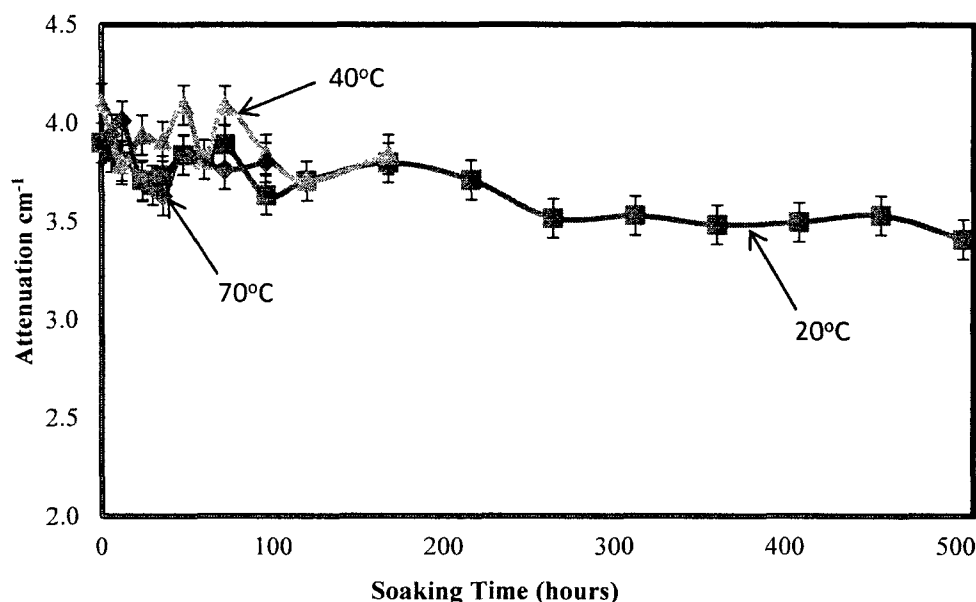


Figure 5.16. Attenuation of switchgrss/biopolymer composite for 3.5MHz at three different temperatures.

Figure 5.16 shows decrease in attenuation values observed for switchgrss/biopolymer composite material at 3.5MHz for three different temperatures. At 20°C and 40°C the decrease in attenuation was 13% and 7% respectively. At 70°C the attenuation reduced by 2.5%. Attenuation values decreased as the temperature increased.

### 5.4.3 Attenuation in switchgrass/biopolymer composite at 10MHz

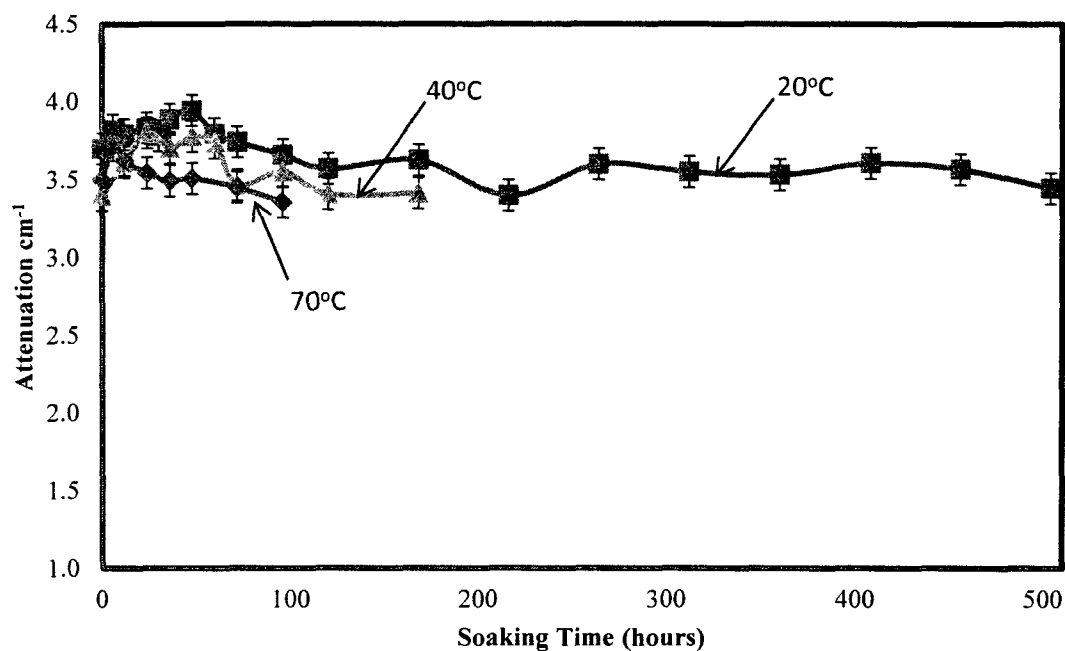


Figure 5.17. Attenuation of switchgrass/biopolymer composite for 10MHz at three different temperatures.

Figure 5.17 shows at 10MHz frequency values of attenuation collected at each temperature. At 40°C the 10MHz frequency is not sensitive as there was no change in the attenuation values. At 20°C and 70°C the decrease in attenuation was 7% and 3% respectively.



#### 5.4.4 Attenuation in switchgrss/biopolymer composite vs. Weight change% at 2.25MHz

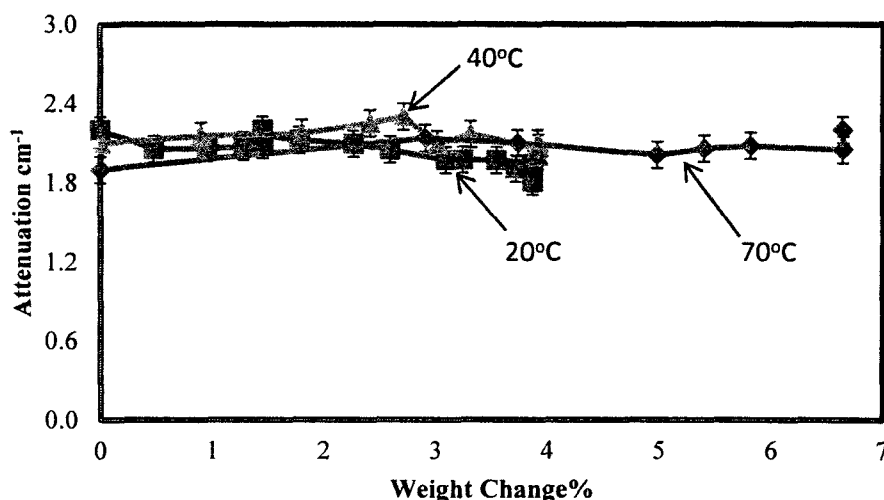


Figure 5.18. Attenuation of switchgrss/biopolymer composite vs. Weight% for 2.25MHz at three different temperatures.

Figure 5.18 presents the attenuation measured at 2.25MHz for switchgrss/biopolymer composite at various temperatures. For switchgrss/biopolymer composite material at 20°C the decrease in attenuation value was 15% with an increase in weight by 3.86% compared to starting material. For 40°C there was no significant change in the attenuation values. For 70°C attenuation values lowered by 16% with an increase in mass of the sample by 6.63% compared to dry sample.

#### 5.4.5 Attenuation in switchgrss/biopolymer composite vs. Weight change% at 3.5MHz

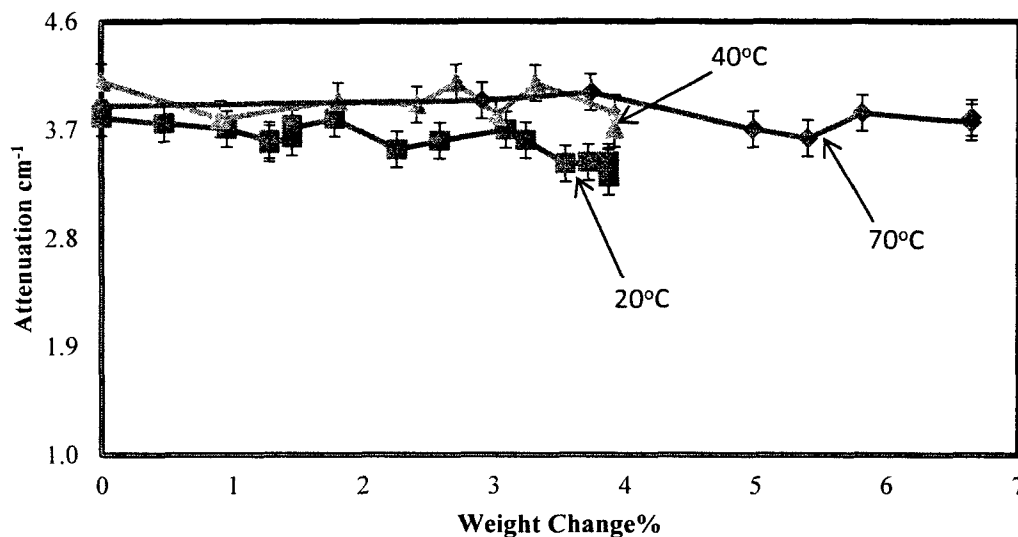


Figure 5.19. Attenuation of switchgrss/biopolymer composite vs. Weight% for 3.5MHz at three different temperatures.

Figure 5.19 present the attenuation values of the switchgrss/biopolymer composite sample versus weight change measured at 3.35MHz for different temperatures. At 20°C the attenuation values was found to be 13% lower with an increase in mass of 3.86% compared to the initial material. For 40°C 7% decrease in attenuation with an increase in weight of 3.91% compared to that of dry sample. At 70°C decrease in attenuation value was 2.5% with an increase in mass of 6.63% compared to starting material.

#### 5.4.6 Attenuation in switchgrass/biopolymer composite vs. Weight change% at 10MHz

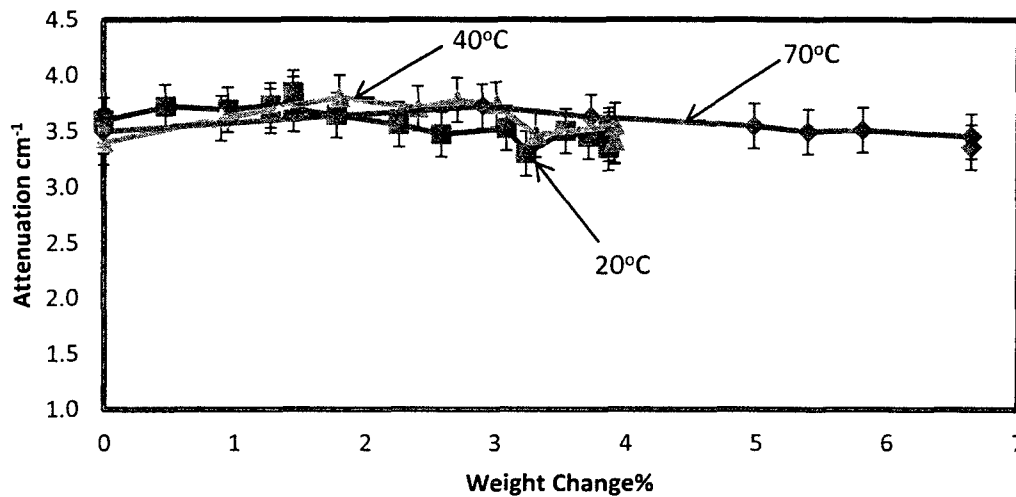


Figure 5.20. Attenuation of switchgrass/biopolymer composite vs. Weight% for 10MHz at three different temperatures.

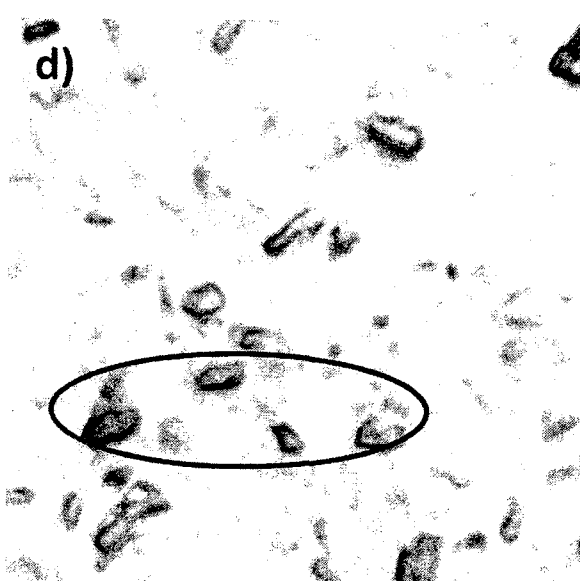
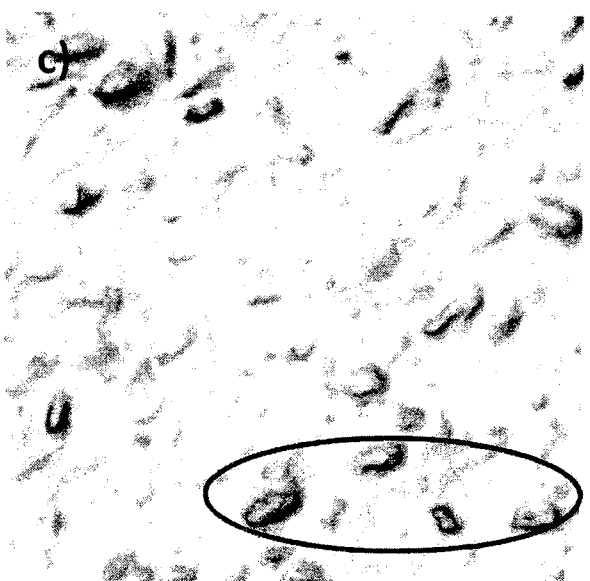
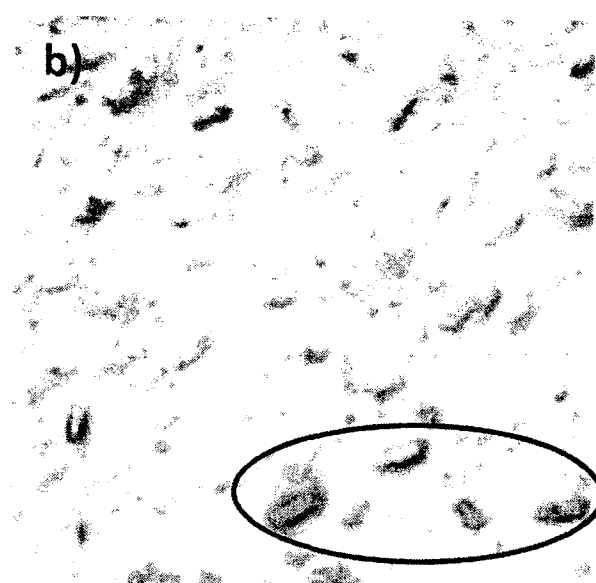
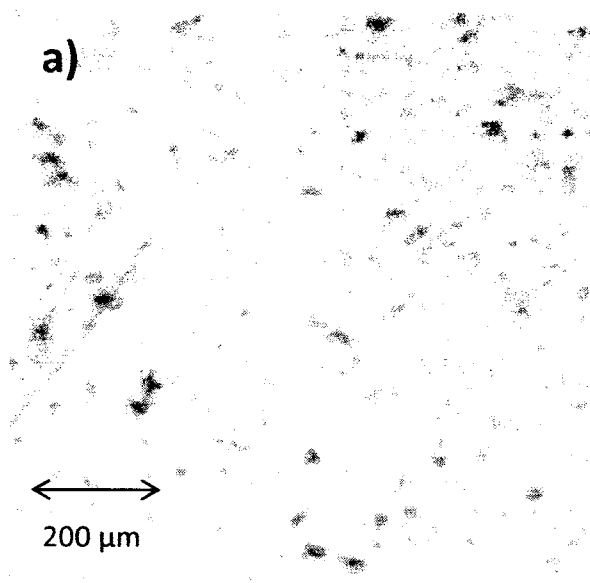
Figure 14.20 presents attenuation values measured at 10MHz frequency for switchgrass/biopolymer composite samples at each temperature. At 40°C there was no significant change in the attenuation values. At 20°C decrease in attenuation was found to be 7% with an increase in weight of 3.86% compared to dry sample. For 70°C 3% lower attenuation values with an increase in mass by 6.63% compared to initial material.

In the attenuation process ultrasonic sound wave penetrates (scattered) into the material through the transducer and gets reflected back from the bottom of the sample. Attenuation was found to be decreased for the switchgrass/biopolymer composite sample at three different temperatures. As the water content increased in the sample, the ultrasound reflection from bottom of the sample would not reach back to the transducer. As a result the pulse receiver shows decrease in attenuation values.

## 5.5 Acoustic Images

A Scanning Acoustic Microscopy Sonix HS-1000 was used to get the acoustic images. From the images it was observed that as the immersion time increases for samples the water absorption by fibers also increases. The fibers gradually become exposed from the surface of the sample and increase as the time progresses. Acoustic scans were performed to examine the nature of the biopolymer/switchgrass fiber interface and any modifications that appears during immersion of the samples in water. A fifty Mega Hertz (50MHz) transducer was used to get the acoustic images. Figure 5.21 shows the typical modifications that appear at the interface of biopolymer/switchgrass fiber under the influence of water at 20°C. Acoustic images clearly show the presence of fibers throughout the interface.

Figure 5.21a the acoustic image at 0hrs (dry sample, not immersed in water) shows the plain surface (fibers were not visible). Fibers began to appear as they absorbed water when the switchgrass/biopolymer composite samples were immersed in water. This can observe in figures 5.21b,c a& d. The circles were drawn on the image show some of the fibers expand out from the matrix. These images were taken at different time intervals.

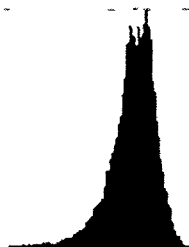


5.21. Acoustic images of the switchgrass/biopolymer composite samples exposed to water at different time intervals. a) 0hrs b) 24hrs c) 120hrs d) 360hrs.

## 5.6 Histograms

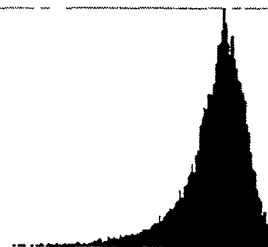
Analysis of the acoustic image histograms gives contrast ratio. Actually the acoustic images represent a stochastic spatial arrangement of the elastic moduli in the switchgrass/biopolymer composite material. A number of pixels of certain brightness in the image histograms are represented as a function of pixel brightness, which gives us elastic moduli distribution statistically in the material as this parameter is primarily related to amplitude of the reflected signal. Histogram width represent the contrast ratio of the images. X-axis of the histograms represents the pixel brightness (scale is 0-256) and Y-axis represents the number of pixels with certain brightness. All the histogram images (Figure 5.22a,b,c & d) show the same peak maximum position (biopolymer matrix). Maximum peak is same for all images which means the reflection coefficient is same for the matrix. The reason for this may be that the matrix did not absorb water. Darker area corresponds to fibers appearance at the surface and water absorption by them. The brightness of the images started decreasing as the immersion time increased for the samples. A decrease in the reflection coefficient means the properties of material becomes closer to water. The higher the water content in the material, the less bright the image will be. Figures 5.22b, 5.22c and 5.22d on the X-axis observed that widening of the histogram indicates the decrease in surface uniformity. Brightness of the image pixel depends on how the properties of material (elastic modulus and density) differ from water properties.

**A) Number  
of pixels**



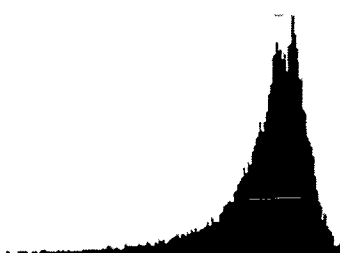
Brightness level of pixel

**B) Number  
of pixels**



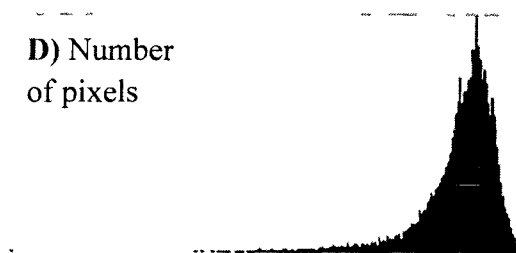
Brightness level of pixel

**C) Number  
of pixels**



Brightness level of pixel

**D) Number  
of pixels**



Brightness level of pixel

5.22 Histograms of the switchgrass/biopolymer composite samples exposed to water at different time intervals. A) 0hrs B) 24hrs C) 120hrs D) 360hrs.

## CONCLUSIONS

As the temperature increased water absorption of WPC and switchgrass/biopolymer composite also increased. The higher temperature 70°C causes water absorption of switchgrass/biopolymer composite to become 1.7 times higher than the switchgrass/biopolymer composite samples absorption of the water at 20°C and 40°C. Water absorption of WPC samples at 70°C causes water absorption to become higher and 1.3 times higher than the WPC sample absorbs the water at 20°C. The percentage of water absorbed by WPC compared to the switchgrass/biopolymer composite sample at three different temperatures was found to be two times higher. The reason could be the amount of water absorption in WPC is due to delignifying ligno-cellulosic material. In WPC lignin found to be the main cause for contributing fading. Therefore removal of the lignin from fillers has become important.

It was proven that the higher temperature (70°C) can accelerate the water absorption rate for both WPC and switchgrass/biopolymer composite materials.

The water diffusion coefficient of the WPC sample at 70°C was about 3 times higher than the WPC sample at 40°C and 8 times higher than WPC sample at 20°C. The switchgrass/biopolymer composite water diffusion coefficient value at 70°C was about 2 times higher than the switchgrass/biopolymer composite sample at 40°C and 8 times higher than switchgrass/biopolymer composite sample at 20°C. Hydrogen bonds are formed between cellulose and water molecules during water absorption. Therefore there is no chemical reaction between hydroxyl group of cellulose and water molecules. Yang et al proved this condition<sup>29</sup>.

SEM micrographs of WPC samples shows poor interfacial bonding due to water absorption. SEM micrographs of water-saturated switchgrass/biopolymer composite sample at



70°C shows poor interfacial adhesion. This will lead to poor mechanical performance of these materials. Acoustic images clearly show fibers are absorbing water and exposing out from the surface. WPC and switchgrass/biopolymer composites are less sensitive to the acoustic techniques.

## REFERENCES

- (1) Mohanty, A.K., M. Misra and G. Hincrichern, Biofibers, biodegradable polymers and biocomposites. An overview. *Macromolecular Material Engineering*. 2000, (1)25, 276-277.
- (2) Laranjeira E., Carvalho, L.H.D., S.M.D.L. Silva and J.R.M. DAlmeida, Influence of Fiber orientation on the mechanical properties of polyester/Jute composites. *Journal of Reinforced plastics and composites*, 2000 **25**(12); 1269-1278.
- (3) D. H. Müller, and A. Krobjilowski, New Discovery in the Properties of Composites Reinforced with Natural Fibers. *Journal of Industrial Textiles*, 2003. **33**(2): 111-130.
- (4) Pickering, K.L., Properties and performance of natural-fiber composites, *Woodhead Publishing in Materials*. 2008.
- (5) C. Maier, and T. Calafut, Polypropylene the definitive user's guide and data book. *Norwich. NY: Plastics Design Library*. 1998.
- (6) Qiu, W.L., Zhang, F.R., T. Endo, and T. Hirotsu, Effect of maleated polypropylene on the performace of polypropylene/cellulose composite. *Polymer Composites*. 2005. **26**(4): 448-453.
- (7) Panthapulakkal, S., M. Sain, and S. Law, Effect of coupling agents on rice-husk filled HDPE extruded profiles. *Polymer International*. 2005. **54**(1): 137-142.
- (8) Rowell, R.M., Challenges in biomass-thermoplastic composites, *Journal of Polymers and the environment*. 2007. **15**(4): 229-235.
- (9) Liu, H., Xie, F., Yu, L., L. Chen, and L. Li, Thermal processing of starch-based polymers. *Progress in Polymer Science*. 2009. **34**(12): 1348-1368.
- (10) Lange, J-P., Lignocellulose conversion: an introduction to chemistry, process and economics. *Biofuels Bioproducts and Biorefining*, 2007. **1**(1):39-48.
- (11) Fisher, T., Hajaligol, M., B. Waymack, and D. Kellogg, Pyrolysis behavior and kinetics of biomass derived material. *Journal of Analytical and Applied Pyrolysis*, 2002. **62**(2): 331-349.
- (12) Jiménez, A., and R.A. Ruseckaite, Binary mixtures based on polycaprolactone and cellulose derivative. *Journal of Thermal Analysis and Calorimetry*, 2007. **88**(3): 851-856.
- (13) Ruseckaite, R.A. and A. Jiménez, Thermal degradation of mixtures of polycaprolactone with cellulose derivatives. *Polymer Degradation and Stability*, 2003. **81**(2): 353-358.

- (14) Fraga, A., R.A. Ruseckaite, and A. Jiménez, Thermal degradation and pyrolysis of mixtures based on poly(3-hydroxybutyrate-8%-3-hydroxyvalerate) and cellulose derivative. *Polymer Testing*, 2005. **24**(4): 526-534.
- (15) Chen, H., M. Miao, and X. Ding, Influence of moisture absorption on the interfacial strength of bamboo/vinyl ester composites. *Composites Part A: Applied Science and Manufacturing*, 2009. **40**(12): 2013-2019.
- (16) Comyn, J., *Polymer permeability*, London: Chapman & Hall, 1985.
- (17) Bismarck, A., Aranberri-Askargorta, I., Springer, J., Lampke, T., Wielage, B., Stamboulis, A., et al., Surface Characterization of Flax, Hemp and Cellulose Fibers; Surface Properties and the Water Uptake Behavior. *Polymer Composites*, 2002. **23**(5): 872-894.
- (18) Espert, A., F. Vilaplana, and S. Karlsson, Comparison of water absorption in natural cellulosic fibres from wood and one-year crops in polypropylene composites and its influence on their mechanical properties. *Composites Part A: Applied Science and Manufacturing*, 2004. **35**(11): 1267-1276.
- (19) Alvarez, V.A., R.A. Ruseckaite, and A. Vazquez, Aqueous Degradation of MATER BI Y–Sisal Fibers Biocomposites. *Journal of Thermoplastic Composite Materials*, 2007. **20**(3): 291-303.
- (20) di Franco, C.R., Cyras, V.P., Busalmen, J.P., R.A. Ruseckaite, and A. Vázquez, Degradation of polycaprolactone/starch blends and composites with sisal fibre. *Polymer Degradation and Stability*, 2004. **86**(1): 95-103.
- (21) Stark, N., Influence of moisture absorption on mechanical properties of wood flour-polypropylene composites, *Journal of thermoplastic composite materials*. 2001. **14**(5): 421-432.
- (22) Dhakal, H.N., Z.Y. Zhang, and M.O.W. Richardson, Effect of water absorption on the mechanical properties of hemp fibre reinforced unsaturated polyester composites. *Composites Science and Technology*, 2007. **67**(7-8): 1674-1683.
- (23) Le Duigou, A., P. Davies, and C. Baley, Seawater ageing of flax/poly(lactic Acid) Biocomposites, *Polymer Degradation and Stability*. 2009. **94**(7): 1151-1162.
- (24) Devi, L.U., Joseph, K., K.C.M. Nair, and S. Thomas, Ageing Studies of Pineapple Leaf Fiber–Reinforced Polyester Composites, *Journal of Applied Polymer Science*. 2004. **94**(2): 503-510.

- (25) Varghese, S., B. Kuriakose, and S. Thomas, Short sisal fiber reinforced natural rubber composites, high-energy radiation, thermal and ozone degradation, *Polymer degradation and stability*.1994. **44**(1): 55-61.
- (26)Joseph, P.V., Rabello, M.S., Mattoso, L.H.C., K. Joseph, and S. Thomas, Environmental effects on the degradation behaviour of sisal fibre reinforced polypropylene composites, *Composites Science and Technology*. 2002. **62**(10-11): 1357-1372.
- (27) Beg, M.D.H., and K.L. Pickering, Accelerated weathering of unbleached and bleached Kraft wood fibre reinforced polypropylene composites, *Polymer Degradation and Stability*. 2008. **93**(10): 1939-1946.
- (28) Islam, M.S., K.L. Pickering, and N.J. Foreman, Influence of accelerated ageing on the physico-mechanical properties of alkali-treated industrial hemp fibre reinforced poly(lactic acid) (PLA) composites, *Polymer Degradation and Stability*, 2010. **95**(1): 59-65.
- (29)Yang, H.-S., Kim, H.-J., Park, H.-J., B.-J. Lee, and T.-S. Hwang, Water absorption behavior and mechanical properties of lignocellulosic filler–polyolefin bio-composites, *Composite Structures*. 2006. **72**(4): 429-437.
- (30) Kim, J.S., H.J. Kim, and D. Cho, Thermal analysis of hydrolysis and degradation of biodegradable polymer and Bio-composite, *Journal of thermal Analysis and Calorimetry*. 2009. **96**(1), 211-218.
- (31) Tajvidi, M., S.K. Najafi, and N. Moteei, Long-Term Water Uptake Behavior of Natural Fiber/Polypropylene Composites *Journal of Applied Polymer Science*. 2006. **99**(5): 2199-2203.
- (32) Rouison, D., Couturier, M., Sain, M., B. MacMillan, and B.J. Balcom, Water absorption of Hemp Fiber/Unsturated Polyester composites, *Polymer Composites*.2005. **26**(4): 509-525.
- (33) Jayaraman, K., Manufacturing sisal–polypropylene composites with minimum fibre degradation, *Composite Science and Technology*. 2003. **63**(3-4): 367-374.
- (34) Rong, M.Z., Zhang, M.Q., Liu, Y., G.C. Yang, and H.M. Zeng, The effect of fiber treatment on the mechanical properties of unidirectional sisal-reinforced epoxy composites, *Composite Science and Technology*. 2001. **61**(10): 1437-1447.
- (35) John, M.J., and S. Thomas, Biofibres and biocomposites, *Carbohydrate Polymers*. 2008. **71**(3): 343-364.

- (36) Morales, J., Olayo, M.G., Cruz, G.J., P. Herrera-Franco, and R. Olayo, Plasma Modification of Cellulose Fibers for Composite Materials. *Journal of Applied Polymer Science*. 2006. **101**(6): 3821-3828.
- (37) Weyenberg, I.V., Truong, T.C., B. Vangrimde, and I. Verpoest, Improving the properties of UD flax fibre reinforced composites by applying an alkaline fibre treatment, *Composites Science and Technology*. 2006. **37**(9): 1368-1376.
- (38) Bledzki, A.K., and J. Gassan, Composites reinforced with cellulose based fibres, *Progress in Polymer Science*. 1999. **24**(2): 221-274.
- (39) Zafeiropoulos, N.E., C.A. Baillie, and J.M. Hodgkinson, Engineering and characterisation of the interface in flax fibre/polypropylene composite materials. Part II. The effect of surface treatments on the interface, *Composite Science and Technology*. 2002. **33**(9): 1185-1190.
- (40) Bledzki, A.K., S. Reihmane, and J. Gassan, Properties and Modification Methods for Vegetable Fibers for Natural Fiber Composites, *Journal of Applied Polymer Science*. 1996. **59**(8): 1329-1336.
- (41) Pothan, L.A., S. Thomas, and G. Groeninckx, The role of fibre/matrix interactions on the dynamic mechanical properties of chemically modified banana fibre/polyester composites *Composite Science and Technology*. 2006. **37**(9): 1260-1269.
- (42) Herrera-Franco, P.J., A. Valdez Gonzalez, and M. Cervantes-Uc, Development and characterization of a HDPE-sand-natural fiber composite, *Composites Part B: Engineering*. 1997. **28**(3): 331-343.
- (43) Herrera-Francoand, P.J., and M. de J. Aguilar-Vega, Effect of Fiber Treatment on the Mechanical Properties of LDPE–Henequen Cellulosic Fiber Composites, *Journal of Applied Polymer Science*. 1997. **65**(1): 197-207.
- (44) Valdez Gonzalez, A., Cervantes-Uc, J.M., R. Olayo, and P.J. Herrera-Franco, Chemical modification of heneque'n fibers with an organosilane coupling agent, *Composites Part B: Engineering*, 1999. **30**(3): 321-331.
- (45) Xue, Y., Veazie, D.R., Glinsey, C., M.F. Horstemeyer, and R.M. Rowell, Environmental effects on the mechanical and thermomechanical properties of aspen fiber–polypropylene composites, *Composites Part B: Engineering*. 2007. **38**(2): 152-158.
- (46) Colom, X., Carrasco, F., P. Pages, and J. Canavalc, Effects of different treatments on the interface of HDPE/lignocellulosic fiber composites, *Composites Science and Technology*. 2003. **63**(2): 161-169.

- (47) Zheng, Y.-T., Cao, D.-R., D.-S. Wang, and J.-J. Chen, Study on the interface modification of bagasse fibre and the mechanical properties of its composite with PVC, *Composites Part A: Applied Science and Manufacturing*. 2007. **38**(1): 20-25.
- (48) Cao, Y., S. Shibata, and I. Fukumoto, Mechanical properties of biodegradable composites reinforced with bagasse fibre before and after alkali treatments, *Composites Part A: Applied Science and Manufacturing*, 2006. **37**(3): 423-429.
- (49) M. Brahmakumar, C. Pavithran, and R.M. Pillai, Coconut fibre reinforced polyethylene composites: effect of natural waxy surface layer of the fibre on fibre/matrix interfacial bonding and strength of composites, *Composites Science and Technology*. 2005. **65**(3-4): 563-569.
- (50) Nam, T.H., Ogihara, S., N.H. Tung, and S. Kobayashi, Effect of alkali treatment on interfacial and mechanical properties of coir fiber reinforced poly (butylene succinate) biodegradable composites: *Composites Part B: Engineering*. 2011. **42**(6): 1648-1656.
- (51) Elsabbagh, A., L. Steuernagel, and G. Ziegmann, Effect of fiber/matrix chemical modification on the mechanical properties and water absorption of extruded flax/polypropylene composite, *Journal of Applied Polymer Science*. 2009. **111**(5): 2279-2289.
- (52) Chem, D., J. Li, and J. Ren, Influence of fiber surface-treatment on interfacial property of poly(l-lactic acid)/ramie fabric biocomposites under UV-irradiation hydrothermal aging, *Material Chemistry and Physics*. 2011. **126**(3): 524-531.
- (53) Samal, R.K., Panda, B.B, S.K. Rout, and M. Mohanty, Effect of chemical modification on FTIR spectra. I physical and chemical behaviour of coir, *Journal of Applied polymer science*, 1995. **58**(4): 745-752.
- (54) George. J, S.S. Bhagawan, and S. Thomas, Improved interactions in chemically modified pineapple leaf fiber reinforced polyethylene composites, *Composite Interfaces*. 1998. **5**(3): 201-223.
- (55) Hristov, V., and S. Vasileva, Dynamic mechanical and thermal properties of modified poly(propylene) wood fiber composites, *Macromolecular Materials Engineering*. 2003. **288** (10): 798-806.
- (56) Mwaikambo, L.Y. and M.P. Ansell, Chemical modification of hemp, sisal, jute and kapok fibers by alkalization, *Journal of Applied Polymer Science*. 2002. **84**(12): 2222-2234.
- (57) Wong, S., R. Shanks, and A. Hodzic, Interfacial improvements in Poly(3-hydroxy butyrate)-flax fiber composites with hydrogen bonding additives, *Composites Science and Technology*. 2004. **64**(9): 1321-1330.

- (58) Gwon, J. G., Lee, S. Y., G.H. Doh, and J. H. Kim, Characterization of Chemically modified wood fibers using FTIR spectroscopy for biocomposites, *Journal of Applied Polymer Science*. 2010. **116**(6): 3212-3219.
- (59) Bledzki, A.K., and A. Jaskiewicz, Mechanical performance of biocomposites based on PLA and PHBV reinforced with natural fibres – A comparative study to PP, *Composites Science and Technology*. 2010. **70**(12): 1687-1696.
- (60) Sawpan, M.A., K.L. Pickering, and A. Fernyhough, Improvement of mechanical performance of industrial hemp fibre reinforced polylactide biocomposites, *Composites Part A: Applied Science and Manufacturing*. 2011. **42**(3): 310-319.
- (61) Tajvidi, M., and G. Ebrahimi, Water Uptake and Mechanical Characteristics of Natural Filler-Polypropylene Composites, *Journal of Applied Polymer Science*. 2003. **88**(4): 941-946.
- (62) Simonsen, J., R. Jacobson, and R. Rowell, Properties of Styrene-Maleic Anhydride Copolymers Containing Wood-Based Fillers, *Forest Products Journal*. 1998. **48**(1): 89-92.
- (63) Bledzki, A.K., A.A. Mamun and J. Volk, Physical, chemical and surface properties of wheat husk, rye husk and soft wood and their polypropylene composites, *Composites Part A: Applied Science and Manufacturing*. 2010. **41**(4): 480-488.
- (64) Ng, Z.S., Bulk orientation of Agricultural Filler- Polypropylene composites, *University of Waterloo*. 2008.
- (65) Lee, M.W., S.O. Han, and Y.B. Seo, Red algae fiber/poly(butylene succinate) Biocomposites: the effect of fiber content on their mechanical and thermal properties, *Composites Science and Technology*. 2008. **68**(6): 1266-1272.
- (66) Kim, H.-S., Lee, S.-H., Lee, S., H.-J. Kim, and J.R. Dorgan, Enhanced interfacial adhesion, mechanical and thermal properties of natural flour-filled biodegradable polymer biocomposites. *Journal of Thermal Analysis and Calorimetry*. 2011. **104**(1): 331-338.
- (67) Rosa, M.F., Chiou, B.-S., Medeiros, E.S., Wood, D.F., Williams, T.G., Mattoso, L.H.C., W.J. Ortos, and S.H. Imam, Effect of fiber treatments on tensile and thermal properties of starch/ethylene vinyl alcohol copolymers/coir Biocomposites, *Bioresource Technology*. 2009 **100**(21): 5196-5202.
- (68) Bhat, I-U-H., Abdul Khalil, H.P.S., M.R. Nurul Fazita, and C.K. Abdullah, Hybridized Biocomposites from Agro-Wastes: Mechanical, Physical and thermal characterization, *Journal of Polymers and the Environment*. 2011. **19**(1): 49-58.

- (69) Moriana, R., Vilaplana, F., S. Karlsson, and A. Ribes-Greus, Improved thermo-mechanical properties by the addition of natural fibers in starch-based sustainable Biocomposites. *Composites Part A: Applied Science and Manufacturing*. 2011. **42**(1): 30-40.
- (70) Briggs, A. In *Acoustic Microscopy*; Monographs on the Physics and Chemistry of Materials; Clarendon Press: Oxford, NY, 1992, pp 25-59.
- (71) [www.geosci.ipfw.edu/sem.semedx.html](http://www.geosci.ipfw.edu/sem.semedx.html)
- (72) Vilaplana, F., E. Stromberg, and S. Karlsson, Environmental and resource aspects of sustainable Biocomposites, *Polymer Degradation and Stability*. 2010. **95**(11): 2147-2161.
- (73) Mohanty, A.K., M. Misra, and T.D. Lawrence, Natural Fibers, Biopolymers and Biocomposites, *Taylor & Francis Group*. ISBN 0-8493-1741-X. 2005.
- (74) Klyosov, A., Wood-Plastic Composites, *Wiley*. 2007. 405
- (75) Zadorecki, P., and P. Flodin, Surface modification of cellulose fibers III. Durability of cellulose–polyester composites under environmental aging, *Journal of Applied Polymer Science*. 1986. **31**(6): 1699-1707.
- (76) M.M. Thwe, and K. Liao, Effects of Environmental Aging on the Mechanical Properties of Bamboo-Glass Fiber Reinforced polymer matrix Hybrid composites, *Composites Part A: Applied Science and Manufacturing*. 2002. **33**(1): 43-52.
- (77) Loos, A.C., and G.S. Springer, Moisture Absorption of polyester- E-glass composites, Environmental Effects on Composite Materials, *Technomic Publishing Co. Inc.*, CT, USA. 1981. 51-62.
- (78) Wang, W., and J.J. Morrell, Water sorption Characteristics of two wood-plastic composites, *Forest Products Journal*. 2004. **54**(12): 209-212.
- (79) Doan T.T.L., S.L. Gao and E. Mader, Jute/polypropylene composites I. Effect of matrix modification, *Composites Science and Technology*. 2006. **66**(7-8): 952-963.
- (80) Bledzki, A.K., Letman, M., A. Viksne, and L. Rence, A comparison of compounding processes and wood type for wood fiber-PP composites, *Composites Part A: Applied Science and Manufacturing*. 2005. **36**(6): 789-797.



- (81) Stamboulis, A., Baillie, C.A., Garkhail, S.K., H.G.H. Van Melick, and T. Peijs, Environmental durability of flax fibers and their composites based on polypropylene matrix, *Applied Composite Materials*. 2000. **7**(5-6): 273-294.
- (82) Panthapulakkal, S., and M. Sain, Studies on the Water Absorption properties of short Hemp-Glass fiber Hybrid Polypropylene composites, *Journal of Composite Materials*. 2007. **41**(15): 1871-1883.
- (83) Ke, T.Y., and X. Sun, Physical properties of poly(lactic acid) and starch composites with various blending ratios, *Cereal Chemistry*. 2000. **77**(60): 761-768.
- (84) Wang, H., X.Z. Sun, and P. Seib, Strengthening blends of poly(lactic acid) and starch with methylene diphenyl diisocyanate. *Journal of Applied Polymer Science*. 2001. **82**(7): 1761-1767.
- (85) Crank, J., Mathematics of Diffusion, *Oxford University Press*, Oxford. 1956. 347.
- (86) Marcovich, N.E., M.M. Reboredo, and M.I. Aranguren, Moisture Diffusion in polyester wood fiber Composites, *Polymer*. 1999. **40**(26): 7313-7320.
- (87) Qina, L., Qiu, J., Li, M., Ding, S., Shao, L., Lu, S., Zhang, G., Y. Zhao, and X. Fu, Mechanical and thermal properties of poly(lactic acid) composites with rice straw fiber modified by poly(butyl acrylate), *Chemical Engineering Journal* 2011. **166**(2): 772-778.
- (88) Y.Y. Leu, and W.S. Chow, Kinetics of water absorption and thermal properties of poly(lactic acid)/organomontmorillonite/poly(ethylene glycol) Nanocomposites, *Journal of Vinyl & Additive Technology*. 2011. **17**(1): 40-47.
- (89) V. Bucur, Anisotropy characterization of structural flackboard with ultrasonic methods. *Wood and Fiber Science*. 1992. **24**(3): 337 – 346.
- (90) Bekhta, P. A., P. Niemz, and L. J. Kucera, The study of sound propagation in the wood-based composite material. *Proceeding of 12th International Symposium on Nondestructive Testing of Wood*, Sopron, 2000. 33 – 41.
- (91) Vun, Y. R. , Wu, Q. , M. Bhardwaj, and G. Stead, Through – thickness ultrasonic transmission properties of oriented strandboard. *Proceeding of 12<sup>th</sup> International Symposium on Nondestructive Testing of Wood* , Sopron. 2000. 76 – 68

- (92) Kazemi Najafi S., V. Bucur, and Gh. Ebrahimi, Elastic constants of particleboard with ultrasonic technique. *Material Letters*. 2005. **59**(16): 2039-2042.

**VITA AUCTORIS**  
**GANESH M. VENUKADASULA**

**Education**

- 2009-2011 M.Sc. Candidate, Chemistry  
Department of Chemistry and Biochemistry, University of Windsor  
Advisor: Dr. Elena Maeva
- 2002-2004 M.Sc. Organic Chemistry  
Osmania University, AP, INDIA
- 1998-2001 B.Sc. Biology, Chemistry  
Osmania University, AP, INDIA

**Awards**

- 2009-2011 Received International Graduate Student Scholarship, University of Windsor,  
Canada
- 2008 Received Parker fellowship, Wichita State University, USA

**Employment history**

- 2009-2011 **Research Assistant**  
Department of Chemistry and Biochemistry,  
University of Windsor, Windsor, CANADA
- 2009-2011 **Graduate Assistant**  
Department of Chemistry and Biochemistry,  
University of Windsor, Windsor, CANADA
- 2007-2008 **Research Assistant**  
Department of Chemistry,  
Wichita State University, Wichita, USA
- 2005 **Research Assistant**  
National Chemical Laboratory, Pune, INDIA

**Publications**

1. Through-Bond Photoinduced Electron Transfer in a Self-assembled Porphyrin-Fullerene Conjugate Held by a Hamilton type Hydrogen Bonding motif:  
Francis D'Souza, **Ganesh M. Venukadasula**, Ken-ichi Yamanaka, Navaneetha K Subbaiyan, Melvin E.Zandler and Osamu Ito. *Org. Biomol. Chem.*, **2009**, 7, 1076 – 1080
2. Preparation and Selected properties of an improved composite of the Electrophoretically Deposited Single-Wall Carbon Nanotubes, Electrochemically coated with a C60 – Pd and Polybithiophene mixed polymer Film.

Piotr Pieta, **Ganesh M. Venukadasula**, Francis D'Souza and Wlodzimierz Kutner  
*J. Phys. Chem. C* **2009**, *113*, 14046–14058

3. Conductive, capacitive and visco-elastic properties of a new composite of the C60-Pd Conducting polymer and single-wall carbon nanotubes.  
Piotr Pieta, Emilia Grodzka, Krzysztof Winkler, Magdalena Warczak, Andrzej Sadkowski, Grazyna Z.Sukowska, **Ganesh M. Venukadasula**, Francis D'Souza, and Wlodzimierz Kutner. *J. Phys. Chem. B* **2009**, *113*, 6682–6691
4. Preparation and selected properties of a composite of the C60-Pd Conducting polymer and Single-Wall Carbon Nanotubes.  
Piotr Pieta, Emilia Grodzka, Krzysztof Winkler, **Ganesh M. Venukadasula**, Francis D'Souza and Wlodzimierz Kutner, *phys. stat. sol. (b)* *245*, No. 10, 2292–2295 (**2008**)

### Poster Presentations

1. “Self-Assembled Carbon Nanotube Based Donor-Acceptor Ensembles for Photo-Induced Electron Transfer Studies”. ACS Midwest meeting, Kansas City, Kansas, United States. Nov 7-9, 2007
2. “Self-assembled Porphyrin-Fullerene Conjugate via Hamilton type Hydrogen Bonding motif”. ACS Midwest meeting, Nebraska, Kearney, United States, Oct 8-10. 2008
3. Study of the Defects and Water Absorption Behaviour in Biocomposites using Acoustic Methods, 5th Biannual Research Meeting. Guelph, Ontario November 24, 2010.
4. Biocomposites for Automotive Applications: Non-Destructive Evaluation of the Composites Properties and their Deterioration, 2010 CAP Congress, Toronto, Ontario, June 7, 2010 - June 11, 2010
5. Nondestructive Evaluation of Natural Fiber Reinforced Composites: Material Properties and their Deterioration. 12th International Symposium on Nondestructive Characterization of Materials. Virginia Tech , Blacksburg, USA, June 19-24, 2011
6. Effect of Composition and Fibers Dimensions on Acoustic Properties of Natural Fiber Reinforced Composites. ASNT 20th Annual Research Symposium & Spring Conference, March 21-25, 2011. San Francisco, California, United States.

### Oral Presentation

1. Water absorption, diffusion characterization and dimensional stability of biocomposite materials, **The Ontario BioCar Initiative 7<sup>th</sup> Biannual Research Meeting, University of Toronto, June 3<sup>rd</sup> 2011**